THE UNIVERSITY OF CHICAGO

TUMOR CELL-INTRINSIC DEFECTS IN STING PATHWAY SIGNALING AND TYPE I INTERFERON EXPRESSION

A DISSERTATION SUBMITTED TO
THE FACULTY OF THE DIVISION OF THE BIOLOGICAL SCIENCES
AND THE PRITZKER SCHOOL OF MEDICINE
IN CANDIDACY FOR THE DEGREE OF
DOCTOR OF PHILOSOPHY

INTERDISCIPLINARY SCIENTIST TRAINING PROGRAM: IMMUNOLOGY

BY

BLAKE ALAN FLOOD

CHICAGO, ILLINOIS

DECEMBER 2020

If you can make one heap of all your winnings
And risk it on one turn of pitch-and-toss,
And lose, and start again at your beginnings
And never breathe a word about your loss;
If you can force your heart and nerve and sinew
To serve your turn long after they are gone,
And so hold on when there is nothing in you
Except the Will which says to them: 'Hold on!'

If you can talk with crowds and keep your virtue,
Or walk with Kings—nor lose the common touch,
If neither foes nor loving friends can hurt you,
If all men count with you, but none too much;
If you can fill the unforgiving minute
With sixty seconds' worth of distance run,
Yours is the Earth and everything that's in it,
And—which is more—you'll be a Man, my son!

- If, Rudyard Kipling

TABLE OF CONTENTS

LIST OF FIGURES

LIST OF TABLES

ACKNOWLEDGEMENTS

I've been recently reflecting on how I have changed while working on my PhD and what led me to even get this opportunity. It is clear that the work presented in this thesis is not solely my own but, rather, a result of collaboration and support from many sources.

From a young age I was always interested in math and science. There are several teachers that helped foster that curiosity but I think my particular interest in molecular biology began in Mrs. Epperson's high school class. She taught with such skill and passion that it made biology enticing. Mr. Sparks, who taught chemistry, was equally skilled and did a great job introducing basic scientific philosophies. It was in his class that I had the opportunity to do a self-directed, independently-designed research project that made me want to pursue scientific research as a career. Then, in my first year of college, Rudy Fratti allowed me to join his lab. It was in Rudy's lab that I confirmed my love of science and realized that I wanted to do clinically-relevant work. Looking back, I'm amazed at how much he trusted me to work on an independent project and helped me push it forward. Many other researchers only trust undergraduates with simple, repetitive work but he truly treated me like a scientist. I think his influence is a large part of why I ultimately chose to continue pursuing science. There were also several people in his lab that helped me learn science and made lab an enjoyable place including: Surya Karunakaran, Mat Star, and Greg Miner.

After college I was very fortunate to be accepted to the University of Chicago's MSTP program. As I began to transition into the PhD phase of my training, Doug Kline and Justin Kline helped me become familiar with immunologic research. I remember a particular practice presentation with Doug where I became aware of the level of detail and precision that are necessary in science, which has made me a tangibly better scientist. Ultimately, I joined Tom

Gajewski's lab. I don't think I can ever truly thank him enough for the opportunity he provided and impact he has had on me as a scientist. In college I heard that the main thing you get from a PhD is "how to think" more than the raw information or data. I didn't really believe it because there is so much information to learn and data to collect but I now realize that was true. I think Tom is the single person who has had the greatest impact on my approach to science and I feel fortunate to be mentored by one of the best in this regard. In Tom's lab there have been so many people that have helped me in a myriad of ways. When I first joined the lab, Leticia Corrales taught me a lot about techniques and about how to be a productive scientist. There were others who were instrumental in teaching me techniques such as Jason Williams, Shuyin Li, Akinola Emmanuel Jr., and Ken Hatogai. Others were a lot of fun to talk about broad scientific ideas with such as Stefani Spranger, Jon Trujillo, Emily Higgs, and Jessica Fessler. Yet others simply made it fun to come to lab including Vyara Matson, Brendon Horton, Kyle Cron, Alex Cabanov, Jeffrey Bloodworth, and Andrea Ziblat. More recently I've gained a set of informal clinical mentors to help me transition back to a medical mindset including Sherin Rouhani, Athalia Pyzer, Randy Sweis, and Jon Trujillo. I also couldn't have done this without mentorship by Marissa Alegre and my thesis committee: Marcus Clark, Justin Kline, Fotini Gounari, and Seungmin Hwang. Their help and guidance has been instrumental.

Finally, there is my family which transcend this timeline. My extended family have always been there for me and I am lucky to have such a large support network. In particular, my parents are truly amazing. They shaped me as a kid and instilled in me the values I have today. They taught me honesty, fostered my curiosity, and taught me the importance of always giving your best in anything you pursue. Moreover, they provided me with a level of love and support that I know is not common and will never take for granted. I love you guys.

ABSTRACT

It has previously been shown that immunogenic tumors spontaneously activate the innate immune system through the STING pathway. Based on this observation, STING agonists have been developed and are being tested as a pharmacologic approach to activate the pathway and promote anti-tumor immunity. As part of these studies, we observed that tumor cells themselves usually fail to produce IFN-β in response to STING agonists or cytoplasmic DNA, arguing that loss of activation of this pathway might occur regularly as a component of oncogenesis. Understanding failed activation of this pathway might lead to new therapeutic strategies to re-engage tumor cell-intrinsic IFN-β production, which would be predicted to cause immune-mediated tumor control. We found that B16 tumor cells retained expression of each gene in the STING pathway, and that STING signal transduction was intact up to and including nuclear translocation of IRF3. In tumor cells, ChIP assays revealed that IRF3 failed to bind the IFN-β promoter but still bound to other gene promoters and induced expression of those genes. This was likely due to an epigenetic block because Mϕ epigenetically opened the IFN-β promoter region after STING activation, but tumor cells lacked this opening event. Previous work had implicated the NF-κB pathway in the epigenetic opening of the IFN-β locus, and so we examined this pathway in B16 tumor cells. Indeed, we found failed nuclear translocation of the p65 component of NF-κB following STING agonist application. Heterokaryon fusion studies indicated that a dominant-negative mechanism was operational, suggesting that an inhibitory factor was present in tumor cells that blunted NF-κB activation. Treatment with cycloheximide to allow degradation of a putative inhibitory factor restored both NF-κB signaling and IFN-β expression by B16 tumor cells. A genome-wide CRISPR screen identified multiple candidates that, when knocked out, augmented tumor cell-intrinsic NF-κB signaling and IFN-β expression.

Chapter 1: Introduction

1.01 Overview: The immune system can oppose cancer

Cancer develops as a consequence of the accumulation of somatic mutations. Most mutations are deleterious but if the mutations confer a cell with enhanced proliferation and survival it will necessarily lead to the accumulation of those cells [1]. This expansion causes the most aggressive and resilient clones to become enriched. In this way, cancer can progress over time from benign tumors to metastatic disease.

However, mutation and altered gene expression in cancer cells can also serve as a means for recognition by the host immune system. Our mechanistic understanding of anti-tumor immunity was catalyzed by the observation that patients with a higher degree of immune infiltration into their tumors tend to have a better prognosis. In particular, a higher level of $CD8^+$ cytotoxic T cells in a tumor is associated with prolonged patient survival [2–5]. $CD8^+$ T cells may have developed evolutionarily to fight viral infections by recognizing and killing compromised cells through recognition of virus-encoded antigens. It seems that the same components of the immune system can recognize and destroy malignant cells through recognition of mutated or

newly expressed tumor antigens. Just as $CD8^+$ T cells can differentiate healthy from infected cells based on the presence of virus, they can also identify malignant cells based on the underlying mutations found in cancer [6,7].

Perhaps the best evidence the immune system can oppose cancer is the fact that cancer cells often express inhibitory ligands on their surface that suppress $CD8^+$ T cells and that therapies designed to target these molecules have been clinically successful. For example, several types of cancer upregulate expression of PD-L1, a ligand that binds an inhibitory receptor, PD-1, on the surface of $CD8^+$ T cells [8,9]. Checkpoint blockade immunotherapies designed to block these inhibitory ligand/receptor interactions have been developed and are FDA-approved to treat a broad range of tumor types [10]. However, only a minority of patients respond to checkpoint blockade immunotherapy. Patients that respond to checkpoint blockade tend to have a higher level of pre-existing $CD8^+$ T cell infiltration prior to therapy [11]. This argues the majority of patients that don't respond might benefit from therapies designed to generate and recruit $CD8^+$ T cells and other critical immune components into the tumor microenvironment. New strategies to achieve these events could have the potential to treat a wide range of cancers, by expanding the percentage of patients capable of responding to checkpoint blockade.

There are many conceptual approaches to cancer therapy. Therapies like radiation or chemotherapy are thought to exploit the aggressive proliferation of cancer cells to damage and kill them [12]. More recently developed targeted therapies block key pathways that are mutated or functionally active in cancer cells which drive their growth and survival. However, there are dozens of potentially altered pathways which can be affected at multiple levels, so that a relatively long list of drugs would need to be developed to target different molecular pathways. Cancer immunotherapy is conceptually much simpler. It relies on an initial innate immune

response to alert the immune system to the tumor, subsequent recruitment of immune cells into the tumor microenvironment, and, ultimately, a functional anti-tumor adaptive immune response. Evidence suggests that patients with the first 2 steps successfully completed represent the "T-cell inflamed" subset of patients that are more likely to respond to checkpoint blockade immunotherapies [11,13,14]. Therefore, finding therapies designed to promote the initiation of an anti-tumor immune response has the potential to benefit many patients and is the general motivation behind this thesis.

1.02 Developing tumors overcome inhibitory mechanisms

During oncogenesis, there are several pathways that can oppose tumor formation. Genes encoding molecules in such pathways are defined as "tumor suppressor" genes [1]. Tumor suppressor genes are commonly mutated or inactivated in cancers. One of the most commonly inactivated tumor suppressor genes is p53, which is mutated or lost in over half of human tumors [15,16]. p53 is a transcription factor that regulates expression of hundreds of genes. In response to DNA damage, it induces cell cycle arrest and DNA repair. If signaling is strong enough or prolonged enough, p53 can also promote cell death via apoptosis [17]. p53 therefore opposes cancer by deleting cells with too much DNA damage and thus helps to prevent cells from accumulating mutations. Tumor suppressor genes are an obstacle that tumor cells must overcome during oncogenesis. The immune system is similarly thought to oppose tumor formation and necessitate tumor cell adaptation.

Tumors form more rapidly in immunocompromised mice than wild-type (WT) mice. When tumor cells that developed in WT mice are transplanted into immunocompromised mice, they grow rapidly. However, if tumor cells derived from immunocompromised mice are transferred into WT mice with the same genetic background, tumor cells are immunologically

rejected unless those recipient mice are depleted of key immune cells like $CD8^+$ T cells [18,19]. These observations demonstrate that an anti-tumor immune response can delay tumor outgrowth by opposing tumor formation. It also demonstrates that tumors developing in the face of an ongoing anti-tumor immune response are forced to adapt to become less immunogenic. Thus, the immune system can act as a tumor cell-extrinsic tumor suppressor that delays the formation of cancer and shapes its final form. Understanding how the immune system responds to cancer and, in turn, how tumors suppress or evade immunity is a major factor in improving cancer immunotherapy.

1.03 Immunologic responses coordinate innate and adaptive immunity

The immune system can be broadly divided into the innate and adaptive immune system. The innate immune system is an evolutionarily ancient system that evolved before the divergence of plants and animals [20]. The innate immune system represents the first set of cells that respond to an infection or other threat. It senses the presence of a pathogen using "Pattern Recognition Receptors" (PRRs) which can detect "Pathogen-Associated Molecular Patterns" (PAMPs) released by pathogens or "Damage-Associated Molecular Patterns" (DAMPs) released by damaged host cells [21–23]. PRR activation stimulates a signal transduction cascade converging on several different transcriptions factors most typically NF-κB, IRF3, and AP-1 [24]. Collectively these transcription factors induce expression of hundreds of genes including inflammatory cytokines and chemokines. Secretion of these inflammatory mediators alerts surrounding cells to the infection and also recruits other cell types to the site of the infection. For example, PRRs that detect a viral infection will promote the expression of type I interferons such as IFN-β that interfere with viral replication. Signaling through IFNAR, the type I interferon receptor, causes infected cells to stop proliferating, induces upregulation of interferon-stimulated genes that

disrupt viral replication, and can even induce cell death in an attempt to kill infected cells [25]. Chemokines induced by PRR signaling can recruit innate cells such as monocytes. Monocytes express CCR2 which bind the chemokines CCL2 or CCL7 to recruit monocytes to inflamed tissue [26]. At the site of inflammation, monocytes can differentiate into macrophages or dendritic cells (DCs) [27]. Macrophages are equipped with their own PRRs and are phagocytic cells that can engulf extracellular bacteria to digest them. These innate cellular and molecular effectors are capable of clearing an infection independently but, in circumstances where they fall short, the innate immune system can mobilize the adaptive immune system. Antigen-presenting cells (APCs), such as DCs, are innate cells recruited to the site of an infection by inflammatory cytokines and they are tasked with stimulating cells of the adaptive immune system.

In general terms, APCs are phagocytic cells that take up exogenous material and process it for presentation on Major Histocompatibility Complex (MHC) molecules [28,29]. APCs express their own PRRs and can also sense inflammatory cytokines. These signals indicate the presence of a pathogen and stimulate APCs to undergo maturation. Mature DCs upregulate CCR7 and migrate from the inflamed tissue through the lymphatics to the lymph node that drains the site of infection [30,31]. In the draining lymph node, DCs present peptides initially acquired at the site of infection to naïve T lymphocytes having corresponding T cell antigen receptors (TCRs) [32]. Inflammatory signals also stimulate APCs to increase their expression of co-stimulatory molecules, including CD80 and CD86, that help promote productive activation and maturation of T cells [29]. By this mechanism, the innate immune system stimulates an adaptive immune response.

The adaptive immune response is slower to become activated but is more specific to an individual pathogen and can form memory to protect against re-exposure to a pathogen. The

adaptive immune system is comprised of two main cell types, B and T lymphocytes. Each T lymphocyte expresses a TCR on the surface that recognizes oligopeptides presented on MHC molecules on other cells [29,33]. During T cell development in the thymus, the germline-encoded TCR gene segments undergo random recombination to generate a single TCR for a given cell. The combinatorial nature of this process means that an estimated 10^{15}-10^{20} distinct TCRs can be produced among the peripheral T cell repertoire [33,34]. An individual host is thought to have approximately 10^{6}-10^{7} distinct T cell clonotypes at one time with most T cells expressing only one TCR [35–37]. After TCR recombination, developing T cells are exposed to self-antigens in the thymus and any T cells expressing TCRs that strongly recognize self-antigens are deleted from the repertoire. T cells that recognize self-antigens relatively weakly are driven to become T regulatory cells that have immunosuppressive functions and help to maintain immune tolerance [38]. The immense diversity produced by TCR gene recombination combined with the selection process to remove strongly auto-reactive T cell clones produces a naïve T cell repertoire with the ability to recognize a broad universe of exogenous antigens.

In addition to central tolerance, which occurs during T cell development, naïve T cells are also constrained by peripheral tolerance mechanisms. Peripheral tolerance is mediated by the restriction of T cell activation to APCs with the proper costimulatory signals [38]. If naïve T cells recognize antigen presented by APCs without the proper costimulatory molecules, then the T cells are functionally inactivated or deleted [38]. If naïve T cells recognize peptides presented by APCs simultaneously with costimulatory molecules, then the T cells undergo maturation. T cell maturation causes them to rapidly proliferate and increase their numbers exponentially [39]. This allows a single naïve T cell with a TCR specific for a pathogen to produce as much as 500,000 daughter cells which can then combat the infection or antigen-expressing tumor cells. Mature T

cells also express effector molecules and alter their chemokine receptor expression patterns. For example, $CD8^+$ cytotoxic T cells express granzymes and perforin which, when released, can enter target cells to induce apoptosis [40]. $CD8^+$ T cells can also express FasL which can bind Fas on target cells to induce apoptosis [41]. Yet another effector mechanism employed by $CD8^+$ T cells is IFN-γ expression which causes further inflammation, remodeling the surrounding microenvironment, and can directly induce cell death [42–44]. Collectively, the coordination between innate and adaptive immunity leads to expansion of antigen specific T cells, causes them to home to the site of an infection or inflamed tumor site, and provides an adaptive immune response to clear antigen-expressing cells.

1.04 A subset of human tumors are infiltrated by $CD8^+$ T cells

A major subset of patients with cancer have high levels of $CD8^+$ T cells infiltrating their tumors, apparently reflecting an endogenous immune response [3,5,45]. This observation raises the question of why such tumors are not rejected spontaneously by the host immune response. Subsequent observations were made demonstrating that tumors with high levels of $CD8^+$ T cell infiltration also contain several immunosuppressive mechanisms that prevent the T cells from carrying out their effector functions [46]. These mechanisms include the presence of T regulatory cells and increased expression of inhibitory factors on tumor cells such as PD-L1. PD-L1 is a ligand which binds the PD-1 receptor on $CD8^+$ T cells. PD-1 signaling inhibits T cell effector function and drives them toward a dysfunctional state [47]. Therefore, while there may be $CD8^+$ T cells in the tumor microenvironment of many patients, with at least a subset of those $CD8^+$ T cells being specific for tumor antigens [48], such tumors are not rejected because these T cells are dysfunctional or suppressed. Checkpoint blockade antibodies against PD-L1/PD-1, and also

against a second inhibitory receptor CTLA-4, have been approved by the FDA for a wide range of cancer types [10].

However, most patients fail to respond to checkpoint blockade immunotherapy. Translational research studies trying to understand why this is the case began to look for predictive biomarkers for response to therapy. One key observation is that patients with high levels of pre-existing $CD8^+$ T cell infiltration into their tumor were more likely to respond with tumor shrinkage [11,13]. Treatment with anti-PD-1 results in an expansion of $CD8^+$ T cells within the tumor site as assessed by post-treatment biopsies. Together, these results suggest that anti-PD-1 therapy helps to improve the function of tumor-infiltrating $CD8^+$ T cells, and therefore patients that have already successfully primed and recruited effector T cells into the tumor microenvironment are more likely to respond. However, this paradigm raises the question as to how such T cells become primed and recruited in the first place. It was of interest to determine which innate immune pathways, as well as inflammatory cytokines and chemokines, are required upstream to generate the T cell-inflamed tumor microenvironment phenotype.

1.05 T cell priming and recruitment is promoted by type I interferon signaling

Type I IFNs had been evaluated as a cancer immunotherapy since the 1970s, long before the mechanism of action of these cytokines was understood [49]. Type I interferons can have direct anti-tumor effects by inhibiting proliferation and angiogenesis [25,43,50,51]. Type I interferons are also associated with the T cell-inflamed tumor phenotype. In human metastatic melanoma, genes expressed by T cells correlated with type I interferon-stimulated gene expression [52]. In mice deficient for the type I interferon receptor, IFNAR, there was a defect in tumor-specific $CD8^+$ T cell priming. Mixed bone-marrow chimeras demonstrated that IFNAR deficiency exclusively in the Batf3-lineage of DCs led to defective tumor-specific $CD8^+$ T cell priming. The Batf3 lineage

of DCs is known to be superior at cross presenting exogenous antigens on MHC I for cross-priming of tumor-specific $CD8^+$ T cells [53–55]. Therefore, it seems type I IFN signaling in the $Batf3^+$ DC subset is critical for inducing APC maturation and optimal priming of tumor-specific $CD8^+$ T cells [52,56]. During T cell priming, direct exposure of T cells to type I interferons are also beneficial because they can enhance T cell proliferation [57] and effector function [58,59]. Thus, type I interferons play an important role in priming the anti-tumor adaptive immune response.

Following activation and differentiation, effector T cells are recruited to inflamed peripheral tissues through a process dependent upon chemokines. CXCL9/10 is induced at high levels by type I IFN signaling through IFNAR [60]. In the context of cancer, CXCL9/10 is critical for recruiting $CD8^+$ T cells to the tumor microenvironment. In mice, CXCL9/10 is expressed by APCs in the tumor microenvironment and the receptor for CXCL9/10, CXCR3, is expressed on tumor infiltrating $CD8^+$ T cells [61]. Similarly, Batf3-deficiency in the hematopoietic compartment led to a loss of CXCL9/10 expression in the tumor microenvironment and ultimately loss of tumor-infiltrating T cells, arguing for a role for DCs in T cell recruitment and not just in T cell priming. Pre-activated T cells still failed to infiltrate the Batf3 DC-deficient tumors unless the tumors were injected with exogenous activated DCs. These data suggest $Batf3^+$ DCs sense type I interferons and express CXCL9/10 to recruit T cells into the tumor microenvironment independently of T cell priming [62].

Type I interferons therefore promote both priming and recruitment of $CD8^+$ T cells into the tumor microenvironment. Mechanistically, it seems that $Batf3^+$ DC maturation is induced by type I interferons which then stimulates $CD8^+$ T cell cross-priming. At the tumor site, type I interferon signaling on $Batf3^+$ DCs promotes chemokine expression to recruit effector $CD8^+$ T

cells to the tumor microenvironment. These observations make type I IFN signaling an important component of the dynamic and multi-step generation of an anti-tumor T cell response.

1.06 Tumors can induce type I interferon expression via activation of the STING pathway in host cells

It became of interest to determine the innate immune pathway(s) necessary for induction of type I IFN production by host APCs in the context of cancer. To identify the innate immune pathway activated by tumors, several different knockout mice lacking innate immune adaptors or receptors were tested for their ability to prime a tumor-specific $CD8^+$ T cell response. While most knockout mice retained normal T cell priming, mice lacking STING demonstrated a marked reduction in the induction of tumor antigen-specific $CD8^+$ T cells. This defect was identified based on IFN-γ ELISPOT analysis of splenocytes after tumor injection [63]. Mice deficient for STING also showed defective IFN-β gene expression by tumor infiltrating immune cells when compared to wildtype controls and showed faster tumor outgrowth. STING knockout mice also lacked accumulation of tumor-specific $CD8^+$ T cells in the tumor microenvironment. Therefore, upon implantation of tumors in vivo, the host STING pathway becomes activated in APCs, elicits a type I interferon response, promotes T cell priming, and this leads to $CD8^+$ T cell accumulation in the tumor microenvironment.

STING stands for the "STimulator of INterferon Genes" and was discovered in a screen for genes regulating type I interferon gene expression [64–66]. The STING pathway is activated by cytosolic DNA sensed by cyclic GMP-AMP (cGAMP) synthase (cGAS) [67]. After binding DNA, cGAS synthesizes a small molecule second messenger, cGAMP. cGAMP binds directly to STING in its homodimerization domain and causes an inhibitory domain to be displaced [68,69].

This causes STING to translocate from the endoplasmic reticulum through the golgi apparatus, and it ultimately ends up on perinuclear vesicles [64,70,71]. During this process, STING recruits the kinase TBK1 [72] and the transcription factor IRF3, which is phosphorylated by TBK1 [73]. More recent observations have indicated NF-κB can also be activated by STING activation including IKK-β phosphorylation, IκBα degradation, and phosphorylation of NF-κB RelA [64,74,75]. However, the molecular details and importance of this arm of STING signaling has not fully been established.

Based on the knowledge that the STING pathway is activated by implanted tumors, pharmacologic STING agonists were developed with the goal of deliberately activating the STING pathway as a potential therapeutic [76]. These agonists generally mimic cGAMP and are capable of directly stimulating STING itself. Mice injected with STING agonists intratumorally rejected B16 melanoma and other tumors. STING KO mice lacked any response indicating the effects were mediated through STING pathway signaling on host cells. STING agonist injection elicited high levels of type I interferon expression in the tumor microenvironment and IFNAR-deficient mice failed to reject tumors. The heightened levels of type I interferons led to an increased frequency of tumor antigen-specific $CD8^+$ T cells, and depletion of $CD8^+$ T cells eliminated a large proportion of the anti-tumor effect. Thus, STING agonists can promote tumor rejection in an IFNAR- and $CD8^+$ T cell-dependent manner.

1.07 IFN-β transcriptional initiation requires cooperation by several factors

Type I interferons were the first cytokines to be discovered in 1957 and are important for antiviral immunity as well as anti-tumor immunity [77]. Type I interferons, in general, include both IFN-α and IFN-β. There are 13 or 14 different IFN-α genes in humans and mice, respectively, but there is only 1 IFN-β gene in each species [78]. IFN-α expression tends to be primarily induced

via autocrine signaling through the type I interferon receptor IFNAR [79,80]. In this way, type I interferon expression typically has a biphasic expression pattern. Shortly after innate immune activation, IFN-β is expressed and stimulates autocrine IFNAR signaling. This autocrine signal promotes a second phase with higher expression of IFN-β and initiation of IFN-α expression. Aberrant expression of type I interferons can contribute to several diseases collectively termed "interferonopathies" including Aicardi-Goutières Syndrome and several Lupus-like diseases [81].

IFN-β gene expression is tightly regulated by a 50 bp promoter region approximately 100 bp upstream of the transcriptional start site [82]. The interferon promoter contains binding sites for several transcription factors including the p50/p65 NF-κB heterodimer [83], IRF3 or IRF7 [84,85], and AP-1 [86]. Activating each of these factors individually is insufficient to induce high level expression, and therefore optimal IFN-β gene expression appears to require the cooperative action of multiple transcription factors [87]. While the IFN-β promoter is epigenetically closed at baseline, there are 3 distant NF-κB binding sites that are epigenetically accessible and relatively nearby the IFN-β promoter based on chromatin conformation capture experiments. After activation, NF-κB can bind these sites very quickly and can bind the IFN-β promoter shortly after [88]. Shortly after NF-κB binding, other transcription factors, such as IRF3, can bind the IFN-β promoter [89]. The binding of these transcription factors is also assisted by HMGA1 which binds to DNA and induces a bend that promotes other transcription factor binding [83,90,91]. The effect of HMGA1 leads to interactions with several transcription factors and makes their collective binding cooperative. Together, these data argue that NF-κB signaling at early timepoints remodels the IFN-β promoter to allow itself and other transcription factors to bind to the promoter and the combined action of multiple transcription factors is required for IFN-β expression.

Once multiple transcription factors have bound the IFN-β promoter they then recruit several cofactors to induce transcription. This includes PCAF [92] which acetylates H4K8 and H3K9 sites of nearby histones [93]. While in vitro PCAF activity is not very specific, its activity at the IFN-β promoter is relatively more specific, likely due to combinatorial interactions with other factors. The histone modifications induced by PCAF promote further modifications including H3S10 phosphorylation and H3K14 acetylation. PCAF then releases from the IFN-β promoter and is replaced by CBP. CBP is cooperatively recruited by interacting with multiple transcription factors at the IFN-β promoter. Manipulation of the activation domains of the transcription factors or rearranging their binding sites to disrupt their continuous protein interface causes them to lose cooperative CBP recruitment and decreases IFN-β expression [94]. Once recruited, CBP helps recruit SWI/SNF and RNA polymerase II [95]. SWI/SNF along with TFIID and TBP then reposition the nucleosome blocking the IFN-β transcriptional start site to enable transcriptional initiation by RNA polymerase II [96,97]. Artificially repositioning nucleosomes to make the promoter region accessible allows for IFN-β expression at earlier timepoints and in response to individual transcription factors rather than requiring multiple transcription factors together [98].

1.08 Evidence supports suppression of tumor cell-intrinsic innate signaling

To date, studies of innate immunity in cancer have primarily focused on tumor-infiltrating immune cells rather than tumor cell-intrinsic signaling. For example, we know that STING signaling in tumor-infiltrating immune cells can induce IFN-β expression, and that type I interferon signaling on APCs is important for priming adaptive anti-tumor immunity [52,63]. When tumor cells are transduced to constitutively express IFN-β the tumors are spontaneously controlled [50]. In fact, injection of a mixture of tumor cells in which as few as 10% of the cells expressed IFN-β still led to tumor control. This indicates that IFN-β expression even by a small

subset of a tumor can lead to slowed growth of the whole tumor even if most cells don't express IFN-β. Mechanistically, tumor control was partially dependent on IFNAR signaling on both hematopoietic and endothelial cells. Tumor cell-intrinsic expression of high levels of type I interferon therefore has both immune-dependent and immune-independent anti-tumor effects.

Consistent with this notion, previous studies have found deletion of the IFN locus in some tumors [99]. In fact, more recent surveys of cancer genomic databases found homozygous deletion of the IFN locus in approximately 7% of patients. Highlighting its importance, the IFN locus represented 13% of all homozygous deletions across all tumor types and was the locus with the second-highest level of homozygous deletion. The deletion of the IFN-β locus also correlated with a worse prognosis and lack of response to checkpoint blockade immunotherapy. In this study, only 1 out of the 27 responders to checkpoint blocked had deletion of interferon genes. Intriguingly, this 1 responder with partial IFN locus deletion retained the IFN-β gene which is thought to initiate type I IFN signaling [100].

Therefore, it seems there may be selective pressure for tumor cells to adapt and delete the type I interferon locus. This observation, combined with the preclinical data showing tumor cells constitutively expressing IFN-β are spontaneously controlled, argues that type I interferon expression by tumor cells is deleterious for cancer growth. This notion raises the question as to whether other processes could lead to defective type I interferon production in cancer cells. The STING pathway is a major mechanism for type I interferon expression by tumor-infiltrating immune cells, and this pathway is broadly expressed by most cell types. Collectively, these ideas led us to study the mechanisms of defective STING pathway activation in cancer cells, with a focus on B16 melanoma cells for deeper study. Conceptually, understanding the precise

molecular aberrations responsible for loss of IFN-β production could lead to new strategies to reverse this process and perhaps improve immune-mediated tumor control therapeutically.

Chapter 2: Materials and Methods

2.01 Cell lines and cell culture

Unless otherwise stated, all cell lines were passaged in "Complete DMEM" that contains 10% fetal bovine serum, 100 U/mL Penicillin/Streptomycin (Fisher #15140122), and 1% Non-Essential Amino Acids in DMEM (Fisher #11140076). The TRAMP cell lines were passaged in DMEM high glucose (Fisher #12430054) with 5% fetal bovine serum, 5% Nu-Serum IV (Fisher #CB51004), 5 μg/mL human recombinant insulin, 25 U/mL Penicillin/Streptomycin (Fisher #15140122), and 10 nM R1881 (Sigma # R0908).

2.02 Primers

Primers are summarized in the tables below for both qRT-PCR and ChIP-qPCR.

Table 1. Mouse-Specific qRT-PCR Primers

Probe	Name	Sequence
Roche #9	mu GAPDH F9	agcttgtcatcaacgggaag
	mu GAPDH R9	tttgatgttagtggggtctcg

Table 1. Mouse-Specific qRT-PCR Primers, continued		
Roche #108	mu IFNb1 F108	ggaaagattgacgtgggaga
	mu IFNb1 R108	cctttgcaccctccagtaat
Roche #3	mu CXCL10 F	gctgccgtcattttctgc
	mu CXCL10 R	tctcactggcccgtcatc
Roche #1	mu Oas2 F	tgatcaagcactggtacaaaca
	mu Oas2 R	cctgctcccaggcataca
Roche #1	mu Trex1 F	tggacaagctctctctgtgc
	mu Trex1 R	agctcagctttgctcagacc
Roche #3	mu Ifit3 F	tgaactgctcagcccaca
	mu Ifit3 R	agagattcccggttgacctc
Roche #91	mu Trib1 F	cctgaagctcaggaagttcg
	mu Trib1 R	ccaggctttccagtctaagc
Roche #53	mu Icam1 F	gctaccatcaccgtgtattcg
	mu Icam1 R	aggtccttgcctacttgctg
Roche #76	mu Rgs1 F	tctgctagcccaaaggattc
	mu Rgs1 R	tgttttcacgtccattccaa
Roche #106	mu Ifih1 F106	cttgtcacgaacgagatagcc
	mu Ifih1 R106	ccaggacatacgtgctttca
Roche #71	mu Isg15 F	agtcgacccagtctctgactct
	mu Isg15 R	ccccagcatcttcaccttta
Roche #79	mu TNFa F79	ctgtagcccacgtcgtagc
	mu TNFa R79	ggttgtctttgagatccatgc
Roche #42	mu STING F	aacaccggtctaggaagcag
	mu STING R	catatttggagcggtgacct
Roche #13	mu TBK1 F	agaggaagtgtccaagtatcaagac
	mu TBK1 R	gaggctgcgagcattttc
Roche #17	mu IRF3 F	caagaggcttgtgatggtca
	mu IRF3 R	gcaagtccagggttttcagt
Roche #80	mu Blimp1 F	tgcggagaggctccacta
	mu Blimp1 R	tgggttgctttccgtttg
Roche #94	mu YY1 F	ctggagaaaagccctttcag
	mu YY1 R	gtcgaaggggcacacatag
Roche #108	muRpl13a F	atccctccaccctatgacaa
	muRpl13a R	gccccaggtaagcaaactt
Roche #46	muRpl19 F	ccacaagctctttcctttcg
	muRpl19 R	gcctcttctgtagcctgagc
Roche # 92	IkK-beta F (92)	ccggaaagtgtcagctgtatc
	IkK-beta R (92)	cctcagctggaagaaggaga

Table 1. Mouse-Specific qRT-PCR Primers, continued		
Roche # 47	p65 F (47)	cccagaccgcagtatccat
	p65 R (47)	gctccaggtctcgcttctt
Roche # 38	NFKBIA qPCR38 F	acgagcaaatggtgaaggag
	NFKBIA qPCR38 R	atgattgccaagtgcagga
Roche # 80	rtTA F (80)	cttttcggcctggaactaatc
	rtTA R (80)	gccgctttcgcactttag
Roche #6	IL6 F (6)	gctaccaaactggatataatcagga
	IL6 R (6)	ccaggtagctatggtactccagaa
Roche #38	IL1b F (38)	agttgacggaccccaaaag
	IL1b R (38)	agctggatgctctcatcagg
Roche #62	mu CCL2 F	catccacgtgttggctca
	mu CCL2 R	gatcatcttgctggtgaatgagt
Roche #89	mu CCL7 F	ttctgtgcctgctgctcata
	mu CCL7 R	ttgacatagcagcatgtggat
Roche #12	mu RNaseh1 F	cactcagggcatggacatc
	mu RNaseh1 R	gctcctctgctcagtcctca
Roche #81	mu Dnase IIa F	agtgccacagaggaccactc
	mu Dnase IIa R	ttcctattcatgtcacccacac

Table 2. Human-Specific qRT-PCR Primers

Probe	Name	Sequence
Roche #25	hu IFNb1 F	cgacactgttcgtgttgtca
	hu IFNb1 R	gaagcacaacaggagagcaa
Roche #34	hu CXCL10 F	gaaagcagttagcaaggaaaggt
	hu CXCL10 R	gacatatactccatgtagggaagtga
Roche #3	hu GAPDH F	gcacaagaggaagagagagacc
	hu GAPDH R	aggggagattcagtgtggtg
Roche #36	hu Ifih1 F	aggcaccatgggaagtgat
	hu Ifih1 R	ggtaaggcctgagctggag
Roche #23	hu Isg15-F	gcgaactcatctttgccagta
	hu Isg15-R	ccagcatcttcaccgtcag
Roche #79	hu TNFa-F	agcccatgttgtagcaaacc
	hu TNFa-R	tctcagctccacgccatt
Roche #57	hu IRF3 F	aaggaaggaggcgtgtttg
	hu IRF3 R	ccttccgtgaaggtaatcaga
Roche #72	hu TBK1 F	tgttttgcgagatgtggtg
	hu TBK1 R	cttcccctataacacgcatga

Table 2. Human-Specific qRT-PCR Primers, continued		
Roche #1	hu STING F	gatatctgcggctgatcctg
	hu STING R	gcaggttgttgtaatgctgatt
Roche #66	hu cGAS F	gaccacctgctgctcagact
	hu cGAS R	tcaaattcattaggtgcagaaatc
Roche #40	hu IL6 F 40	gatgagtacaaaagtcctgatcca
	hu IL6 R 40	ctgcagccactggttctgt
Roche #48	hu ICAM1 F 48	gaagtggtgggggagacata
	hu ICAM1 R 48	cccaataggcagcaagtttc

Table 3. Mouse-Specific ChIP-qPCR Primers

Name	Sequence
muIRF3_bind_Ifn1b F	gctccagctccaagaaagga
muIRF3_bind_Ifn1b R	gatcttgaagtccgccctgt
muIRF3_bind_Ifih1 F	gaggctacttggtacctgcg
muIRF3_bind_Ifih1 R	aggtggcagtgaatgtgtcc
muIRF3_bind_Isg15 F	gcccagctacaatagggtcttaat
muIRF3_bind_Isg15 R	atcagaattgcccaaagacaactg

Table 4. Human-Specific ChIP-qPCR

Name	Sequence
huIRF3_bind_Ifnb1 F	tcctctgaatagagagaggacca
huIRF3_bind_Ifnb1 R	cagagcaaaggcttcgaaagg
huIRF3_bind_Cxcl10 F	aagaaacagttcatgttttggaaag
huIRF3_bind_Cxcl10 R	tgtagcctccaagttacgga

2.03 Quantitative real-time PCR

Total RNA was extracted from 0.5-2 million cells using the RNeasy Micro Kit (Qiagen) substituted with EconoSpin® All-in-one silica membrane mini spin columns (Epoch Life Science) using Qiagen's buffers and following Qiagen's protocol. The concentration of RNA was measured by nanodrop and 1.5 µg total RNA was treated with DNase I (Sigma # 4716728001) according to the manufacturer's protocol. cDNA was synthesized from the purified RNA with a high-capacity reverse transcriptase (Fisher # 4368814) according to the

manufacturer's protocol. This cDNA was then resuspended to a final volume of 200 µL and 5 µL used for qRT-PCR with a final volume of 25 µL. All mRNA quantification was performed using the Taqman gene expression master mix (Fisher # 4369514) and all ChIP DNA quantification was performed using the SYBR green PCR master mix (Fisher # 4309155) on a StepOne Plus real-time PCR system (Applied Biosystems # 4376600).

2.04 *In vitro* stimulation assays

Cells were grown in tissue-culture treated 6 well plates seeded with 0.5-1 million cells. Then next day cells were treated with various conditions depending on the experiment.

For direct STING activation of murine cell lines by DMXAA, cells were treated with complete DMEM containing DMXAA at various concentrations (typically 50 µg/mL) for various amounts of time (typically 2h for RNA isolation or 8h for ELISA).

For stimulation of murine and human cell lines by agonists unable to spontaneously cross the plasma membrane (DNA, cGAMP, or GpAp), 30 µL lipofectamine 2000 was mixed in Opti-MEM media to a final volume of 1 mL and left at room temperature for 5 min. In parallel, 1 mL of agonist solution was mixed in Opti-MEM and subsequently added to the lipofectamine solution. This mixture was then added to cells growing in antibiotic-free media with 1/3 volume agonist added to 2/3 volume media. The final concentrations varied by experiment and agonist but was typically 5 ng/uL DNA or 150 µg/mL cGAMP/GpAp.

For treatment with the epigenetic modulating drugs (Aza, AzaD, TSA, mocetinostat, TMP269) and cycloheximide, a high-concentration stock was initially prepared in DMSO. This was then diluted to prepare a 1000x stock in water which was diluted to 1X in complete DMEM to treat cells. The final concentration of each drug was 5µM Aza, 0.2 µM AzaD, 10 µM TSA, 10

μM mocetinostat, 10 μM TMP269, and 10 μg/mL cycloheximide. Cells were grown in each drug for 24, 48, or 72 hours depending on the experiment but most commonly 24 hours.

2.05 SDS-PAGE and Western blotting

Cells were washed with PBS and resuspended in triton lysis buffer (50 mM Tris-Cl pH 8.0, 150 mM NaCl, 1% v/v Triton-X) at a final concentration of 10 million cells per 1 mL lysis buffer. The protein concentration was measured using the Biorad DC Protein Assay (#5000112) according to the manufacturer's protocol. 20 μg of protein was loaded on a 10% SDS-PAGE gel and run for 30 min at 60V then 1.5 hours at 100V. The gel was transferred to a PVDF membrane and blotted with various primary antibodies (see table) and the LI-COR IRDye secondary antibodies. Blots were visualized using a LI-COR Odyssey® Fc Imaging System.

Table 5. Western Blot Antibodies

Antigen	MW (kDa)	Vendor	Catalog #	Specificity	Isotype
β-Actin	42	Cell Signaling	490	Hu, Mu	Rabbit
GAPDH	35	Cell Signaling	2118	Hu, Mu	Rabbit
IκBα	39	Cell Signaling	4812	Hu, Mu	Rabbit
IKKβ	87	Cell Signaling	2684	Hu, Mu	Rabbit
IRF3	45	Cell Signaling	4302	Hu, Mu	Rabbit
phospho-IKKα/β	85, 87	Cell Signaling	2697	Hu, Mu	Rabbit
phospho-IRF3	45,55	Cell Signaling	4947	Hu, Mu	Rabbit
phospho-TBK1	84	Cell Signaling	5483	Hu, Mu	Rabbit
STING	33, 35	Cell Signaling	3337	Hu, Mu	Rabbit
TBK1	80	Cell Signaling	3504	Hu, Mu	Rabbit
p65	65	Cell Signaling	8242	Hu, Mu	Rabbit
phospho-p65	65	Cell Signaling	3033	Hu, Mu	Rabbit
cGAS	62	Cell Signaling	31659	Murine	Rabbit
cGAS	62	Cell Signaling	15102	Human	Rabbit

2.06 Immunofluorescent Imaging Flow Cytometry

A minimum of 2 million cells per sample were washed with PBS and resuspended in the fixation/permeabilization buffer from the eBioscience Foxp3 transcription factor staining buffer set (Fisher # 00-5523-00). Intracellular staining was then performed for various antigens using the same primary antibodies used for Western Blotting. Secondary staining was performed using goat anti-rabbit secondary antibodies conjugated to APC. Finally, samples were stained with 2 drops per mL DAPI (Akoya #FP1490) in permeabilization buffer for 5 min at room temperature and washed twice with PBS. Sample images were acquired on an Amnis ImageStreamX and analyzed using the IDEAS application according to the manufacturer's guidelines. In particular, nuclear translocation was quantified using the "Nuclear Localization" guided analysis algorithm.

2.07 Chromatin-immunoprecipitation assay

A minimum of 10 million cells were resuspended in 4 mL media and 250 µL of 37% formaldehyde added. To cross-link, samples were incubated 15 minutes at room temperature with gently rocking then cross-linking was stopped by the addition of 125 mM glycine final concentration. Cells were spun down, rinsed with PBS, and lysed with 0.8M RIPA buffer (10 mM Tris-Cl pH 7.4, 1 mM EDTA, 1% Triton X-100, 0.1% Sodium Deoxycholate, 0.8 M NaCl, 0.1% SDS) with protease inhibitors (Fisher # 78429). 10 million cells were lysed in 200 µL of lysis buffer at 4oC for 10 minutes then sonicated to shear the DNA for 10 minutes with a pulse setting of 30 second on / 15 seconds off. The chromatin was cleared of cell debris by centrifuging 10 minutes at 21,000 xg at 4oC and the supernatant kept going forward. "Input" samples were set aside and the remaining sample split in half. Each half received either target-specific antibodies or isotype control antibodies and left rocking overnight at 4oC. The next day, protein G agarose beads (Roche # 11719416001) were blocked then added to the mixture and left to rock overnight at 4oC. Finally, the beads were spun down, rinsed with excess 0.5 M RIPA

twice, then eluted using ChIP elution buffer (2% SDS, 20 mM Tris-Cl pH 6.8). Eluted samples were de-crosslinked using RNase and proteinase treatment. The relative abundance of different promoter regions was measured by RT-PCR comparing the immunoprecipitated samples to the isotype and input controls.

2.08 Assay for transposase accessible chromatin

After harvesting cells, 100,000 cells were washed with PBS and resuspended in 50 µL of cold ATAC lysis buffer (10 mM Tris-Cl pH 7.4, 10 mM NaCl, 3 mM MgCl2, 0.1% IGEPAL CA-630). This was spun down immediately and the transposition reaction performed using the Nextera DNA flex library prep kit (Illumina # 20018704). This was done according to the manufacturer's guidelines and purified using the Qiagen MinElute Kit (Qiagen # 28004). The transposed DNA fragments were then amplified using the Nextera PCR Primers 1 & 2 for 12 cycles before purification by the Qiagen PCR purification kit (Qiagen # 28104). These samples were then submitted for sequencing and the resulting data aligned to the genome to plot the relative accessibility of various sites throughout the genome.

2.09 Heterokaryon formation

Autoclaved PEG 1500 was mixed with complete DMEM to 50% w/v final concentration and the pH adjusted to 7.0-7.4 with HCl. Harvested cells were mixed in a 1:1 ratio in 5 mL serum-free media. They were spun, washed in 1 mL serum-free media for 10 min at room temperature, and spun again. To fuse the cells, they were resuspended in 1 mL 50% PEG within 30 seconds and incubated 2 min at room temperature. Then 10 mL serum-free media was slowly added and samples incubated 30 min at room temperature. The cells were finally washed twice with 50 mL serum-free media and resuspended in 100 mL complete media. They were incubated

1 hour at 37°C in a smaller flask before transfer to a larger flask overnight. Then next day, the fused cells were purified by FACS. A few days after the initial sort the cells were re-sorted to ensure only stably double-positive cells remained for further analysis.

2.10 Whole-genome CRIPSR gRNA screen

B16 tumor cells stably expressing WT cas9 were generated using an adenoviral vector (ABM #K004) and selected using blasticidin. An NF-κB-GFP reporter was stably integrated into B16-cas9 cells using the pGreenFire 2.0 lentivector (System Biosciences # TR412PA-P) and selected with puromycin. Once reporter activity was validated, a pooled whole-genome CRISPR gRNA library was used to transduce the B16-cas9-NF-κB-GFP cells. To generate the whole-genome CRISPR library, 6 million HEK293T cells were seeded on a 10cm dish and transduced using 1 mL Opti-MEM containing 30 µL lipofectamine 3000, 30 µL p3000 reagent, 5 µg pooled gRNA library, 5 µg psPAX2 (Addgene), and 2.5 µgpMD2.G (Addgene). The lipofectamine and p3000/DNA mixtures were prepared separately and combined before adding to the cells. 48 hours later the virus-containing supernatant was filtered through a 0.45 um filter and diluted 1:2 with antibiotics-free media. The virus-containing media was then added to 60 million B16-cas9-NF-κB-GFP cells. To select cells transduced with the CRISPR library, 48 hours later the BFP+ cells were purified by FACS with an efficiency below 30% to avoid multiple gRNA insertions. These cells were passaged an additional 5 days to allow for complete knock-out of target genes and then stimulated 16 hours with DMXAA. The activated cells were then sorted into 4 separate populations with varying levels of NF-κB reporter activity. The cells with the highest reporter activity that were successfully expanded after sorting were then lysed and their gRNA sequences amplified from gDNA with forward (cgggccctacgcgttactcg) and reverse (attggatccaaaaaaagcaccgactcg) PCR primers. The PCR product was then double digested with

ApaI and BamHI, ligated into the pKLV vector (Addgene # 62348), and recombinant plasmids introduced into Stbl3 cells. Plasmids purified from single clones were then sequenced to look for enrichment of particular gRNAs.

2.11 Targeted CRISPR gRNA knockouts

gRNA sequences were designed using the atum.bio CRISPR gRNA design tool (https://www.atum.bio/eCommerce/cas9/input) using an NGG PAM sequence and designed for WT cas9. To clone the gRNA into the pKLV vector (Addgene # 62348), I designed a pair of partially overlapping anti-sense oligonucleotides that, once annealed, would contain an overhang compatible for ligation into pKLV. For example, the gRNA targeting Ubxn1 was made using top (caccgCTCCCTTACGCGCGTCCCCTgt) and bottom (taaaacAGGGGACGCGCGTAAGGGAGc) oligonucleotides where the gRNA sequence is capitalized. I mixed the top and bottom oligonucleotides together in a 1:1 ratio, placed them in a boiling water bath, turned the bath off, and allowed them to cool overnight to anneal. The next day, I ligated the resulting dsDNA into the Bbsi-digested pKLV vector after which the recombinant plasmids were introduced into Stbl3 cells. Plasmids purified from individual colonies were then sequenced to verify proper gRNA insertion. These single gRNA vectors were then packaged using HEK293T cells and transduced into B16 tumor cells according to the same packaging protocol used for the whole-genome CRISPR screen.

2.12 Whole-genome sequencing & somatic variant calling

Tumor cells were expanded until a minimum of 100,000 cells were ready for analysis. The cells were lysed and genomic DNA purified according to the manufacturers protocol using the Qiagen Blood and Cell Culture DNA Kit (Qiagen #13323). This genomic DNA was then

submitted for whole genome sequencing at the University of Chicago core facility. The resulting sequences were processed using the GDC's "DNA-Seq Analysis Pipeline" including the optimizations for somatic variant calling in cancer. Briefly, sequences were aligned with BWA, processed with Picard tools, and variants identified with the HaplotypeCaller. The resulting list of variant bases were then processed with SnpEff to identify which variants caused changes in amino acid composition of genes. This list of variant genes was then annotated with the human-curated uniport database of annotations and filtered for key terms including "NF-kB" to identify genes functionally associated with NF-κB function.

Chapter 3: Results

3.01 Of the cell types in the B16 melanoma tumor microenvironment, only tumor cells fail to express IFN-β following STING agonist treatment

Prior studies have established type I interferons as important anti-tumor cytokines capable of promoting tumor-specific T cell priming and generation of a T-cell infiltrated tumor microenvironment. The STING pathway is the major innate immune pathway activated by endogenous tumors to elicit IFN-β expression, and previous work has shown that intratumoral injection of STING agonists directly into the tumor microenvironment can promote tumor rejection [63,76]. To gain deeper mechanistic insight into this effect, we investigated which cell types could respond to STING agonists and produce IFN-β. We measured IFN-β gene expression by qRT-PCR following STING pathway activation in several cell types present in the tumor microenvironment (Figure 3.1). We treated each cell type with DMXAA, a synthetic STING agonist that directly binds STING to initiate STING pathway signaling. We found the highest expression of IFN-β within the BMDC population, but every cell type responded with IFN-β expression. This is consistent with the expression of the components of the STING pathway in a

broad range of cell types. However, the B16 melanoma tumor cells themselves failed to express IFN-β. Previous studies have shown that transfection of B16 tumor cells to force IFN-β expression driven by a constitutive promoter led to spontaneous tumor control upon implantation in vivo [50]. Thus, if tumor cells could produce their own IFN-β they would be predicted not to grow. These observations suggested the notion that tumor cells may be selected to lose tumor cell-intrinsic STING signaling and IFN-β expression, as a component of oncogenesis.

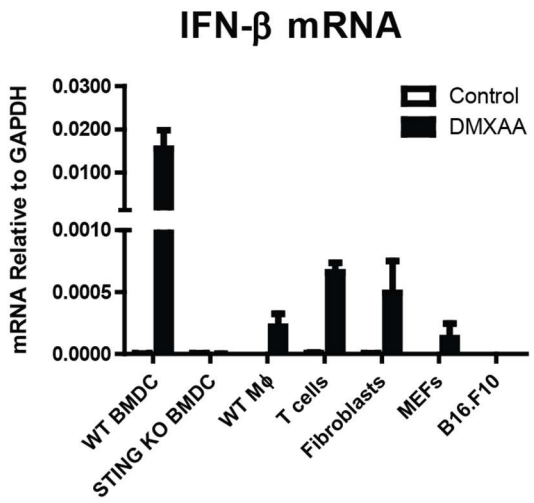

Figure 3.1 Tumor cells fail to produce IFN-β after STING pathway activation in contrast to all other cell types in the tumor microenvironment that express IFN-β.
Several different cell types present in the tumor microenvironment were stimulated with 50 μg/mL DMXAA for 2 hours then IFN-β mRNA measured by qRT-PCR.

3.02 The vast majority of tumor cell lines fail to express IFN-β after STING pathway activation

We wondered whether the lack of IFN-β expression in B16 tumor cells was unique to that cell line or whether it was true of tumor cells more generally. We thus stimulated a broad range of both mouse (Figure 3.AB) and human (Figure 3.CD) tumor cell lines with either the STING agonist DMXAA or DNA + lipofectamine, which activates the STING pathway via cGAS.

These cell lines were selected based on the fact that they represent several tumor cell types in order to avoid any biases that may be introduced by only studying a single tumor subtype. We found that the majority of tumor cell lines failed to express IFN-β in response to both DNA and DMXAA, with the only exception being the TRAMP prostate cancer cell line. TRAMP cells are known to grow slowly both in vitro and in vivo, making it possible that tumor-intrinsic IFN-β expression may partially explain this phenotype. Based on the fact that most of the tumor cells failed to express IFN-β, it was of interest to investigate the molecular mechanism responsible for their lack of IFN-β expression in cancer. In particular, we focused on B16 melanoma cells, as the immunobiology of this tumor model has been investigated in detail. We speculated that by understanding this molecular mechanism we might be able to reverse the phenotype to enable tumor-intrinsic STING signaling and IFN-β expression, which could point in the direction of a new innate immunotherapeutic strategy.

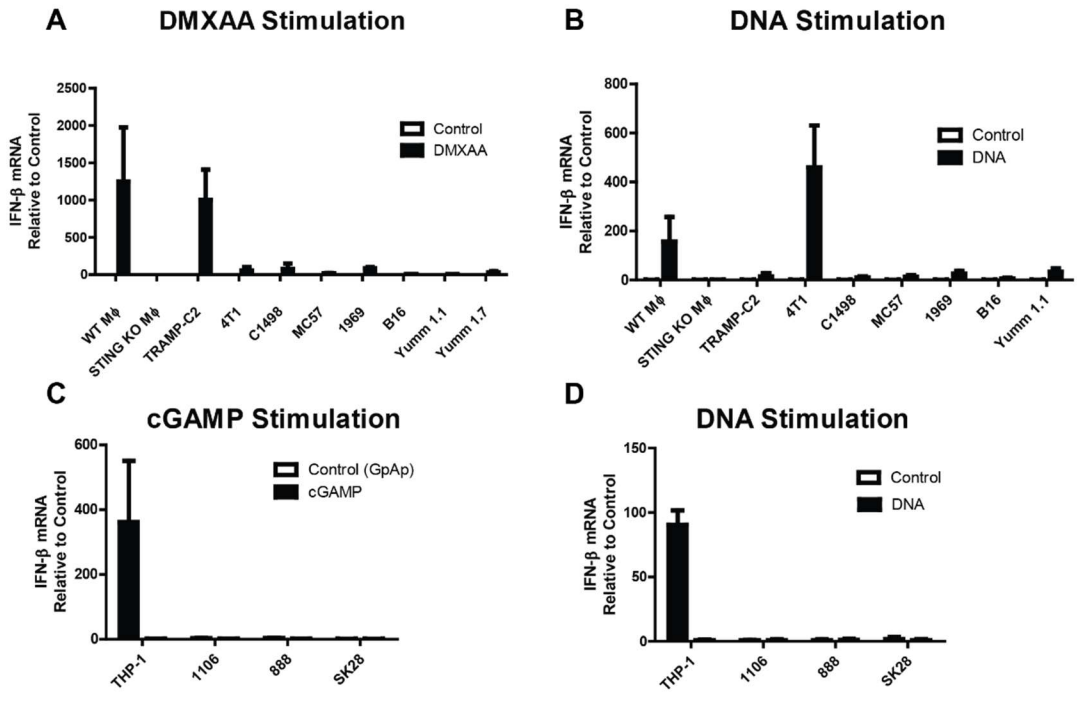

Figure 3.2 Similar to B16 tumor cells, most tumor cells fail to express IFN-β in response to STING pathway activation.

Figure 3.2, continued.
(AB) Various mouse tumor cell lines or Mϕ controls were stimulated with 50 μg/mL DMXAA or 1 μg/mL DNA with lipofectamine. After 2 hours (A) or 4 hours (B) the cells were lysed and IFN-β mRNA measured by qRT-PCR. (CD) Various human tumor cell lines with stimulated with cGAMP or DNA with lipofectamine for 4 hours (C) or 8 hours (D) and IFN-β mRNA measured by qRT-PCR.

3.03 Tumor cells fail to express IFN-β after STING agonist treatment across a broad range of doses and durations

The STING pathway involves several biochemical signal transduction events which occur over a period of several hours. We wondered whether there might be differences in the kinetics of STING signaling and whether tumor cells might simply be expressing IFN-β at later timepoints than we initially tested. We therefore performed a time course experiment stimulating both B16 tumor cells and an immortalized bone marrow-derived macrophage (BMDM) cell line with DMXAA for up to 8 hours (Figure 3.3A). Based on qRT-PCR we found that Mϕ control cells expressed peak levels of IFN-β mRNA at 2 hours after treatment. By 8 hours Mϕ lacked detectable IFN-β mRNA, likely due to feedback inhibition of IFN-β expression. Consistent with our initial observations, we found B16 tumor cells did not express IFN-β at any timepoint. We also measured IFN-β protein levels by ELISA and found that Mϕ produced high levels of IFN-β that accumulated up to 8 hours, which was consistent with our observations at the mRNA level. We found that B16 tumor cells did not produce detectable IFN-β protein at any timepoint (Figure 3.3B). These results are consistent with our initial conclusion that B16 tumor cells fail to produce IFN-β and do not simply exhibit delayed kinetics.

We also wondered whether tumor cells might differ in STING pathway sensitivity compared to Mϕ and so we stimulated them with a broad range of STING agonist

concentrations. We found detectable IFN-β expression from Mϕ as low as 5 μg/mL DMXAA, which is 10x less than we typically use for stimulation. On the other hand, we found that B16 tumor cells failed to express IFN-β in response to any concentration of DMXAA (Figure 3.3B). Collectively, these results argue that B16 tumor cells are qualitatively rather than quantitatively different than macrophages with respect to STING pathway signaling.

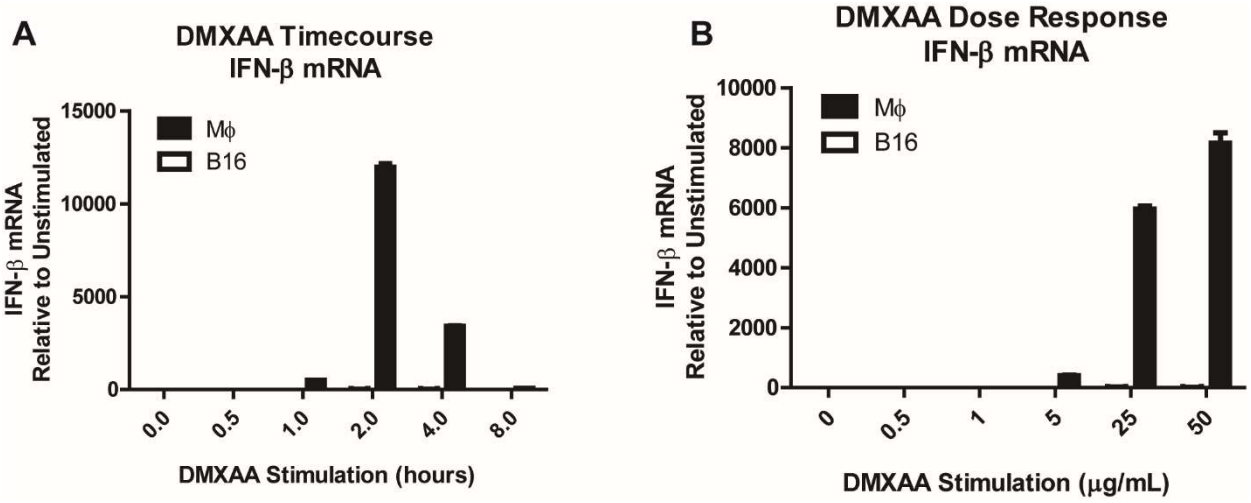

Figure 3.3 Tumor cells fail to express IFN-β in response to STING pathway activation regardless of agonist dose or duration.
(A) B16 tumor cells or Mϕ controls were stimulated with 50 μg/mL DMXAA for various amounts of time. (B) B16 tumor cells or Mϕ controls were stimulated for 2 hours with various concentrations of DMXAA. IFN-β mRNA was then measured by qRT-PCR.

3.04 B16 tumor cells retain expression of the components of the STING pathway

Previous studies have found epigenetic repression of cGAS and STING expression can reduce their expression in tumor cells [101–103]. This phenomenon has been suggested as a mechanism to prevent STING signaling in the context of cancer. Therefore, we measured expression of the components of the STING pathway in B16 tumor cells. Under basal conditions, mRNA levels for cGAS, STING, TBK1 and IRF3 were determined. We found all of these factors were modestly reduced in B16 tumor cells compared to Mϕ. Protein and mRNA levels

don’t always correlate though and there can be as high as 50% discordance [104,105]. To measure protein accumulation, we performed Western blot analysis for each of these factors. We found at the protein level only cGAS was reduced in B16 tumor cells to approximately 50% of the level found in Mϕ.

Some groups have proposed decreased expression of cGAS and STING themselves might be used as a clinical biomarker and may even help predict response to STING agonist therapy. We analyzed multiple cell lines shown in Figure 3. in parallel and plotted the level of expression of both cGAS and STING protein versus mRNA levels. Similar to the results for B16, we found that cGAS mRNA and protein levels correlate quite well across several different cells lines. STING, on the other hand, demonstrated discordance between mRNA and protein levels suggesting STING levels might be additionally regulated at the post-translational level. This observation is consistent with the wide array of regulatory mechanisms governing STING protein stability [71,106–111].

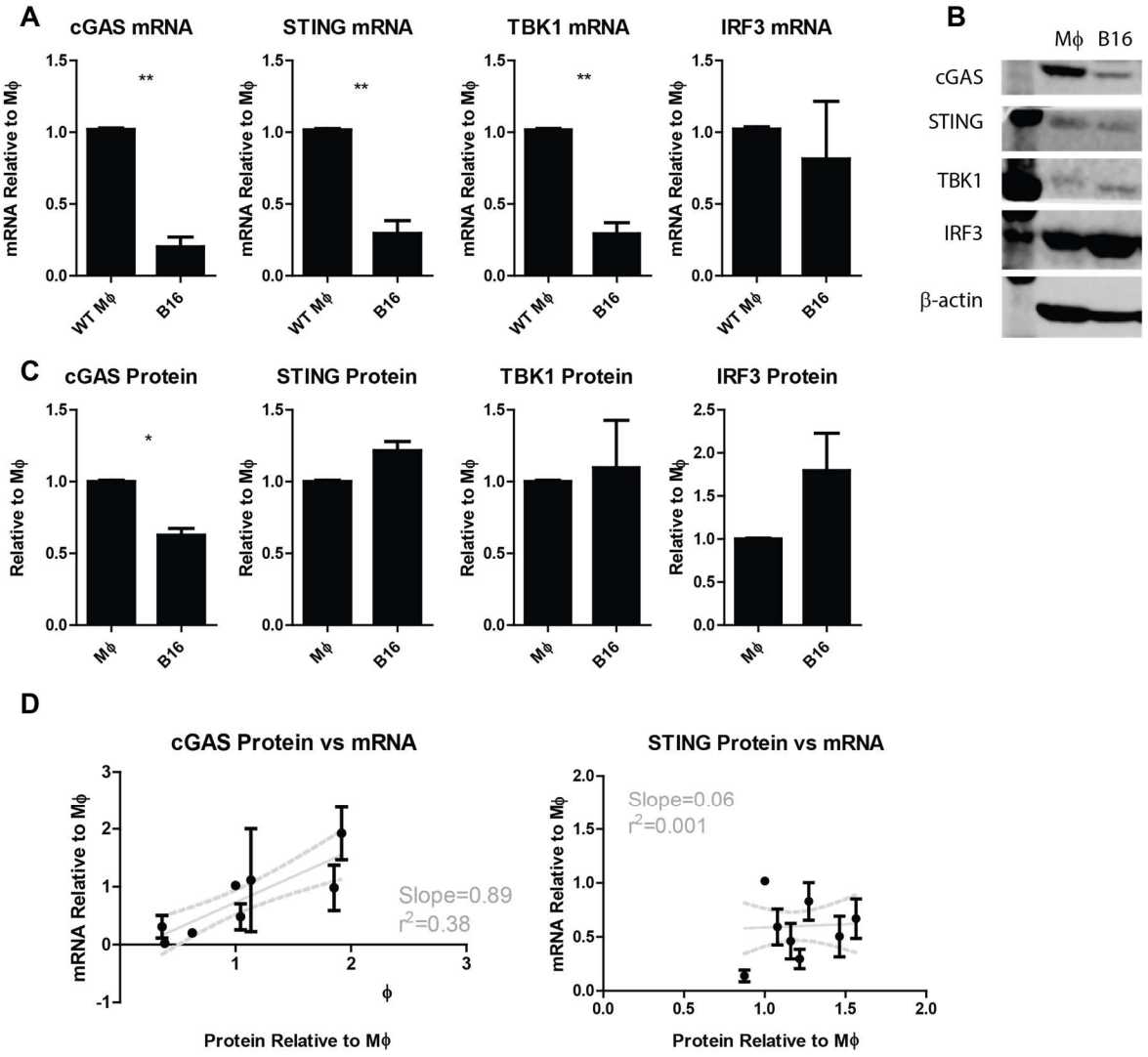

Figure 3.4 Components of the STING pathway are still expressed in tumor cells.
(A) The relative expression of each component of the STING pathway was measured under basal conditions by qRT-PCR (B) An example western blot of B16 tumor cells and Mϕ controls for various components of the STING pathway. (C) Quantification of the Western Blots like shown in B. (D) A correlation plot of the relative expression levels of cGAS and STING for mRNA and protein.

3.05 STING signaling induces phosphorylation of TBK1 and IRF3 in B16 tumor cells

To determine whether the partial reduction in cGAS and STING expression was functionally relevant, we stimulated B16 cells with the STING agonist DMXAA and assessed phosphorylation of TBK1 and IRF3 by Western blot analysis. Even though B16 cells failed to express IFN-β, both TBK1 and IRF3 were phosphorylated in response to DMXAA (Figure 3.5A). When we quantified the Western blot signals, we found that both TBK1 and IRF3 were phosphorylated at quantitatively similar levels in B16 tumor cells compared to Mϕ (Figure 3.5BC). This indicates that the defective STING pathway signaling must lie downstream from phosphorylation of IRF3.

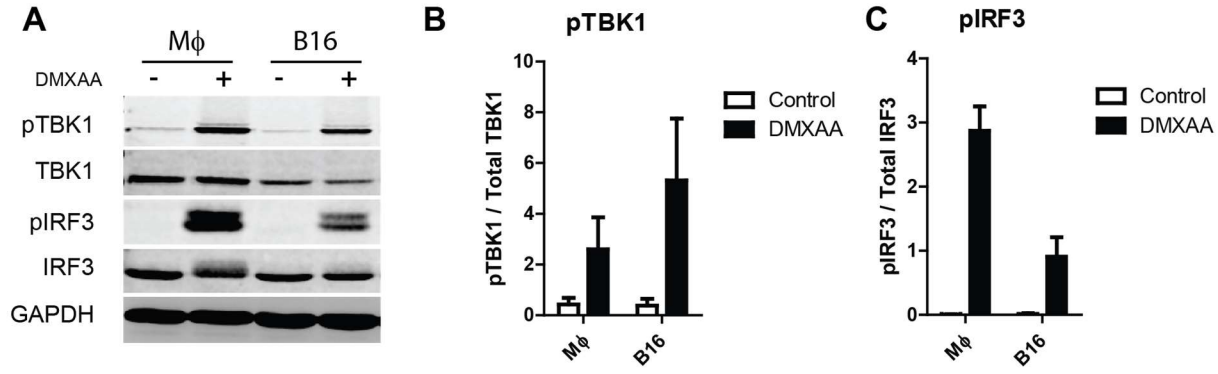

Figure 3.5 STING pathway activation induces phosphorylation of both IRF3 and TBK1 in B16 tumor cells.
(A) A Western Blot for both phosphorylated and non-phosphorylated IRF3 and TBK1. (B) Quantification of blots shown in A.

3.06 STING pathway activation causes nuclear translocation of IRF3 in tumor cells

Following phosphorylation, IRF3 forms a dimer and translocates to the nucleus [70,74,112]. To measure IRF3 nuclear translocation, we stimulated cells with DMXAA and performed intracellular staining for IRF3 as well as DNA using DAPI. We then imaged the cells using Amnis ImageStreamX which is a form of immunofluorescent flow cytometry. Visually, we found that IRF3 translocates to the nucleus of both B16 tumor cells and Mϕ controls. To

quantitatively measure the degree of IRF3 nuclear translocation we measured the overlap in IRF3 vs DNA staining and calculated a similarity index in which a higher value means more nuclear translocation. We found that B16 tumor cells retained IRF3 nuclear translocation, as shown in Figure 3.6A with a histogram representing the distribution of several thousand cells. We further found that the magnitude of nuclear translocation in B16 tumor cells was quantitatively similar to that seen in Mϕ on a per-cell basis (Figure 3.6B) or the percent of cells with nuclear translocation (Figure 3.6C). These results indicate that not only is IRF3 phosphorylated in B16 tumor cells that fail to express IFN-β, but that tumor cells also retain IRF3 nuclear translocation.

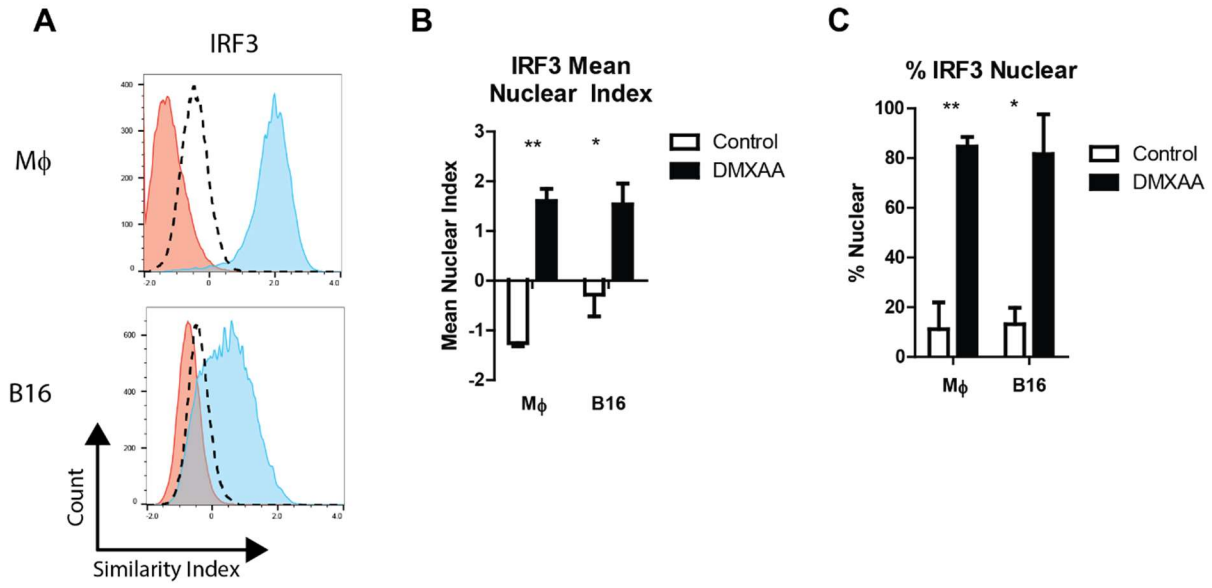

Figure 3.6 ImageStreamX analysis demonstrates IRF3 nuclear translocation in B16 tumor cells.
(A) Quantification in the correlation between the DAPI nuclear stain and IRF3 staining for B16 tumor cells and Mϕ controls. Quantification of the average nuclear index score (B) or percent of cells with nuclear IRF3 (C) across multiple replicates.

3.07 IRF3 fails to bind the IFN-β promoter in B16 tumor cells yet binds to other promoter regions

The IFN-β locus and the regulation of its expression have been carefully studied. Both in vivo and in vitro analyses have carefully mapped binding sites of IRF3 and other transcription factors, and have determined which accessory proteins are necessary for inducing IFN-β gene transcription. IRF3 is known to bind to a particular region approximately 100 bp upstream of the IFN-β gene [82]. To measure IRF3 binding to this locus, we performed a chromatin immunoprecipitation (ChIP) assay. Cells were stimulated with DMXAA to induce STING signaling, and proteins were crosslinked. After immunoprecipitation of IRF3 and purifying the associated DNA, we analyzed binding by qPCR with primers specific to various sites in the genome. We found that in B16 tumor cells, despite IRF3 nuclear translocation, there was no detectable binding of IRF3 to the IFN-β promoter. This was in contrast to Mϕ which demonstrated IRF3 binding to the IFN-β promoter in response to STING activation (Figure 3.7A). This observation finally explains why B16 tumor cells fail to express IFN-β. Thus, in B16 tumor cells following STING pathway activation, IRF3 is phosphorylated and translocates to the nucleus, but it fails to bind the IFN-β promoter and therefore fails to elicit IFN-β transcription.

One hypothesis for failed IRF3 binding was deletion or mutation of the IFN gene locus. However, we sequenced genomic DNA and did not detect any mutations within a 5kb region upstream and a 3kb region downstream of the IFN-β gene (Figure 3.7B). In order to determine whether IRF3 itself was functionally intact, we evaluated the ability of IRF3 to bind to other gene promoters. We found in B16 tumor cells that IRF3 bound the promoters of Ifih1 and CXCL10 to a similar level as seen in Mϕ control cells (Figure 3.7). Taken together, these data

indicate that IRF3 can translocate to the nucleus of B16 cells and bind to DNA, but that it selectively does not bind the IFN-β gene locus.

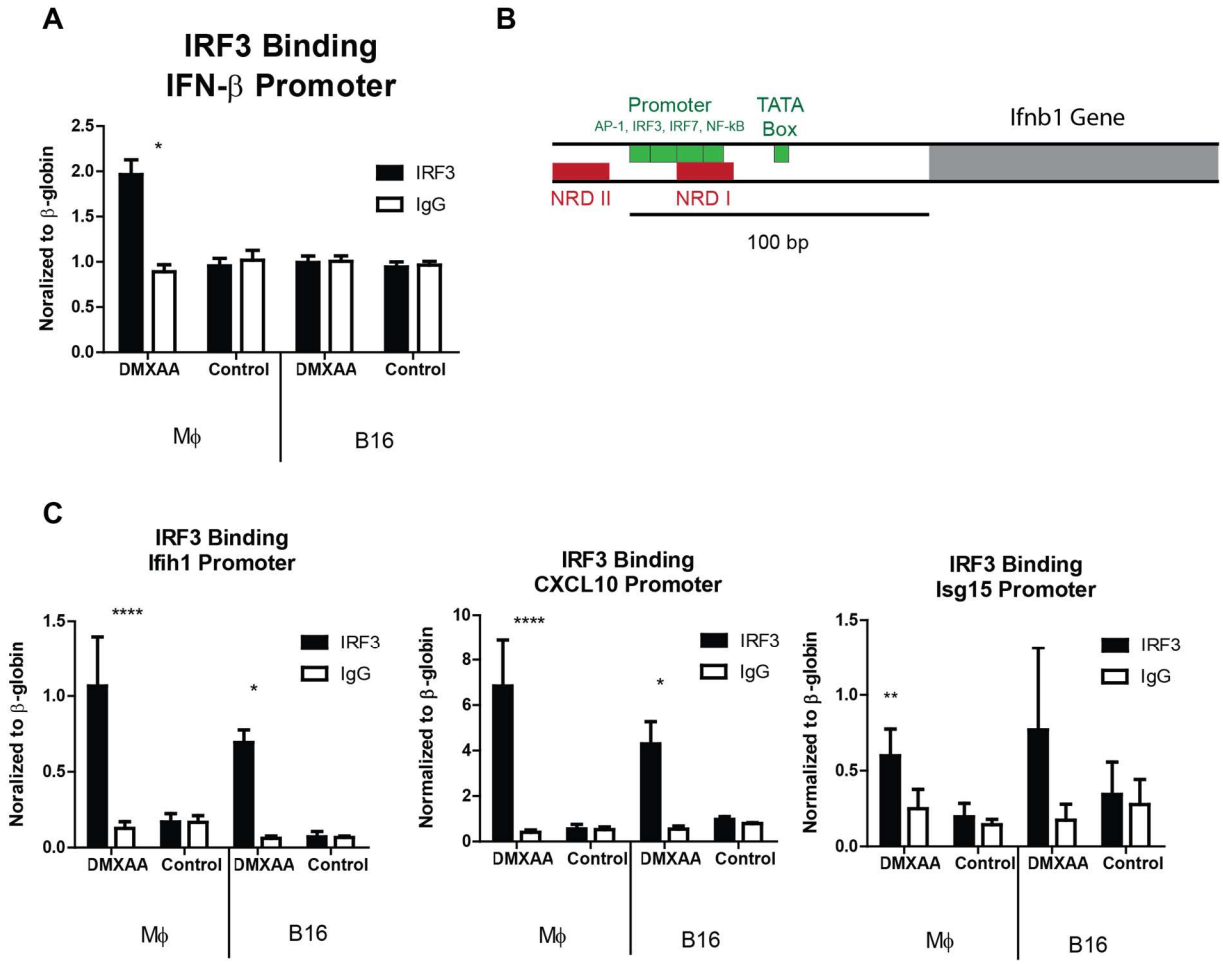

Figure 3.7 IRF3 fails to bind the IFN-β locus but still binds other gene promoters in tumor cells.
(A) Tumor cells or Mϕ controls were stimulated with DMXAA for 2 hours. A ChIP assay was performed for IRF3 and the resulting DNA analyzed by qPCR for enrichment of the IFN-β promoter. (B) A schematic of the binding sites for positive signaling factors (green) and the "negative regulatory domains" (red). Sequencing of this region found no mutations. (C) The same ChIP samples as (A) were analyzed by qPCR for IRF3 binding to other gene promoters.

3.08 STING pathway activation in B16 tumor cells induces transcription of other IRF3 target genes besides IFN-β with similar sensitivity and kinetics to Mϕ control cells

Because we observed IRF3 binding to other gene loci besides IFN-β, we measured expression of those genes to determine whether IRF3 function was intact. Indeed, following stimulation with DMXAA, we found that B16 tumor cells expressed the IRF3 target genes Ifih1, ISG15, and CXCL10.

Time course and dose-response experiments revealed that ISG15 gene expression was similar between B16 tumor cells and Mϕ cells DMXAA doses. We likewise found that ISG15 was expressed in B16 tumor cells at similar levels compared to Mϕ when analyzed over time. Taken together, these results argue that IRF3 is functionally intact in B16 tumor cells, but that the IFN-β gene is selectively not transcribed.

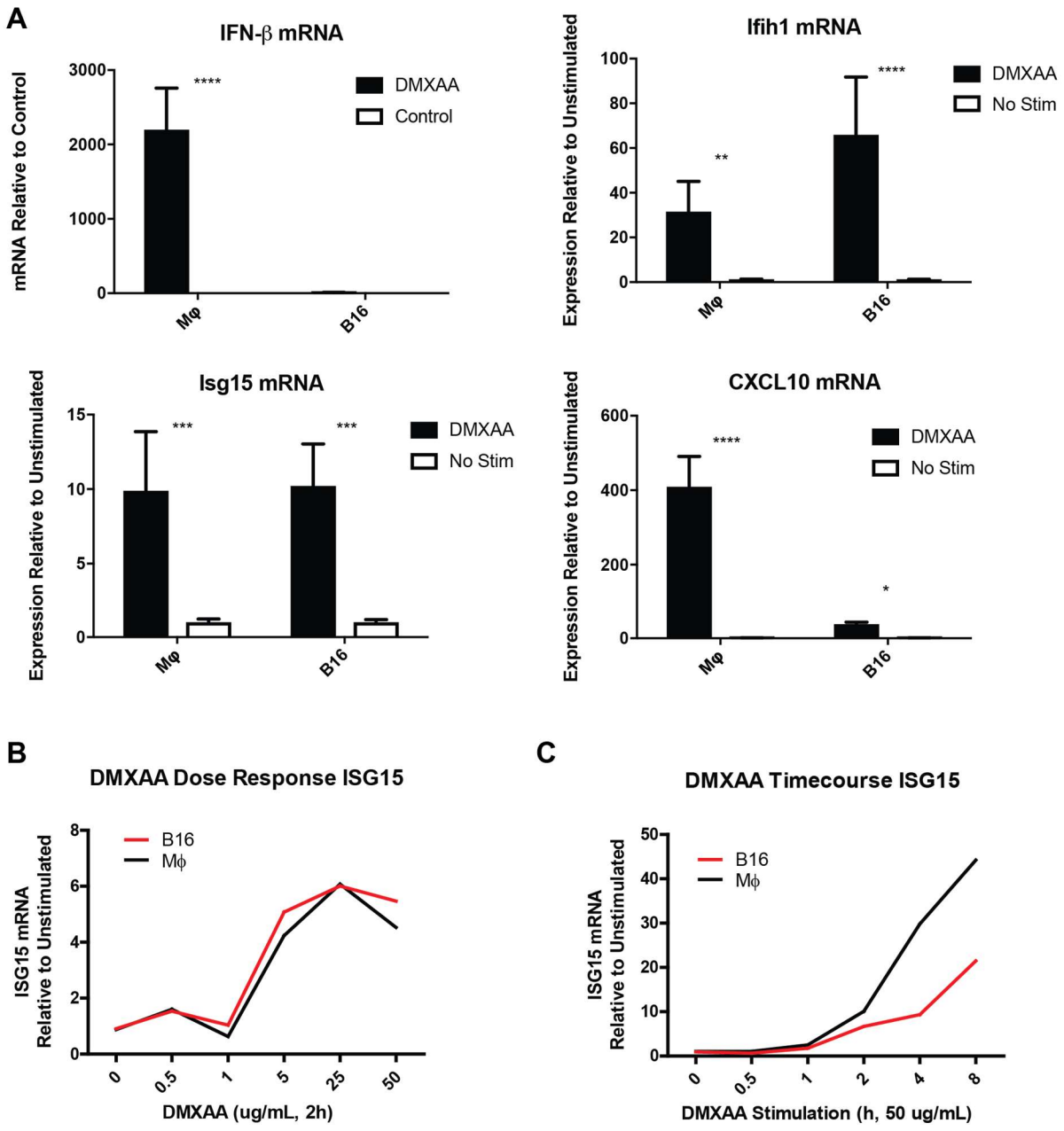

Figure 3.8 Tumor cells retain expression of other IRF3-target genes besides IFN-β. (A) Tumor cells were stimulated with DMXAA for 2 hours and expression of each gene measured by qRT-PCR. (BC) B16 tumor cells were treated for 2 hours with various doses of DMXAA or with 50 µg/mL DMXAA for various amounts of time. Gene expression was then measured by qRT-PCR.

3.09 B16 tumor cells lack IFN-β expression after STING pathway activation by a dominant-negative mechanism

It was of interest to determine the molecular mechanism of failed IRF3 binding to the IFN-β promoter in B16 tumor cells. As a first approach to narrow down possibilities, we aimed to determine whether the lack of IFN-β expression was based on a dominant or recessive mechanism. This was pursued through the generation of heterokaryon fusions of B16 tumor cells with Mϕ. GFP-expressing Mϕ and dsRed-expressing tumor cells were fused using polyethylene glycol (PEG), and the GFP/dsRed double-positive population was isolated by flow cytometric sorting (Figure 3.9). We also sorted dsRed-bright or GFP-bright cells as homotypic fusions as controls. STING signaling was then interrogated by stimulation with DMXAA and measuring IRF3 nuclear translocation as well as IFN-β gene expression. Consistent with what we had observed previously, we found that all 3 populations retained IRF3 nuclear translocation. However, when we measured IFN-β mRNA we found that the heterotypic hybrid population lacked IFN-β gene expression similar to the B16 homotypic control and in contrast to the homotypic Mϕ control. These data indicate that B16 tumor cells lack IFN-β expression by a dominant negative mechanism, and suggest that B16 cells gain a dominant negative factor that opposes IFN-β expression.

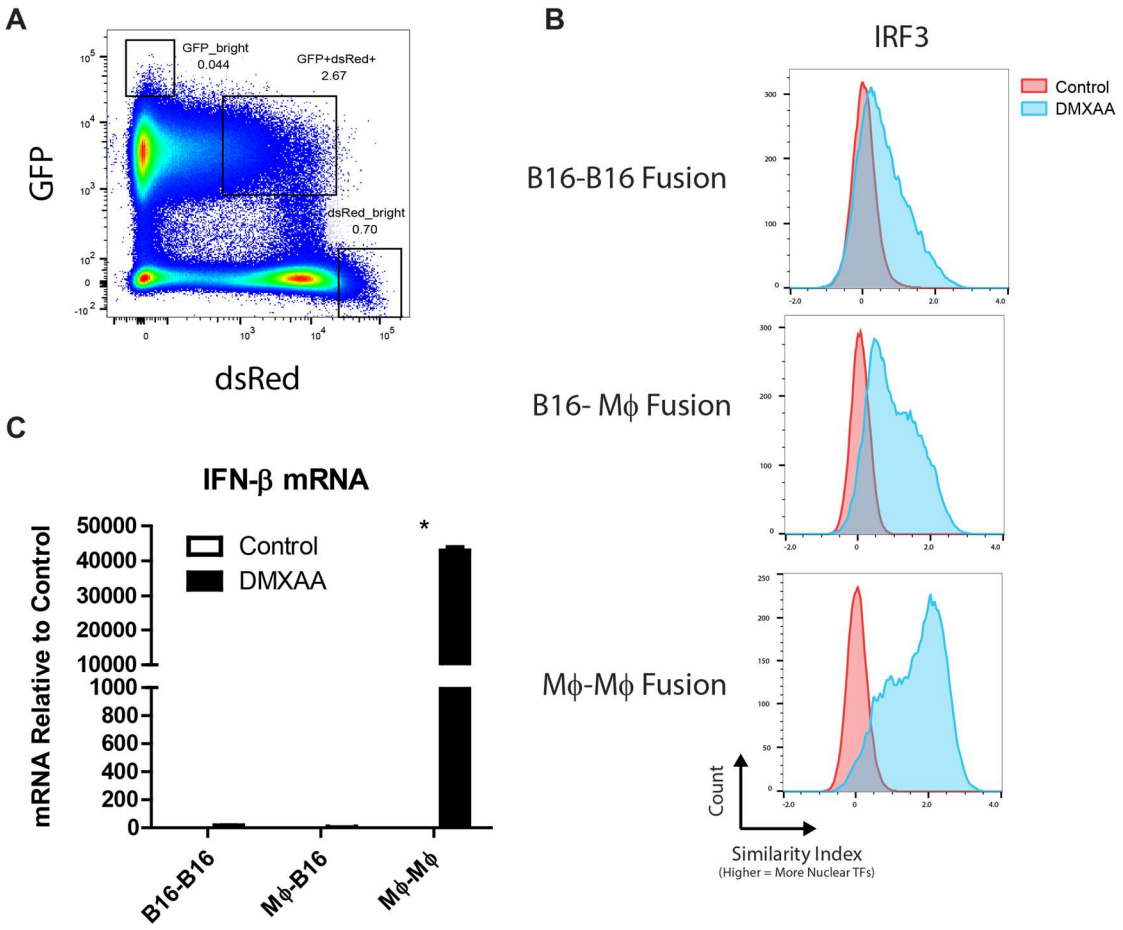

Figure 3.9 B16-Mϕ heterokaryons fail to express IFN-β after STING pathway activation, indicating a dominant-negative mechanism.
(A) ds-Red expressing B16 tumor cells and GFP-expressing Mϕ were mixed with PEG to induce membrane fusion. The double-positive population was then sorted as well as bright populations representing homotypic fusion controls Heterokaryons were stimulated with DMXAA for 2 hours and IRF3 nuclear translocation (B) or IFN-β expression was measured.

3.10 Treatment with cycloheximide enables tumor cells to express IFN-β at comparable levels to Mϕ, presumably due to degradation of an inhibitory factor

Our observations with heterokaryons suggest that B16 tumor cells have a dominant-negative inhibitory factor that prevents IFN-β expression in tumor cells. We reasoned if this was true, then allowing degradation of this inhibitory factor might rescue tumor-intrinsic STING signaling and IFN-β expression. Assuming such a factor was a protein, we treated cells with

cycloheximide (CHX) to block new protein synthesis and allow degradation via natural homeostatic processes. We reasoned that there might be a kinetic window in which the inhibitory factor would be degraded but that the positive signaling factors might remain intact. A time course was performed by pre-treating B16 tumor cells with CHX for various amounts of time then stimulating with DMXAA (Figure 3.10A). We found that after 10h there was high expression of IFN-β mRNA in B16 tumor cells, to a level quantitatively similar to what was seen in Mϕ cells (Figure 3.10B). Analysis by staining with live-dead markers revealed that B16 tumor cells were not killed under these conditions (Figure 3.10C). These results demonstrate that B16 tumor cells are intrinsically capable of IFN-β gene expression, but that negatively regulatory protein(s) prevented IFN-β transcription under steady state conditions.

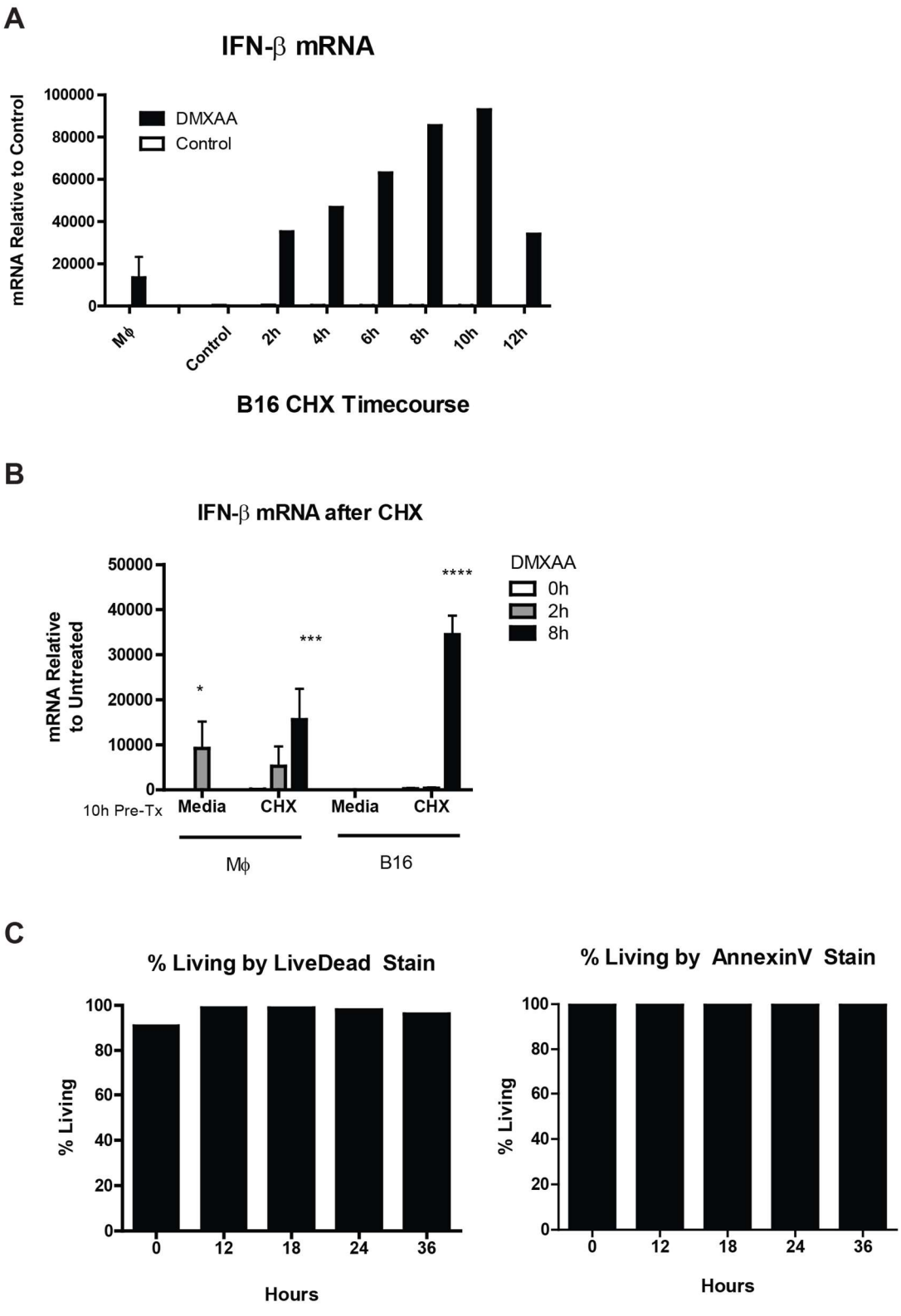

Figure 3.10 Cycloheximide pre-treatment enables tumor cells to express IFN-β in response to STING agonists.

Figure 3.10, continued
(A) B16 tumor cells were treated with cycloheximide (CHX) for various amounts of time and then stimulated for 8 hours with DMXAA and cycloheximide together. (B) Tumor cells or Mϕ controls were grown in media or pre-treated with cycloheximide for 10 hours, then stimulated with DMXAA and cycloheximide for various amounts of time. IFN-β mRNA was measured by qRT-PCR. (C) B16 tumor cells were treated with cycloheximide for various amounts of time then stained with a LiveDead or AnnexinV stain to measure the percent of living cells.

3.11 The IFN-β locus is epigenetically closed at baseline and opens up following STING pathway activation in Mϕ but not tumor cells

Epigenetic regulation is one potential mechanism that could explain why IRF3 can bind other gene promoters but not the IFN-β locus. We therefore directly measured epigenetic accessibility using an assay for transpose-accessible chromatin (ATAC) with deep sequencing to determine which parts of the genome were accessible. In particular, previous studies had described a region just upstream of the IFN-β gene where IRF3 binds (marked in red in Figure 3.11A). Those studies found an approximately 50 bp region around 100 bp upstream of the IFN-β transcriptional start site where multiple transcription factors such as IRF3 and NF-κB can bind [82]. IFN-β gene expression has been linked to a combination of these transcription factors working together to promote transcription. Minimal constructs containing just this 50 bp promoter region led to reporter activity that closely matched endogenous IFN-β expression patterns [87]. Therefore, while other more distant sites may regulate IFN-β gene expression, this key region where IRF3 binds is thought to primarily dictate IFN-β gene expression.

When we measured epigenetic accessibility of this key region, we found it was closed at baseline in both Mϕ and B16 tumor cells. In Mϕ in response to STING pathway activation, the locus became more epigenetically accessible but in B16 tumor cells it failed to open (Figure

3.11). These results argue that IRF3 might not bind the IFN-β promoter in B16 tumor cells because the binding site remains epigenetically closed.

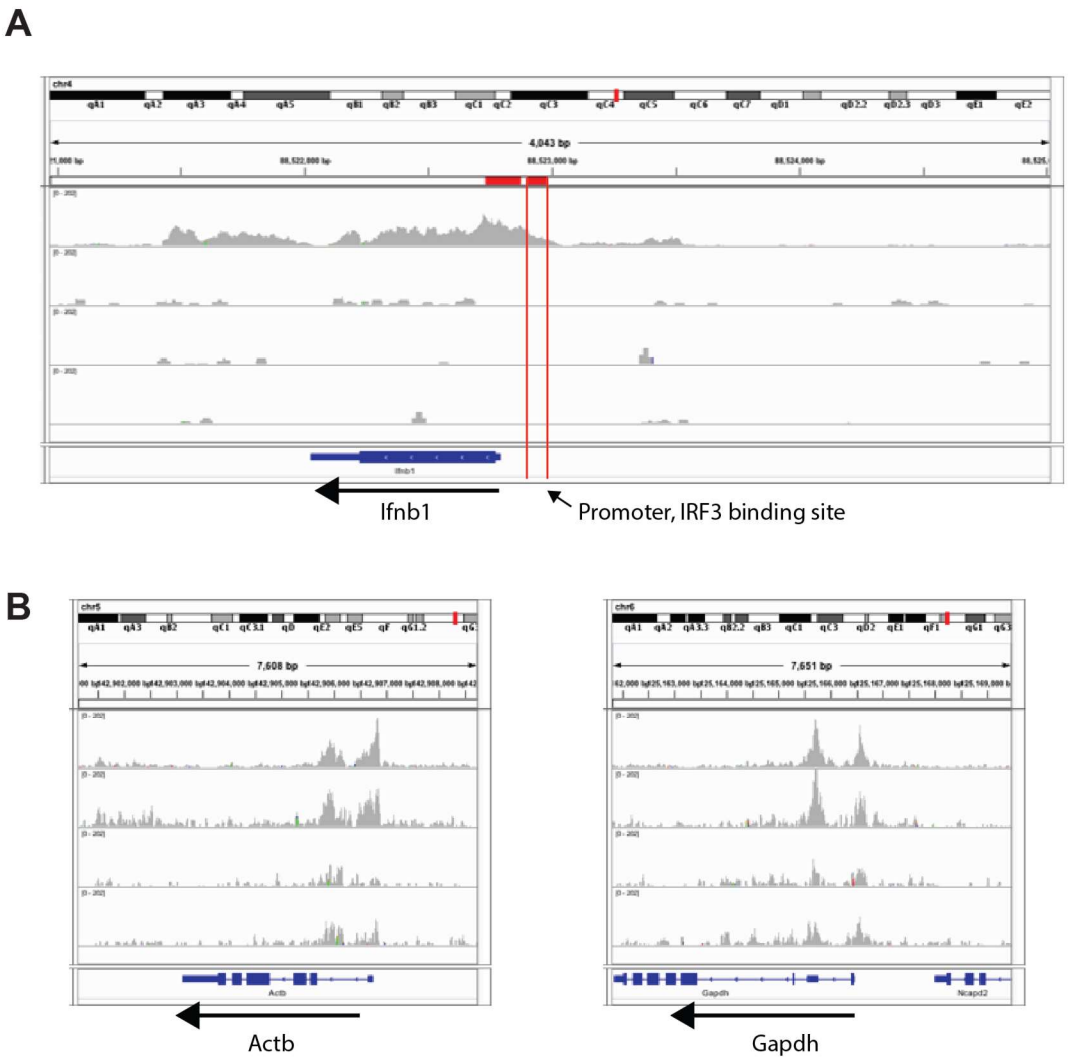

Figure 3.11 ATAC-sequencing reveals the epigenetic accessibility of the IFN-β locus at baseline and following STING pathway activation.
ATAC-sequencing was performed to measure the epigenetic accessibility of the IFN-β locus (A) or other housekeeping genes (B).

3.12 Epigenetic modulation by HDAC and DMT inhibitors fails to enable tumor-intrinsic IFN-β expression by STING pathway activation

There are 2 major possibilities that could explain the failure of B16 tumor cells to open the IFN-β locus epigenetically: 1) tumor cells could actively maintain epigenetic repression of IFN-β via enzymes like histone deacetylases (HDACs) or 2) tumor cells could be missing a cofactor that is necessary for opening the IFN-β locus. To begin to address these possibilities, we investigated whether epigenetic modulating drugs might enable tumor-intrinsic IFN-β expression. B16 tumor cells were treated with several different types of HDAC inhibitors (Figure 3.12A). These drugs were selected because collectively they affect every class of HDACs (Figure 3.12B). However, none of the HDAC inhibitors enabled B16 tumor cells to express IFN-β. In fact, TSA and mocetinostat both suppressed IFN-β expression by control Mϕ cells. We also treated tumor cells with DNA methyltransferase inhibitors across several concentrations but found that neither inhibitor enabled tumor cells to express IFN-β (Figure 3.12CDE). While negative data can be challenging to interpret, these results nonetheless prompted us to focus upon lack of a positive signaling event that is functional in Mϕ yet non-functional in B16 cells.

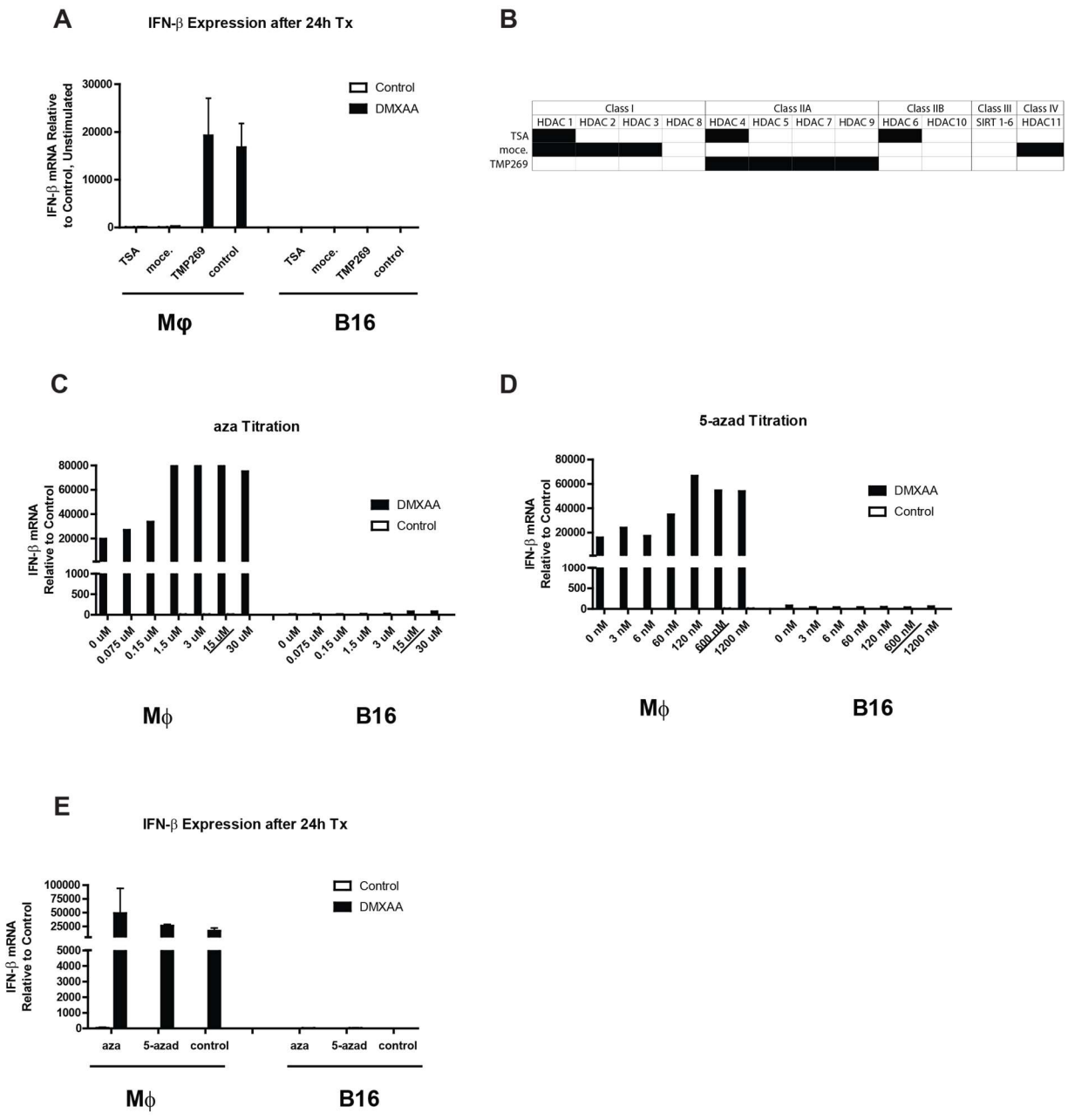

Figure 3.12 Treatment with HDAC inhibitors and DMT inhibitors does not enable tumor cells to express IFN-β in response to STING agonists.
(A) B16 tumor cells or Mϕ controls were treated with high doses of various HDAC inhibitors for 24 hours and stimulated with DMXAA. (B) A summary of which HDACs are inhibited by which drugs. (CDE) Tumor cells or Mϕ controls were treated with azacytidine (aza) or 5-aza-deoxycytidine (5-azad) for various amounts of time (CD) or 24 hours (E) and then stimulated with DMXAA.

3.13 STING pathway activation elicits expression of NF-κB target genes from Mϕ but not B16 tumor cells

Our data to this point suggested that B16 tumor cells might be defective in activation of a pathway required for epigenetically opening the IFN-β gene locus. Based on the literature, NF-κB signaling has been proposed to regulate opening of the IFN-β locus, and also can be activated by STING signaling. Previous studies have found that NF-κB can bind the IFN-β promoter at earlier time points than IRF3 [89]. More recent studies using chromatin conformation capture experiments suggested that there are 3 NF-κB binding sites that associate with the IFN-β promoter region. These sites are found at distant sites in the genome but are physically close to the IFN-β promoter and these NF-κB binding sites are epigenetically accessible at baseline [88]. It is therefore theorized that NF-κB binds to these sites first and then, through a poorly understood mechanism, causes the IFN-β promoter to become epigenetically accessible. This then allows NF-κB to bind to the now epigenetically accessible IFN-β promoter. Shortly after NF-κB binds, IRF3 can then bind the IFN-β promoter and, together, NF-κB along with IRF3 drive IFN-β gene expression.

Therefore, we interrogated NF-κB signaling in B16 tumor cells by evaluating NF-κB p65 binding to the IFN-β promoter by ChIP. In fact, we found NF-κB bound to the IFN-β promoter in Mϕ but not B16 tumor cells (Figure 3.13A). We also investigated induced expression of other target genes, and found that DMXAA induced expression of TNF-α, in Mϕ but not in B16 tumor cells (Figure 3.13B). These results indicate that that NF-κB signaling is activated downstream of STING and drives gene expression in Mϕ but not in B16 tumor cells, and argue that the defect in NF-κB signaling is different than the defect in IRF3 signaling.

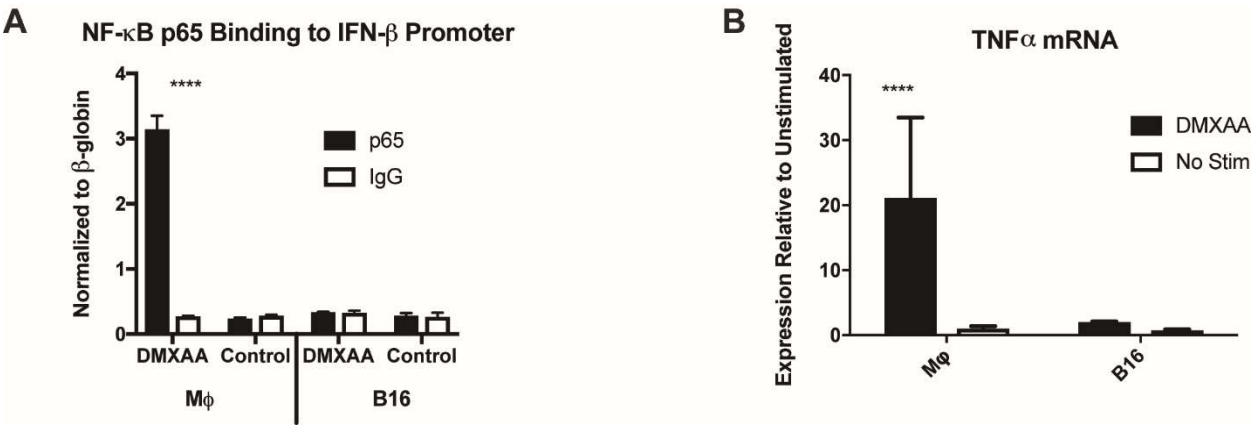

Figure 3.13 NF-κB target gene expression and NF-κB binding to the IFN-β promoter after STING agonist treatment.
(A) B16 tumor cells or Mϕ controls were treated with DMXAA for 2 hours and gene expression measured by qRT-PCR. (B) Tumor cells or Mϕ were treated with DMXAA for 2 hours and NF-κB binding to the IFN-β promoter was measured by ChIP-PCR.

We also stimulated both tumor cells and Mϕ with DMXAA and performed an intracellular stain for NF-κBp65 also known as RelA. In parallel we stained for IRF3 as a positive control. Consistent with our previous observations, we found that IRF3 translocated to the nucleus of both B16 tumor cells and Mϕ. In contrast, NF-κB only translocated to the nucleus of Mϕ (Figure 3.14). These results indicate that the defect in NF-κB signaling is upstream of p65 nuclear translocation.

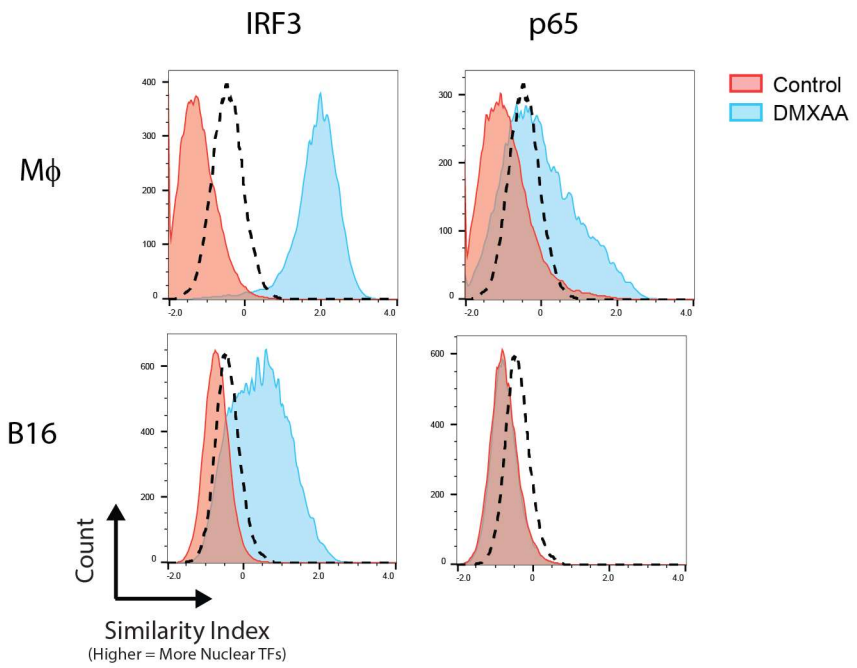

Figure 3.14 ImageStreamX analysis reveals B16 tumor cells lack NF-κB p65 nuclear translocation.
B16 tumor cells or Mϕ controls were treated with DMXAA for 2 hours (blue) and then intracellular staining performed for IRF3 or NF-κB p65. Nuclear translocation was quantified by a similarity index which calculates the correlation between nuclear DAPI staining and antigen staining.

3.14 B16-Mϕ heterokaryons lack NF-κB nuclear translocation, indicating a dominant-negative defect

The observation that Mϕ-B16 heterokaryons fail to express IFN-β demonstrated that B16 tumor cells have a dominant negative mechanism that blocks expression of IFN-β mRNA. If failed NF-κB signaling was responsible for this defect, then we reasoned that p65 nuclear translocation also might be impaired through such a dominant negative effect. To test this hypothesis, we stimulated heterokaryons with DMXAA and measured NF-κB nuclear translocation using ImageStreamX analysis. In fact, we found that Mϕ-B16 hybrid cells lacked NF-κB nuclear translocation after STING pathway activation. This was similar to the B16

homotypic controls and in contrast to Mϕ homotypic controls. These results suggest that dominant negative mechanism that prevents NF-κB signaling in B16 tumor cells might be the core aberration.

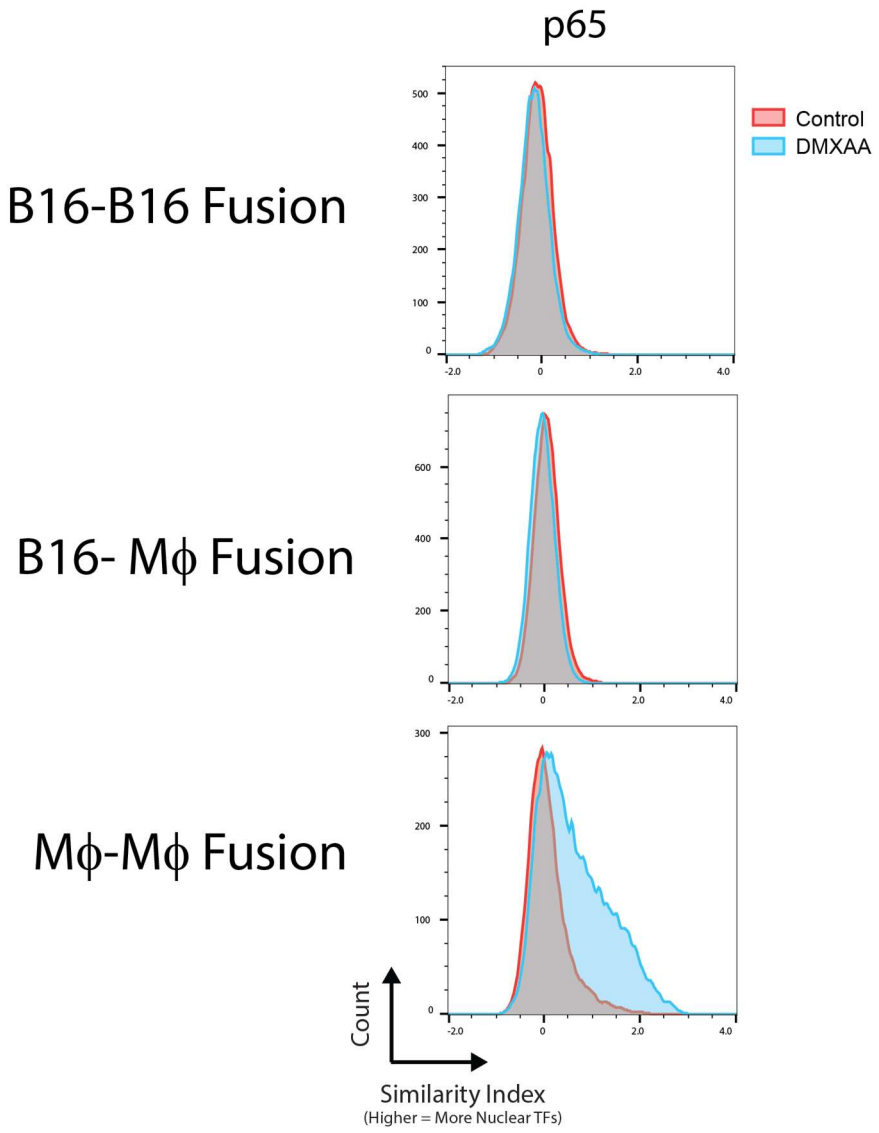

Figure 3.15 Heterokaryons reveal a dominant-negative defect in NF-κB signaling in B16 tumor cells.
Heterokaryons were stimulated with DMXAA for 2 hours and nuclear translocation of NF-κB p65 measured by intracellular staining and ImageStreamX analysis. The similarity index was calculated by quantifying the correlation between nuclear DAPI staining and antigen staining.

3.15 Cycloheximide treatment enables tumor-intrinsic NF-κB nuclear translocation in tumor cells

In as much as we had found evidence for an inhibitory protein in B16 cells that prevented IFN-β gene expression based on CHX treatment experiments, we hypothesized that, if defective NF-κB signaling was mediating this lack of IFN-β expression, then CHX treatment should similarly restore NF-κB signaling. To test this notion, we pre-treated B16 tumor cells with CHX and measured NF-κB p65 nuclear translocation by ImageStream. Indeed, we found that CHX treatment enabled NF-κB translocation into the nucleus (Figure 3.16). Interestingly, treatment with DMXAA did not further augment this process, suggesting that cycloheximide alone was sufficient to induce maximal NF-κB nuclear translocation. This result implies B16 tumor cells may contain a basal propensity for NF-κB signaling.

Importantly, our previous studies did not show any IFN-β expression after CHX treatment alone (Figure 3.10). This result implies that CHX is sufficient to cause NF-κB signaling and nuclear translocation in B16 tumor cells, but this alone does not lead to IFN-β expression. When we treat tumor cells with CHX along with DMXAA, then IFN-β becomes expressed at comparable levels to Mϕ which is likely due to the fact that IRF3 and NF-κB are both activated under those conditions. This phenomenon is similar to what we observe in Mϕ where treatment with DMXAA alone is sufficient to cause both IRF3 and NF-κB signaling.

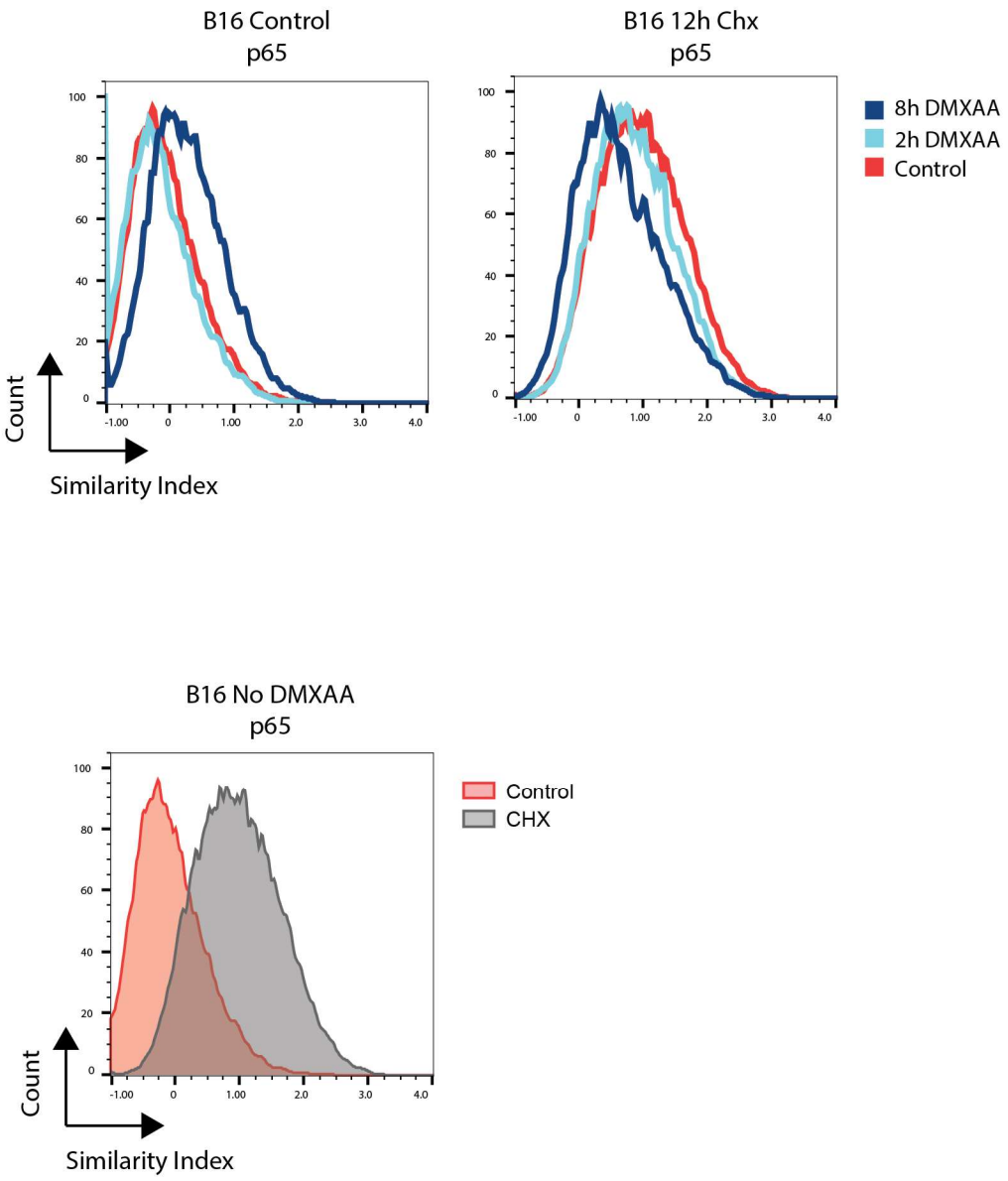

Figure 3.16 Treatment with cycloheximide enables tumor-intrinsic NF-κB nuclear translocation.
B16 tumor cells were treated for 10 hours with cycloheximide (CHX) and then stimulated for various amounts of time with DMXAA and cycloheximide. NF-κB p65 nuclear translocation was measured by intracellular staining and ImageStreamX analysis. The degree of nuclear translocation was quantified by the correlation between DAPI and the antigen stain.

3.16 An NF-κB-GFP reporter recapitulates the phenotype observed in B16 tumor cells

Our collective data implicated an inhibitory protein in B16 tumor cells that prevented NF-κB signaling, thereby leading to defective IFN-β gene expression in response to STING pathway activation. Therefore, we sought to identify gene(s) in B16 tumor cells was responsible for repressing NF-κB signaling. To develop a screen, we introduced an NF-κB reported into B16 tumor cells, and also into Mϕ control cells, to interrogate NF-κB signaling more carefully. We found that DMXAA was sufficient to elicit GFP expression from Mϕ but not tumor cells. However, when B16 tumor cells were pretreated with CHX along with DMXAA treatment, then NF-κB GFP reporter activity was observed (Figure 3.17). A dose response and time course treatment was performed in Mϕ to optimize stimulation. We found that the reporter activity increased over time, and also increased with higher concentrations of DMXAA. These observations confirm that not only does cycloheximide rescue NF-κB nuclear translocation, but that it also rescues expression of an NF-κB transcriptional reporter. These results also established a B16 tumor cell line that could be used to perform a whole-genome screen for candidates that, once deleted, restore expression of NF-κB signaling in B16 tumor cells.

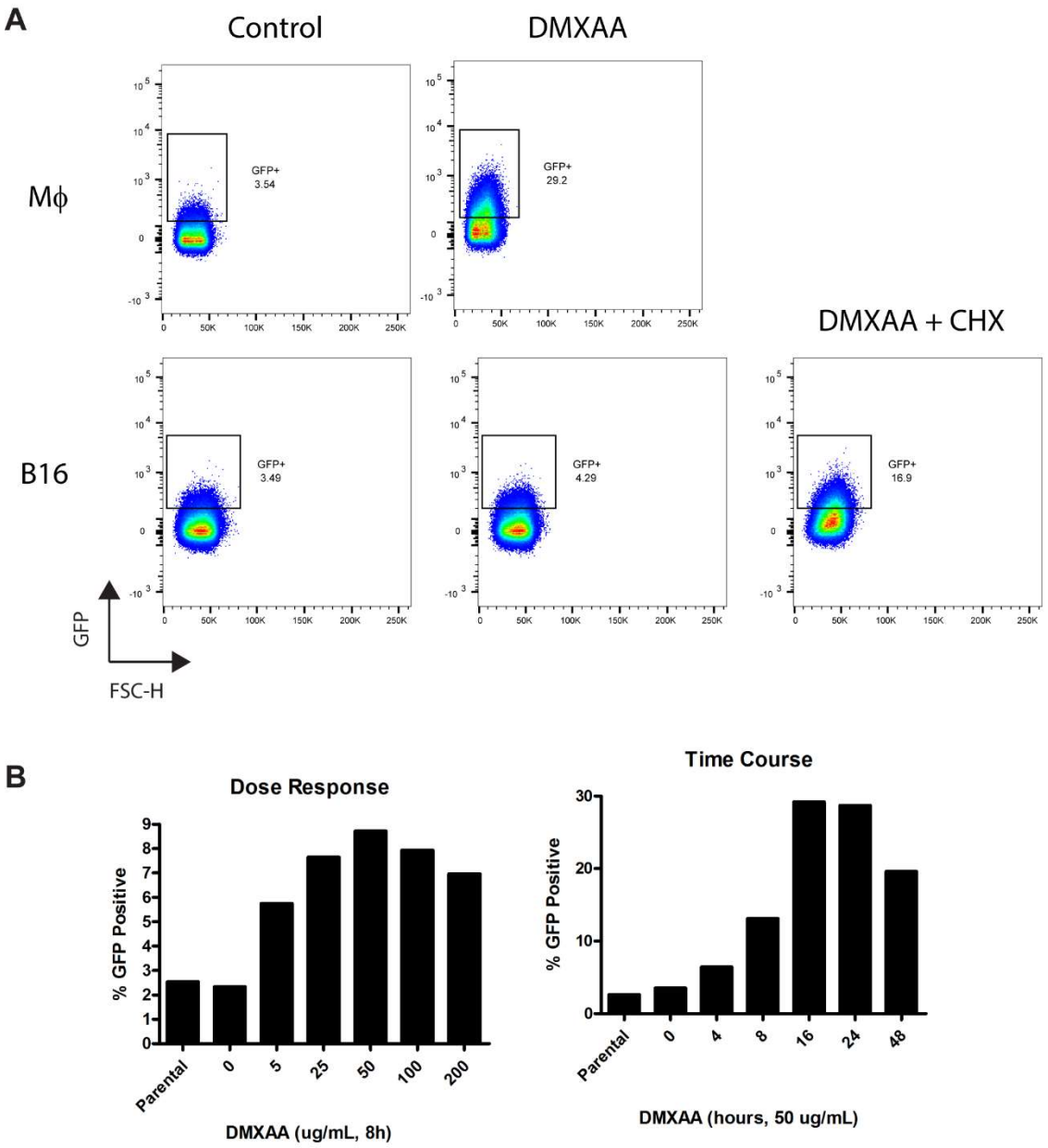

Figure 3.17 An NF-κB GFP reporter measures the response by Mϕ and B16 tumor cells to STING agonists.
Mϕ or B16 tumor cells were treated with DMXAA for 16 hours or tumor cells treated with cycloheximide (CHX) for 10 hours then stimulated with DMXAA and cycloheximide for 8 hours. The cycloheximide treated cells were then grown in normal media 24 hours. Ultimately, flow cytometry was used to measure expression of the NF-κB GFP reporter.

3.17 Expression of a whole-genome CRISPR gRNA library yields rare tumor cells with high NF-κB signaling in response to STING pathway activation

Using B16 tumor cells expressing an NF-κB GFP reporter, we pursued a genome-wide CRISPR screen to identify genes which, when knocked out, restore tumor cell-intrinsic NF-κB signaling. We used a gRNA library containing 87,897 sgRNA sequences targeting 19,150 mouse protein-coding genes. We transduced the library into B16 tumor cells stably expressing both cas9 and the NF-κB GFP reporter. We then expanded the cells and cultured them for 5 days to allow the gene deletion to take effect. The resulting cells were stimulated with DMXAA and then sorted based on high level of GFP expression. We briefly cultured the sorted cells, lysed them to purify genomic DNA, performed PCR specific for the gRNA flanking regions, and sequenced individual gRNAs. Presumably, any genes identified by this screen are acting as dominant negative repressors of NF-κB signaling because deleting them enabled tumor cells to express the NF-κB GFP reporter.

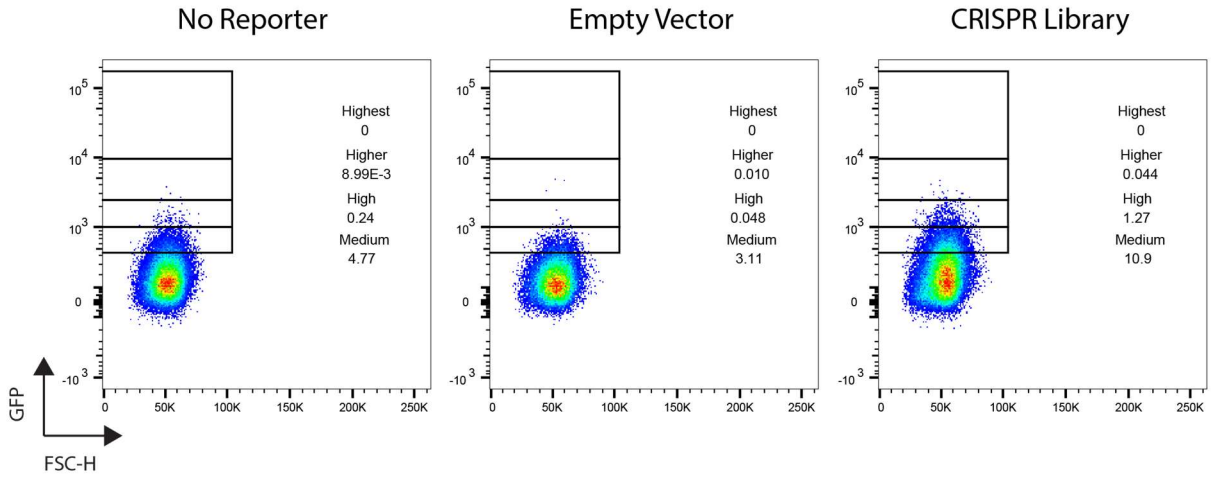

Figure 3.18 Tumor cells were sorted based on expression of the NF-κB GFP reporter after transduction with a genome wide CRISPR gRNA library.
B16 tumor cells stably expressing cas9 and an NF-κB GFP reporter were transduced with a genome-wide CRISPR gRNA library. After 5 days or proliferation the cells were sorted for varying levels of GFP reporter expression for further analysis.

3.18 gRNAs targeting several genes are enriched in a whole-genome CRISPR screen for NF-κB reporter activity

Upon sequencing the gRNAs from B16 tumor cells with exceptionally high NF-κB-GFP reporter expression, we found an enrichment for gRNAs targeting several genes. These included Mast1, Nbeal2, Smad1, Pglyrp2, Stam2, Ifitm2, and Prss50 (Figure 3.19). Based on the literature, several of these genes seemed mechanistically plausible as regulators of NF-κB signaling downstream of STING. For example: Mast1 is a kinase; Smad1 is involved with TGF-β signaling which can cross-talk with STING signaling; Ifitm2 over-expression has been linked to suppression of type I interferon expression after polyI:C stimulation [113]; and Prss50 is a poorly characterized protease. Each of these proteins have functions that could conceivably impact on STING signaling to regulate signal transduction but none of them have been previously identified as regulators of NF-κB signaling. We decided to consider all 12 targets as candidates for further analysis.

Gene	Times Sequenced
Mast1	6
Nbeal2	6
SMAD1	5
Pglyrp2	5
Stam2	4
Ifitm2	4
Prss50	3
Cop1	1
Dcaf6	1
Rad51ap2	1
S1pr5	1
Tshz3	1

Figure 3.19 Several candidate genes are identified by the genome-wide CRISPR screen. Cells sorted from the highest reporter-expressing population were sorted, lysed, and the corresponding gRNAs sequenced. These sequences were then matched to the corresponding genes they target and summarized in the table shown.

3.19 Multiple genes are mutated in B16 melanoma that are known to suppress NF-κB signaling

In parallel to the CRISPR library approach, we also analyzed which genes are mutated in B16 tumor cells compared to Mϕ. We reasoned that any mutations that are present in B16 tumor cells but not Mϕ could explain why they have different phenotypes downstream of STING activation and therefore could explain why B16 tumor cells have a defect in NF-κB signaling.

To identify variants in B16 tumor cells, we performed whole-genome sequencing on both B16 tumor cells and macrophage controls and compared both of them to the published C57BL/6 genome. A total of 554,271 sequence variants were identified in B16 tumor cells compared to Mϕ controls. These variants caused a total of 1,755 genes to have changes to their protein-coding regions. We filtered these genes by functional annotation to identify only genes that had previously been connected to NF-κB signaling, which identified 22 potential candidates. Of these, several had previously been implicated as positive regulators of NF-κB, or had been reported to regulate NF-κB signaling via mechanisms inconsistent with our observations. For example, some factors were described as NF-κB inhibitors but competed with NF-κB for DNA binding which is different than our observation in tumor cells where the defect is upstream of NF-κB nuclear translocation. This type of analysis narrowed the field to 8 promising candidates that were mutated in B16 tumor cells and could theoretically inhibit NF-κB signaling. Among these was Ubxn1, which had previously been shown to suppress NF-κB signaling in response to viral infections [114–116]. Another candidate was Trim30a which regulates stability of TAB2/TAB3 as well as TRAF6 which has been proposed as the adaptor linking STING signaling to NF-κB signaling [75]. We considered all 8 of these genes potential candidates for further evaluation.

		Gene Name	Function (brief):	Mutation Type
NF-κB Suppressors	1	Commd4	interacts with E3 ligase for IkBa, inhibits IkBa degradation	Missense
	2	Ksr2	inhibits MEK activation of MAPK/NFkB	Missense
	3	Nlrc5	binds IKKb and IKKa to block NFkB signaling	Missense/Splice-Region
	4	Prkaca	kinase, can bind the RelA/p50/IkBa complex	Frame-shift
	5	Relb	part of non-canonical NFkB complex (RelB/p52)	Missense
	6	Siva1	suppresses NF-kB in T cells, promotes AICD	Missense/Splice-Region
	7	Trim30a	Causes degrad. of TAB2/TAB3, inhibits TRAF6, blocks NFkB	Missense
	8	Ubxn1	↑ Ubxn1 causes ↓ NFkB by DNA virus, binds IkBa E3 ligase	Missense
NF-κB Activators	9	Aebp1	promotes phosphorylation of IkBa -> degradation	Premature-STOP
	10	Atm	DNA-damage response, can activate NFkB	Missense
	11	Clu	binds the E3 ligase for IkBa to promote degradation	Missense
	12	Il18rap	links IL18 signaling to NFkB activation (promotes)	Missense
	13	Map3k3	part of MAPK pathway, which can act. NFkB	Missense
	14	Slamf1	Slam-/- Mf stim with LPS make less TNFa	Missense
	15	Tlr11	interacts with Myd88 and TRAF6 to promote NFkB signaling	Missense
	16	Tyro3	promote PI3K activity, which -> AKT -> NFkB	Missense
Unlikely Mechanistically	17	Alk	receptor tyrosine kinase, can activate NFkB downstream	Missense
	18	Ascc2	cofactor, binds DNA with NFkB, promotes transcription	Missense
	19	Esr1	estrogen TF, competes w NFkB for DNA binding	Missense
	20	Nfkbiz	IkB-zeta, blocks RelA/p50 DNA binding	Missense
	21	Ror1	receptor for WNT5A -> Ror1 -> canonical NFkB	Missense
	22	Trip4	cofactor that binds DNA with NFkB, promotes transcription	Premature-STOP

Figure 3.20 Whole-genome sequencing identifies multiple mutated genes in B16 melanoma associated with the NF-κB pathway.
gDNA was purified from B16 tumor cells or Mϕ controls. This gDNA was submitted for deep sequencing, aligned to the B6 mouse genome, and variants between B16 tumor cells and Mϕ identified. These variants were screened for effects on protein-coding genes and in genes that are associated with the NF-κB pathway.

3.20 Tumor cells transduced with several candidate gRNAs enable tumor-intrinsic NF-κB reporter activity

After performing whole-genome sequencing and a genome-wide CRISPR screen we found a total of 20 candidate genes (8 from sequencing and 12 from the CRISPR screen) that could theoretically act as inhibitory factors to suppress NF-κB signaling in B16 tumor cells. To test whether any of these candidates actually had an impact on NF-κB signaling we cloned

individual gRNAs targeting each gene. We then transiently transfected these gRNAs into B16 tumor cells expressing the NF-κB GFP reporter, and analyzed the cells by flow cytometry for GFP expression. Using this approach, we estimated that fewer than 50% of the cells would be homozygous knockouts, so we would anticipate a small subpopulation of cells with improved function. We found that introducing gRNAs targeting several candidate genes appeared to produce a "shoulder" in the GFP expression histograms with higher GFP expression after DMXAA treatment. For example, introducing a gRNA targeting Nbeal2 caused a shift in NF-κB GFP reporter expression with around 15% of cells positive after stimulation. While this was not a majority of cells it was in stark contrast to control B16 cells where there was no detectable NF-κB GFP expression (Figure 3.22).

Our previous observations looking at NF-κB nuclear translocation indicated cycloheximide treatment alone was sufficient to drive NF-κB signaling. Based on this observation we speculated B16 tumor cells might have a constitutive drive for NF-κB signaling that is kept in check by an inhibitory factor. We therefore analyzed NF-κB GFP reporter expression in the gRNA-expressing cells at baseline, without DMXAA. Introducing gRNAs targeting Relb seemed to cause a shift in basal NF-κB GFP reporter expression when we compared gRNA-expressing cells to their parental controls. This was in contrast to the introduction of a gRNA targeting Cop1 which seemed to have no effect on basal NF-κB GFP expression. Based on these observations we selected 8 promising gRNAs that led to increased NF-κB reporter expression. Nbeal2, Dcaf6, Prkaca, Smad1, Ubxn1, and Rad51ap2 were selected because they led to a slight increase in GFP expression after DMXAA treatment while Trim30a, Relb, and Commd4 were selected because they led to a shift in basal NF-κB GFP expression.

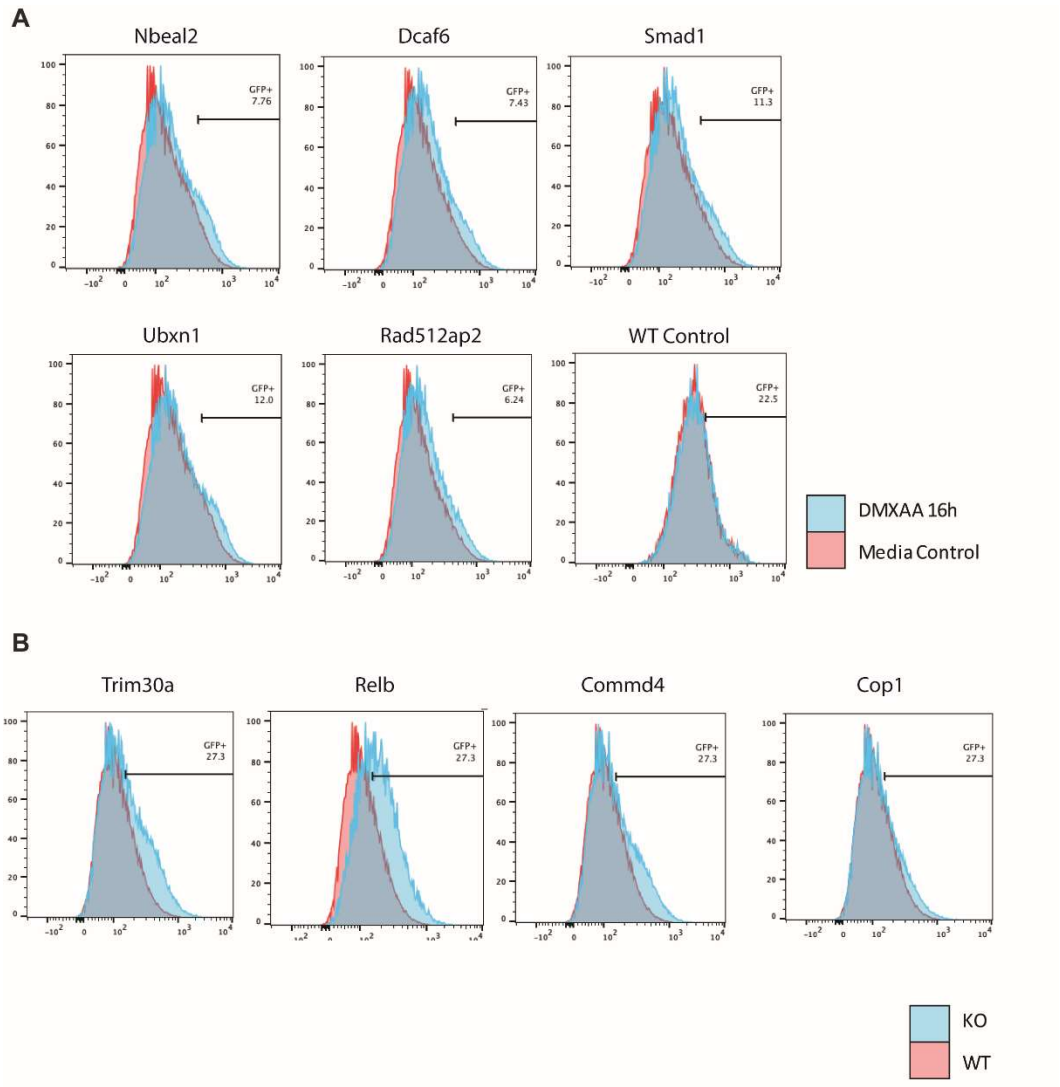

Figure 3.21 Tumor cells with transient expression of single gRNAs lead to increased NF-κB GFP reporter expression.
NF-κB GFP reporter expression was measured in B16 tumor cells. (A) Reporter expression was measured after 16 hours of DMXAA expression and compared to control gRNA expressing cells. (B) Reporter expression was measured under basal conditions in gRNA expressing cells or WT controls without gRNA expression.

3.21 Preliminary data suggests that individual knockout tumor cells can express IFN-β

To further evaluate our 8 top candidates, we stably transfected B16 tumor cells using a lentiviral vector and sorted the transduced cells. These were a bulk population of sorted cells which we estimated would have a higher targeting efficiency than the transiently transfected cells used for NF-κB GFP reporter analysis. We allowed the stably transduced cells to proliferate in order for the genetic recombination to take effect and then stimulated the cells with DMXAA for 2 hours. We found that cells expressing a gRNA targeting several candidates expressed higher IFN-β than B16 control cells without gRNA expression. The top 3 genes were Trim30a, Ubxn1, and Nbeal2, which demonstrated IFN-β expression around 30-45 fold higher than controls. While this was still inferior to the ~500-fold expression observed in Mϕ controls, the transduced B16 cells were not expected to be 100% gene-targeted.

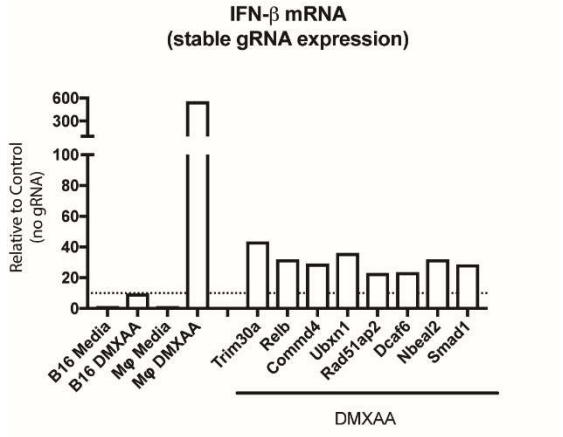

Figure 3.22 Tumor cells stably expressing single gRNAs express higher levels of IFN-β than WT tumor cells.
B16 tumor cells were stably transduced with gRNAs targeting individual candidate genes. Tumor cells were then stimulated with DMXAA for 2 hours and IFN-β expression measured by qRT-PCR

3.22 Other mouse tumor cell lines that fail to express IFN-β also retain IRF3 signaling, similar to B16 tumor cells

Additional tumor cell lines were analyzed to determine whether any had a similar phenotype to B16 melanoma. To measure IRF3 signaling downstream of STING activation, we stimulated multiple tumor cell lines with DMXAA for 2 hours and measured IRF3 nuclear translocation by Amnis ImageStreamX. We found that, similar to B16 tumor cells, all of the tumor cells we tested retained IRF3 signaling. This observation indicates that multiple tumor cell lines retain expression of the STING pathway and IRF3 signaling, and yet fail to express IFN-β itself.

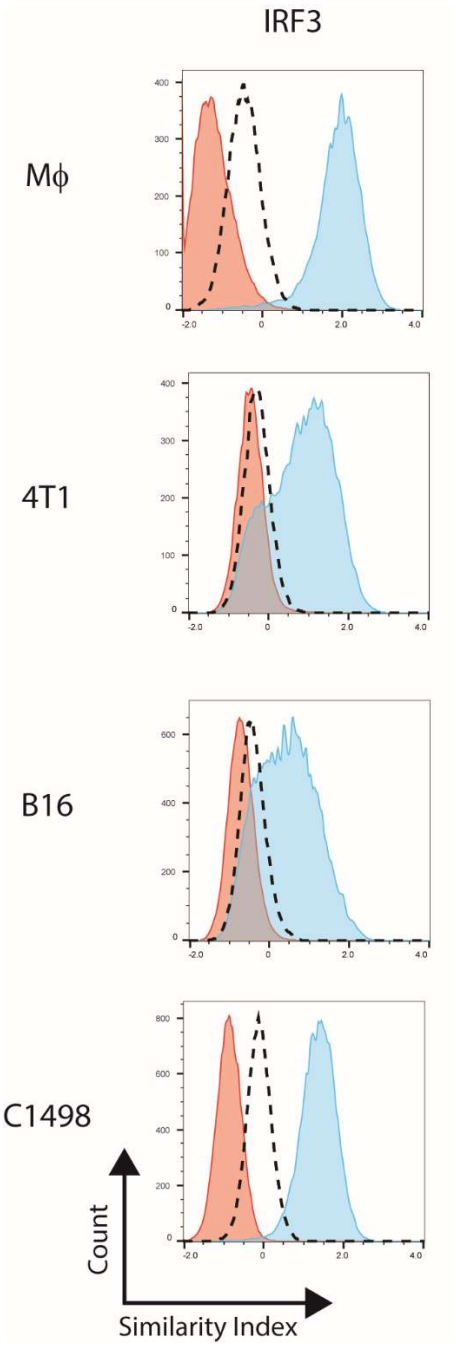

Figure 3.23 IRF3 nuclear translocation still occurs in multiple mouse tumor cell lines. Various tumor cell lines or Mϕ controls were treated with DMXAA and IRF3 nuclear translocation measured by ImageStreamX analysis. The degree of nuclear translocation was quantified by a "similarity index" that measures the correlation between the antigen stain and the DAPI nuclear stain.

3.23 A subset of human tumor cell lines display a similar phenotype to B16 tumor cells

We also evaluated whether the phenotype we observed in mouse tumor cells might also be identified in human cancer cells. Several human melanoma tumor cell lines were stimulated with cGAMP + lipofectamine and analyzed for expression of IFN-β mRNA. We found that none of the human melanoma lines tested expressed IFN-β in response to STING pathway activation (Figure 3.).

Based on the observation that human melanoma cell lines failed to express IFN-β, we examined STING pathway signaling more carefully within these cells. On cell lines, Mel1106, retained IRF3 nuclear translocation as we had seen in B16 cells. To determine whether IRF3 was functionally able to bind DNA and induce gene expression, we measured ISG15 and Ifih1 gene expression. Both of these IRF3 target genes were expressed by Mel1106 at levels quantitatively similar to the THP-1 monocytic controls. We then investigated whether IRF3 could bind to the IFN-β promoter, by ChIP assay. Indeed, no detectable binding of IRF3 to the IFN-β promoter was observed Mel1106. These data clearly show that the overall phenotype that mouse tumor cell lines fail to express IFN-β is also shared by a subset of human tumor cells. Further, these data indicate there are human cancers with similar molecular mechanisms to what we have observed in B16 tumor cells, retaining IRF3 nuclear translocation and expression of other IRF3 target genes but without detectable binding of IRF3 to the IFN-β promoter. The other 2 human melanoma cell lines examined showed lack of IRF3 nuclear translocation. This observation argues they have lost IFN-β gene expression by a distinct mechanism.

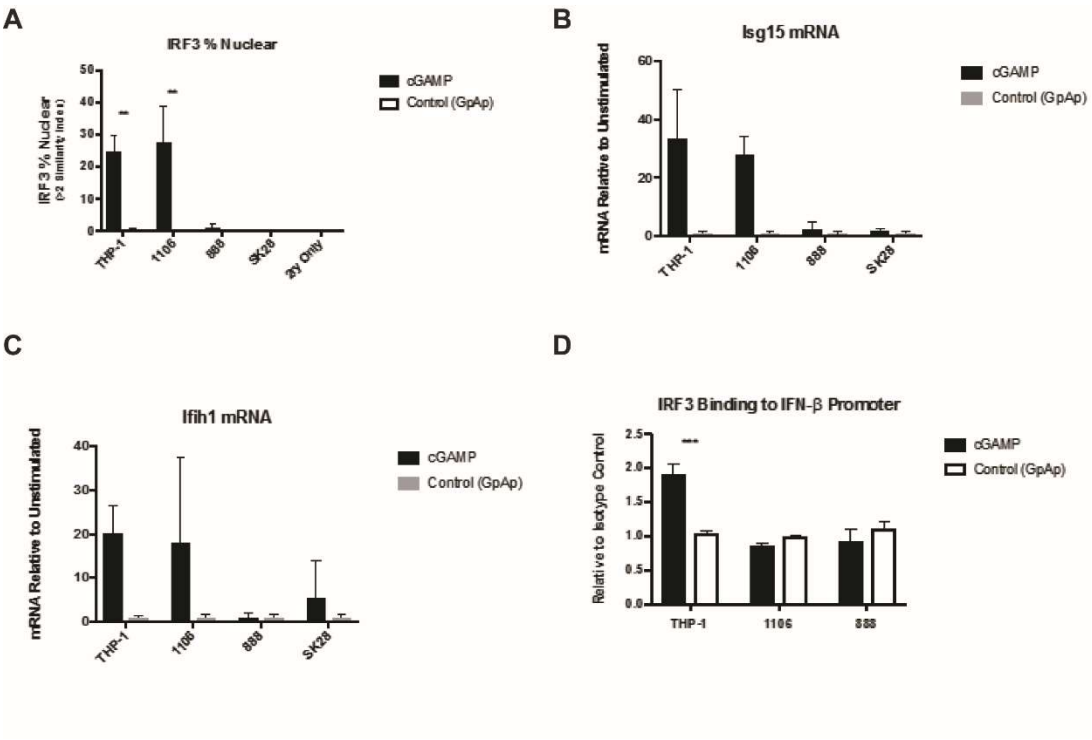

Figure 3.24 A subset of human tumor cell lines have intact IRF3 nuclear translocation and lack IRF3 binding to the IFN-β promoter.
Various human tumor cell lines or THP-1 monocytic controls were stimulated with cGAMP for 4 hours. (A) The percentage of cells with nuclear translocation was then measured by ImageStreamX. (BC) Expression of IRF3 target genes was measured by qRT-PCR. (D) IRF3 binding to the IFN-β promoter was then measured by ChIP-qPCR.

Chapter 4: Discussion

4.01 Overview: B16 tumor cells retain many aspects of STING signaling but lack IFN-β production due to a dominant-negative inhibition of NF-κB signaling

We initially observed that B16 tumor cells failed to express IFN-β in response to STING pathway activation. We found this particularly interesting because when these tumors are implanted in vivo, they induce STING pathway activation within host APCs [63]. Thus, there is intrinsic capability to drive STING pathway activation. In addition, previous studies had indicated that forced expression of IFN-β in tumor cells was deleterious for tumor growth [50]. We tested several tumor cell lines and found the vast majority of them failed to express IFN-β including multiple human melanoma cell lines. In order to more deeply characterize STING signaling, we chose to study the B16 melanoma cell line in-depth to identify the precise molecular mechanism responsible for their lack of IFN-β expression (summarized in Figure 4.1). Our ultimate goal was to identify molecular mechanisms that might allow reversal of this phenotype, which could serve as a therapeutic strategy by restoring tumor cell-intrinsic IFN-β expression so that tumor cells commit "immunologic suicide".

We began characterizing STING signaling by measuring proximal downstream signaling events after activation of STING itself. After STING activation, the central defined signaling events were intact in B16 tumor cells including IRF3 phosphorylation, IRF3 nuclear translocation, IRF3 DNA binding, and transcription of IRF3 target genes. These observations were surprising because they demonstrate the IRF3 branch of STING signaling was wholly intact, but nonetheless the tumor cells failed to express IFN-β. When comparing tumor cells to Mϕ that do express IFN-β, the first difference that we observed was at the level of IRF3 binding to the promoter of IFN-β. Previous studies have identified the precise IRF3 binding site [117] and we found that IRF3 failed to bind this region in B16 tumor cells but did bind in Mϕ after STING activation. IRF3 binding to the IFN-β promoter is required for optimal IFN-β expression and likely explains why tumor cells fail to express IFN-β [82].

There are multiple cofactors that can associate with the IFN-β promoter and a defect in any of them might explain why IRF3 fails to bind the IFN-β promoter. Rather than evaluating these individually we tested heterokaryons for IFN-β expression in response to STING agonists and found they failed to express IFN-β. This indicated that B16 tumor cells lack IFN-β expression in a dominant negative manner. This observation enabled us to focus on pursuing inhibitory factors that narrow the number of candidate mechanisms. Cycloheximide treatment enabled tumor-intrinsic IFN-β expression to levels similar to what was seen in Mϕ, which further supported the notion that B16 tumor cells have an inhibitory factor that acts in a dominant negative manner.

We evaluated the epigenetic accessibility of the IFN-β locus and found that it failed to open up in response to STING activation in tumor cells. This was in contrast to Mϕ controls which epigenetically opened up the IFN-β locus after STING activation. Based on the literature,

we suspected NF-κB signaling was responsible for epigenetic opening of the IFN locus and therefore investigated NF-κB signaling in B16 tumor cells. We found that NF-κB signaling was defective in B16 tumor cells downstream of STING. The lack of NF-κB signaling in tumor cells appeared to be mediated by a defect upstream of nuclear translocation and was a dominant negative mechanism. Similar to IFN-β expression, cycloheximide reversed this phenotype and enabled NF-κB nuclear translocation in tumor cells.

Based on the close correlation between NF-κB signaling and IFN-β expression, we utilized a whole-genome CRISPR screen with an NF-κB reporter to identify which genes, when knocked out, enabled tumor cell-intrinsic NF-κB signaling. We found 12 candidates by the CRISPR screen and, based on whole-genome sequencing, we found 8 additional NF-κB associated genes with non-synonymous mutations. After testing these 20 candidates individually we have found multiple candidates that seem to increase both NF-κB signaling and IFN-β expression in tumor cells. However, these data involving individual candidate genes are still preliminary, and more confirmatory experiments are needed. We have generated single cell clones for each of these candidates which should provide a definitive answer about which gene(s) help to suppress NF-κB signaling in tumor cells and to what level knocking them out affects IFN-β expression.

Regardless of the results of these individual candidates, it is clear that B16 tumor cells fail to express IFN-β in a dominant negative manner and this is likely due to a defect in NF-κB signaling downstream of STING activation. These data provide a proof-of-concept that it is possible to enable tumor-intrinsic IFN-β expression in some tumor cells that appear to lack IFN-β expression under normal conditions. We further postulate that therapies designed to enable

tumor-intrinsic IFN-β expression might represent a promising new innate immunotherapeutic approach.

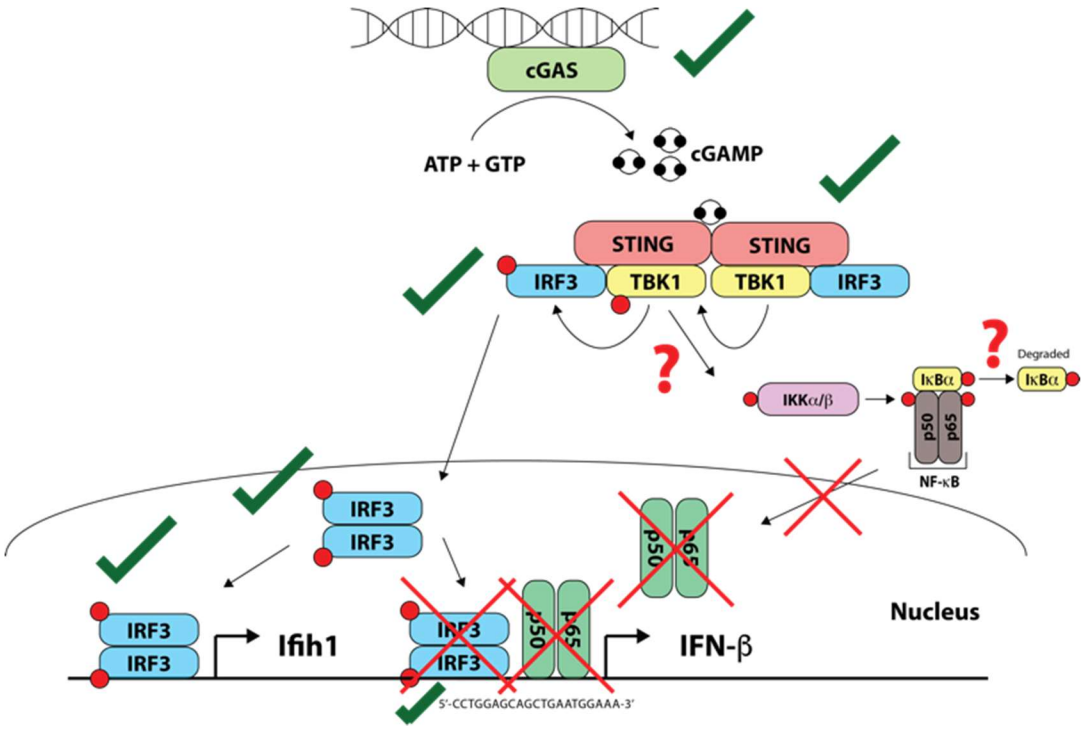

Figure 4.1 STING signal transduction events in B16 tumor cells.
Following STING pathway activation in B16 tumor cells the components of the STING pathway are still expressed and the IRF3 arm of the pathway is functionally intact. However, IRF3 does not bind the IFN-β promoter. This is likely due to a failure to epigenetically open the locus. The NF-κB arm of the STING pathway is defective in tumor cells upstream of nuclear translocation and this is mediated by a dominant-negative mechanism. We have multiple promising candidates that might be this inhibitory factor and are determining whether knocking them out restores NF-κB signaling as well as IFN-β expression.

4.02 Unbiased screening methods identify multiple candidate genes that, when knocked out, appear to enable tumor-intrinsic IFN-β expression

The primary conclusion of this thesis is that most tumor cells fail to express IFN-β after STING pathway activation but, at a mechanistic level, in B16 tumor cells this is not simply due

to deletion of the IFN-β locus or loss of the STING pathway. We find that B16 tumor cells retain STING signaling including IRF3 target gene expression but that IFN-β itself is not expressed and this is associated with a loss of NF-κB signaling. Loss of IFN-β expression and NF-κB signaling are dominant negative phenotypes and reversed by treatment with cycloheximide. Beyond these findings we also have preliminary evidence of single gene knockouts that might enable tumor-intrinsic NF-κB signaling and IFN-β expression. Based on stable expression of gRNAs we find that Trim30a, Ubxn1, and Nbeal2 are all promising candidates that, when knocked out, enable a degree of tumor cell-intrinsic NF-κB signaling and IFN-β expression. While these data are still preliminary, previous studies of these candidate genes suggest plausible mechanistic links to STING signaling and NF-κB activation.

In the context of STING signaling, the mechanism linking STING activation to IRF3 signaling is well characterized [70,74,112]. TBK1 becomes associated with STING as it migrates from the ER through the golgi apparatus [118] and is responsible for phosphorylating several components of the STING complex [72]. IRF3 interacts directly with STING and the precise residues are known [73]. TBK1 ultimately activates IRF3 by direct phosphorylation. The connection between NF-κB and STING is less well established. One study has suggested TRAF6 is involved because TRAF6 KO caused loss of NF-κB signaling downstream of STING [75]. In the context of TLR signaling, TRAF6 can recruit TAB2/3 which in turn recruits the IKK complex that initiates NF-κB signaling [119,120]. Trim30a can inhibit NF-κB activation downstream of TLRs [121]. In this context, Trim30a was found to bind to the TAB2/3 complex that acts as an adaptor between TLR activation complexes and downstream kinases that activate NF-κB. Trim30a association with this complex caused TAB2/3 ubiquitination and degradation, thus opposing NF-κB signaling. Trim30a knockdown increased NF-κB signaling while over expression decreased

NF-κB signaling. Other studies have identified Trim30a in regulating the stability of STING itself but this is likely not happening in tumor cells since they retain IRF3 signaling [111]. Therefore, it seems possible that TRAF6 could associate with the STING complex in order to recruit TAB2/3 which, in turn, recruit the IKK complex. Previous studies have suggested TBK1 phosphorylates the IKK complex to initiate NF-κB activation [75]. If this model is true, then TRIM30a could suppress NF-κB signaling downstream of STING by causing degradation of TAB2/3. This could explain why IRF3 signaling is intact while NF-κB signaling is lost in B16 tumor cell downstream of STING activation.

Another promising candidate that might suppress NF-κB signaling in B16 tumor cells is Ubxn1. Ubxn1 over expression suppresses NF-κB signaling while Ubxn1 knock down causes higher levels of NF-κB signaling in response to both viral infection and TNF-α stimulation [114–116]. Mechanistically, Ubxn1 was found to interact with the E3 ligase that controls IκBα degradation [114]. This led to an accumulation of IκBα in Ubxn1 over-expressing cells, which in turn suppressed NF-κB signaling. In B16 tumor cells, we observe a dominant negative effect in NF-κB signaling that is upstream of nuclear translocation and associated with accumulation of IκBα. This is consistent with the known role of Ubxn1in NF-κB signaling and therefore makes it another promising candidate.

One of the top genes identified by the genome-wide CRISPR screen was Nbeal2. Our preliminary data suggests that Nbeal2 knockdown may increase NF-κB signaling and IFN-β expression, but more confirmatory experiments are needed. Nbeal2 is less well characterized than the other candidates and has primarily been studied in the context of platelets. Mutations in Nbeal2 cause a defect in the formation of α-granules in platelets, resulting in gray platelet syndrome [122]. Without the ability to produce α-granules, platelets are not able to maintain

hemostasis and this causes prolonged bleeding. At the molecular level, Nbeal2 is a cytosolic protein but associates with the plasma membrane via interactions with Dock7, Sec16a, and Vac14 [123]. Previous studies have shown that Dock7 is required for megakaryocyte function and Nbeal2 deficiency caused a loss of Dock7 in megakaryocytes [124]. Based on its association with Dock7, Nbeal2 is thought to play a role in the vesicular trafficking necessary for α-granule biogenesis. STING itself is also regulated via vesicular trafficking. For example, iRhom2, Sec61, TRAPb, Sec5, and VPS34 are all required for trafficking of STING and loss of any of these factors causes a loss of IFN-β expression [70,71,125]. Likewise, treatment with brefeldin A or knockdown of Sar1 both inhibit ER-to-golgi trafficking and have been show to specifically prevent TBK1 association with STING [118]. STING ultimately traffics to perinuclear regions but the exact cofactors that are present on this vesicle are not completely understood [70]. To prevent chronic STING signaling, STING eventually co-localizes with Rab7 and can be degraded by the lysosome [106,107]. Therefore, as a regulator of vesicular trafficking, Nbeal2 has many potential roles in STING signaling. For example, Nbeal2 could regulate the delivery of cofactors to modify STING itself or delivery of adaptors to link STING activation to NF-κB signaling.

It is conceivable that several of these candidates may act together to deregulate STING signaling in tumor cells. Our whole-genome sequencing results have identified mutations in all 3 candidates with a Trp to Cys in Trim30a, Gly to Glu in Ubxn1, and Gly to Asp in Nbeal2. It is possible that each of these mutations plays a partial role in the phenotype we observe in tumor cells in order to help repress NF-κB signaling. One interesting future direction is to generate a triple KO that might ultimately express higher levels of IFN-β than any single KO. These hypotheses are speculative, but I think it is clear that there are multiple candidates that seem

promising and that one or more of them may be responsible for repressing NF-κB signaling in B16 tumor cells.

4.03 Studying tumor-intrinsic innate immune signaling reveals molecular details about IFN-β transcriptional initiation

While our work has largely focused on STING signaling with the perspective of innate immunotherapy of cancer, it also sheds new light on basic mechanisms of IFN-β gene regulation. Often in biology, important insights into biological processes have been gained when a pathway is discovered to be aberrantly regulated. Understanding at which steps viruses inhibit innate immunity or where tumor cells tend to mutate certain pathways reveals new insights into the mechanisms and bottlenecks of those pathways. IFN-β transcriptional regulation has been extensively studied, and one of the general conclusions is that multiple transcription factors must work together to induce IFN-β expression. Our results further confirm this observation. It seems that in B16 tumor cells, a defect in NF-κB signaling leads to a complete loss of IFN-β gene expression. By contrast, Mϕ that inducibly express high levels of IFN-β retain cooperative NF-κB signaling and IRF3 signaling. Most research involving STING signaling has focused on the IRF3 arm of the STING pathway, but more recent work has shown that NF-κB is also activated downstream of STING [75]. Based on our observations, it seems this arm of STING signaling is essential for successful induction of IFN-β expression by STING pathway activation.

Mechanistically, one of the early steps in the initiation of IFN-β gene expression appears to be NF-κB activation. There are 3 "Alu" sites in the genome that associate with the IFN-β promoter based on chromatin conformation capture experiments [88]. While these sites are close to the IFN-β promoter in 3-dimensional space, they are relatively distant in genomic terms because

two of them are on entirely different chromosomes and the third site is on the other arm of the same chromosome as the IFN-β gene. Under basal conditions in macrophages, we find that the IFN-β promoter region is epigenetically closed and that it opens up after STING pathway activation. Previous studies have found that these 3 distant Alu sites are epigenetically open at baseline and that NF-κB can bind these sites at timepoints earlier than it binds the IFN-β promoter [88]. Our data in the context of these other studies further confirm the importance of NF-κB signaling for IFN-β expression and helps to tie it directly to the epigenetic control of the IFN-β promoter region. It is possible that NF-κB binding to the distant Alu sites that are accessible at baseline allows NF-κB to recruit other factors that epigenetically open the IFN-β promoter region. However, more studies are needed to describe the exact process that causes this epigenetic opening of the IFN-β promoter in response to STING signaling.

IFN-β is normally only expressed by a fraction of stimulated cells even under ideal conditions [126,127]. This observation also agrees with our results in which only a fraction of Mϕ demonstrated IRF3 or NF-κB nuclear translocation. One of the big unanswered questions involving IFN-β gene expression is which mechanisms dictate whether individual cells express IFN-β. One of the main theories put forward is that this is a stochastic process and is due to the requirement for several transcription factors working together. This theory argues that these transcription factors have many binding sites throughout the genome and therefore are the limiting factor because there may not be sufficient quantities to bind the IFN-β promoter in every cell. This theory argues that IFN-β is not expressed unless multiple transcription factors bind simultaneously to the promoter and that this only occurs in a subset of cells [82]. There is evidence that IFN-β expression by individual cells is a stochastic process because cloned cells from individual precursors do not change the proportion of IFN-β expressing cells [128]. Consistent with

the idea that transcription factor association with the IFN-β promoter is the limiting factor, over expression of IRF3 or NF-κB leads to a higher proportion of IFN-β-expressing cells [129,130]. Recent studies have found that adding additional copies of the NF-κB binding sites to the distant Alu sites that associate with the IFN-β promoter also can increase the proportion of IFN-β expressing cells [88]. These data argue that NF-κB signaling and, specifically, its association with the IFN-β promoter, may be a major limiting factor that determines whether or not individual cells express IFN-β. Our data support this hypothesis because B16 tumor cells that entirely lack NF-κB signaling lack IFN-β expression and treatment with cycloheximide restores both of these outcomes. We also provide evidence that NF-κB may be acting to regulate epigenetic accessibility of the IFN-β promoter. Therefore, with the initial intention of understanding tumor cell-intrinsic STING signaling, we have also provided new mechanistic insights into IFN-β gene regulation.

4.04 Tumor cells frequently silence cell-intrinsic STING signaling and IFN-β expression

Cancer cells generally inactivate tumor suppressor genes as they undergo oncogenesis. For example, p53 is inactivated in a majority of human tumors and several mechanisms have been described by which tumors can inactivate p53. Most commonly tumors simply delete or mutate the p53 gene but they have also been described to suppress signaling upstream of p53 with negative regulators, use alternative splicing to block function, or even epigenetically suppress p53 expression [131]. There is now growing evidence that the innate immune system can act as a tumor suppressor by recruiting an adaptive immune response and promoting tumor rejection.

Deletion of the IFN locus represents approximately 13% of all homozygous deletion events and occurs in approximately 7% of patients with cancer [100]. This observation supports the notion that the innate immune system, through type I interferon signaling, can also act as a tumor-suppressor and that tumors adapt to silence this process. Tumor cell-extrinsic activation of the STING pathway leads to IFN-β expression by tumor-infiltrating immune cells, which can contribute to immune-mediated tumor control. This observation demonstrates that there are endogenous STING pathway agonists in the tumor microenvironment and that they are sufficient to activate host STING signaling and IFN-β expression [63]. Additionally, some tumor cells show the presence of cytosolic DNA or DNA fragments even in the absence of any therapeutic treatment which, in principle, should stimulate the STING pathway [132]. One study of lung cancer suggested the stressful tumor microenvironment can cause damage to mitochondria and that release of mitochondrial DNA may be a source of STING agonism [133]. Other studies have found perinuclear micronuclei that contain cGAS and might initiate STING signaling in tumor cells [134,135]. These data argue that most tumor cells are likely confronted with high concentrations of STING pathway agonists from multiple sources. The STING pathway is broadly expressed in a wide range of cell types [136] which raised the question as to whether tumor cells themselves sense endogenous STING agonists.

We found that the majority of tumor cell lines tested failed to express IFN-β in response to STING pathway activation. Previous studies of colorectal cancer and melanoma have described epigenetic silencing of both the STING and cGAS genes [101–103]. These studies identified methylation of the cGAS and STING genes as a potential mechanism that lead to a decrease in mRNA levels and support the notion that there is selective pressure to silence tumor cell-intrinsic STING signaling. Another study using a KRAS-driven lung cancer model found a

connection between LKB1 and expression of STING [133]. LKB1-mutations tend to make lung cancer more aggressive and resistant to checkpoint blockade immunotherapy. When trying to uncover the mechanistic link between LKB1 and resistance to immunotherapy, they found that LKB1 caused increased expression of the epigenetic remodeling enzymes DNMT1 and EZH2 which, in turn, caused silencing of STING expression. Bypassing this process with ectopic STING expression impaired the fitness of the tumor cells. This observation provided a direct link between oncogenic events and a selective advantage in tumor cells that are able to silence STING signaling. In our own work, most of the tumor cell lines we tested retained expression of the components of the STING pathway. In fact, there was some discordance between STING mRNA and protein levels suggesting that directly measuring STING protein or even downstream signaling events like IRF3 nuclear translocation are important when evaluating the integrity of the STING pathway.

Restoring tumor cell-intrinsic STING signaling may represent a unique therapeutic strategy for cancer. For most classical tumor suppressor genes, such as p53, restoring signaling in a single tumor cell would likely lead to apoptosis and deletion of that affected cell. Restoring innate immune signaling in tumor cells would likely initiate an immune response capable of killing not only that cell but other bystanders as well. For example, when only 10% of tumor cells were forced to express constitutive IFN-β, the entire tumor was controlled in vivo [50]. Based on this notion, finding ways to lift inhibition of innate immunity, just like anti-PD-1 checkpoint blockade immunotherapy, may represent a promising therapeutic strategy.

4.05 Tumor cells frequently retain certain aspects of STING such as IRF3 signaling

While we found that most tumor cell lines failed to express IFN-β, it was intriguing that B16 cells retained IRF3 signaling. In fact, several of the tumor cell lines that failed to express

IFN-β after STING pathway activation retained IRF3 nuclear translocation. These data confirmed our hypothesis that most tumor cells would lose tumor-intrinsic IFN-β expression because it is such a potent anti-tumor effector. While there are still many mechanisms downstream of STING activation that could cause a failure to express IFN-β while retaining IRF3 signaling, it is interesting that multiple cell lines retained this aspect of STING signaling. One study using radiation to cause tumor-intrinsic DNA damage found that tumor cells with increased STING signaling survived better [137]. Trex1 is a cytosolic DNAse that can attenuate STING pathway activation by degrading the stimulatory cytosolic DNA [138,139]. Trex1-deficient cells therefore have higher levels of STING activation, and it was found that this was associated with improved tumor survival following radiation. Conversely, Trex1-deficient cells that also lacked IRF3 did not have improved survival. This observation argues that there are consequences of IRF3 signaling that may provide pro-tumor effects by directly promoting tumor cell survival.

Transfer of tumor-derived DNA to the cytosol of host APCs is one of the proposed mechanisms for STING activation in tumor-infiltrating immune cells [63,139,140]. If this cytosolic DNA is the source of STING activation in immune cells, then it could be responsible for initiating the anti-tumor immune response by stimulating type I interferon expression and APC maturation. As such, tumor cells that retain STING signaling and DNAse expression might be better at degrading cytosolic DNA to evade detection by the innate immune system. In this way, preserving STING signaling while losing IFN-β expression could provide a benefit to tumor cells by preventing their release of immune-stimulatory DNA.

Another possible pro-tumor effect of STING signaling is autophagy. STING pathway activation can stimulate autophagy in an IFN-independent manner [141]. Autophagy can have anti-tumor effects in developing, pre-malignant cells by helping cells cope with stress. However,

autophagy tends to be more pro-tumor in fully malignant cells [142]. The tumor microenvironment tends to be nutrient-deprived and hypoxic which makes cell survival difficult. Autophagy allows cells to deal with damaged organelles and to recycle cellular components which are both useful under these stressful conditions. Activation of autophagy downstream of STING activation may therefore be a pro-tumor consequence of STING signaling that is independent of type I interferon signaling.

Another potential pro-tumor effect of STING signaling is an effect on $CD8^+$ T cells. $CD8^+$ T cells are anti-tumor effectors but T-cell intrinsic STING signaling can promote apoptosis [143–145]. One study has proposed that cGAMP derived from tumor cells may be taken up by $CD8^+$ T cells to promote their apoptosis [143–146]. If this is true, it is possible that certain aspects of STING signaling including cGAS activity and cGAMP release, may have pro-tumor consequences that are independent of NF-κB signaling or IFN-β expression. Therefore, STING-dependent induction of IFN-β seems to be an important anti-tumor effector and a process that is frequently silenced in tumor cells. However, many tumor cells seem to lack IFN-β expression while retaining other aspects of STING signaling such as expression of STING itself or IRF3 activation. It is interesting to consider whether tumor cells may retain these other aspects of signaling due to pro-tumor effects and, if so, it seems inhibitors of these processes may be useful as combination therapies with innate agonists.

4.06 Tumor-intrinsic STING signaling may be tied to STING activation in tumor-infiltrating immune cells

Host STING is required for IFN-β expression by tumor infiltrating immune cells [63]. This demonstrates that there are STING pathway agonists present in the endogenous tumor

microenvironment and that tumor-infiltrating immune cells can take up these agonists. An important remaining question is how this process occurs. A better understanding of the process of host STING pathway activation by tumor cells could enable the development of new therapies designed to augment it and promote a stronger anti-tumor immune response. The two primary hypotheses are that tumor-derived cGAMP or DNA are transferred from tumor cells to tumor-infiltrating immune cells.

The initial description of STING activation in tumor-infiltrating immune cells found evidence for transfer of labeled tumor DNA [63]. If cGAMP was transferred from tumor cells to immune cells, then it would directly activate STING and bypass the need for cGAS. However, both cGAS and STING appear to be necessary for response to checkpoint blockade in B16 melanoma [147]. These data argue that tumor cells contain DNA capable of activating the STING pathway and that it is transferred to immune cells. The precise mechanism for transfer of DNA to host APCs is not fully understood. One proposed mechanism is the release of extracellular vesicles by tumor cells that could fuse with APCs to directly deliver DNA into the cytosol. In vitro studies of irradiated tumor cells have found tumor-derived exosomes with DNA which, when transferred to DCs, could stimulate the STING pathway [139].

An alternative hypothesis is that cGAMP might be released by tumor cells and taken up via transporters in tumor-infiltrating immune cells. RMA-S and B16-BL6 tumor cells were reported to grow more quickly in STING $^{-/-}$ but not cGAS $^{-/-}$ mice suggesting the transfer of cGAMP rather than DNA [148]. This process was connected to a transporter in tumor-infiltrating immune cells that actively takes up cGAMP. Other studies have also found cGAMP transfer across GAP junctions [149] or extracellular vesicles [150]. These studies suggest that cGAMP might be transferred from tumor cells to immune cells. If this is the case, then tumor-intrinsic STING

signaling, specifically cGAS activity, may be necessary to activate STING in tumor infiltrating cells. One study has proposed this same process can occur in tumor-infiltrating T cells and that it may promote T cell apoptosis to provide a pro-tumor effect [145].

4.07 Innate immunotherapies represent an important new immunotherapeutic strategy

While checkpoint blockade immunotherapy has demonstrated the utility of recruiting the adaptive immune system for fighting cancer, most patients still fail to respond to these treatments. Clinical response to checkpoint blockade correlates with the presence of $CD8^+$ T cells in the tumor microenvironment [11,13,45]. This T cell-inflamed phenotype correlates with a type I interferon gene signature, and type I interferon signaling has been causally linked to tumor-specific $CD8^+$ T cell cross priming [52]. This type I interferon signature, in turn, has been linked to STING activation because STING-deficient mice lack IFN-β expression by tumor-infiltrating immune cells and, as a result, lack tumor-specific $CD8^+$ T cell priming. Taken together, these data argue that the anti-tumor immune response begins with STING pathway activation, IFN-β expression, APC maturation, tumor-specific T cell cross priming, chemokine production, and recruitment of effector T cells into the tumor microenvironment. If tumor cells express inhibitory ligands such as PD-L1 they can then suppress these effector T cells. However, blockade of PD-L1/PD-1 interactions can reverse this phenotype to enable T cell effector function.

It therefore seems that innate immune activation is a pre-requisite for a successful anti-tumor immune response and response to checkpoint blockade. This idea argues that in order to go beyond the successes of adaptive immunotherapies we may need innate immunotherapies.

STING agonists are one such therapy and have shown promise in pre-clinical models [76]. However, such agonists are typically administered via intratumoral injection. This approach works well if the tumor is accessible for direct injection. However, in circumstances where the tumor cannot be directly injected or where it is desirable to affect many metastases at once this strategy is less effective. Therefore, there is a need for systemic innate immunotherapies that can have an effect in the tumor microenvironment.

There are several strategies that are being pursued in an attempt to achieve this [151–153]. For example, ENPP1 is the enzyme that degrades cGAMP, and inhibitors of ENPP1 have been tested as a systemic therapy. Systemic administration of ENPP1 inhibitors promoted STING signaling and resulted in delayed tumor growth [154]. Modified bacteria have also been developed to promote STING signaling. Modified *E. coli* preferentially grow in the hypoxic and immunosuppressed tumor microenvironment. *E. coli* designed to express a di-nucleotide cyclase were able to stimulate STING, promote anti-tumor immune responses, and generate immune memory against tumor antigens (Society for ImmunoTherapy of Cancer Annual Meeting 2018 Poster P624). Another bacteria-based approach used auxotrophic *Salmonella typhimurium* that depend on tumor-derived adenosine. These bacteria expressed a Trex1 siRNA to inhibit Trex1 expression and allow for the accumulation of DNA. After IV delivery, there was a 1000-fold enrichment of bacteria in the tumor compared to liver or spleen and this caused an immune-dependent delay in tumor outgrowth (Society for ImmunoTherapy of Cancer Annual Meeting 2018 Poster P235).

Our work identifying how tumor cells silence tumor-intrinsic STING signaling could lead to the development of analogous therapies. For example, drugs designed to block the dominant negative inhibitor of NF-κB signaling in tumor cells could likely be administered systemically. Based on the fact that this process does not appear to occur in normal cells like the Mϕ controls

that we have studied, it seems like this therapy could have relative tumor selectivity to restore STING signaling locally. This is a particularly attractive approach because most models of STING signaling in cancer begin with tumor-derived DNA or cGAMP. This means that tumor cells are exposed to the highest levels of agonists and represent the greatest proportion of cells in the tumor microenvironment. Therefore, targeting STING signaling in tumor cells could represent a promising strategy. Further, it seems that even in relatively "immunologically cold" tumors that lack any sort of T cells or APCs there will still be tumor cells. If a therapy could re-enable tumor-intrinsic IFN-β expression, then this could stimulate chemokine expression to recruit immune cells and initiate an anti-tumor immune response even in the immunologically "coldest" tumors.

4.08 Future Directions

We found that the vast majority of tumor cell lines, including several human tumor cell lines, failed to express IFN-β after STING pathway activation. As we began to probe this more carefully, we found that B16 melanoma cells preserved IRF3 signaling downstream of STING activation but that these tumor cells lost NF-κB signaling. This defect in NF-κB signaling was mediated by a dominant negative mechanism and was reversed by cycloheximide treatment. IFN-β expression similarly displayed a dominant negative mechanism that was reversed by cycloheximide treatment and enabled tumor cells to express IFN-β at levels quantitatively similar to Mϕ controls. Based on this working model we employed whole-genome sequencing and a genome-wide CRISPR screen with an NF-κB reporter to identify candidate genes responsible for the phenotype. We found several candidates that, when knocked out, seem to augment tumor-intrinsic NF-κB signaling and IFN-β expression. However, these data involving single gene knockouts are still preliminary.

The highest priority follow-up experiments are to test single cell cloned populations with individual gene knockouts. These populations can be tested by Western blot analysis and genomic sequencing to identify whether they are homozygous knockout for each candidate gene. Once confirmed, they can then be tested for NF-κB signaling and IFN-β expression. Such experiments should reveal which genes have the largest effect on both of these outputs. Once these candidates have been fully tested for IFN-β expression, more detailed mechanistic studies will be possible. For example, Ubxn1 has been connected to IκBα protein accumulation. Does this occur in B16 tumor cells and is it reversed in Ubxn1 KO tumor cells? Trim30a has been linked to TAB2/3 degradation. Does this occur in B16 tumor cells and is it similarly reversed in Trim30a KO cells? Nbeal2 has been connected to regulation of vesicular trafficking. At some point the IKK complex must associate with the STING signaling complex on perinuclear vesicles. Is this defective in B16 tumor cells and might it be reversed by Nbeal2 KO? Regardless of which candidate looks promising they can all be tested by ImageStreamX to measure NF-κB nuclear translocation after STING pathway activation in knockout cells.

Once one of the major candidates is validated, it will be interesting to see how WT vs KO cells that have restored IFN-β expression grow in vivo. I hypothesize that tumor cells capable of tumor-intrinsic IFN-β expression will grow more slowly and may even be spontaneously rejected based on past studies [50]. It will be interesting to see how this affects tumor infiltration by myeloid cells, tumor-specific $CD8^+$ T cell cross-priming, $CD8^+$ T cell effector phenotypes, and immunologic memory. It will be especially interesting to see whether KO tumor cells capable of IFN-β expression respond better to checkpoint blockade immunotherapy or STING agonist injection.

Another open question is whether this same process occurs in human tumors. To test this, we have collected histology sections from human melanoma patients and are currently optimizing an RNA in-situ hybridization technique that can identify IFN-β mRNA. It will be interesting to see which cells in the tumor microenvironment express IFN-β. It's possible that human tumor cells will similarly lack IFN-β expression even as nearby myeloid cells express IFN-β. It will also be interesting to see how this phenotype looks when compared to patients that respond or fail to respond to checkpoint blockade immunotherapy.

Ultimately there are still many interesting future directions to directly follow up on my work. Some of the less direct but nonetheless interesting questions are broader questions such as: Does IRF3 signaling still occur downstream of STING in endogenous tumors and might it provide a benefit? What happens with TRAMP cells that are capable of IFN-β expression? How does the immune system respond differently to these cells and might deletion of IFN-β expression by these cells change their growth?

4.09 Conclusion

Ultimately, our results have identified a recurrent phenotype in which activation of the STING pathway fails to elicit IFN-β expression by the vast majority of tumor cells. As we began to probe the molecular mechanism more carefully, we found a number of interesting results. We found that in B16 tumor cells that fail to express IFN-β, the tumor cells retained IRF3 signaling including phosphorylation, nuclear translocation, DNA binding, and target gene transcription from sites other than the IFN-β locus. We found that NF-κB signaling was defective in B16 tumor cells and that this seemed to cause a failure in the epigenetic opening of the IFN-β locus. This failure to epigenetically open the IFN-β locus likely prevents IRF3 from binding the locus and, ultimately, prevents IFN-β expression. We found that the lack of IFN-β expression and the

defect in NF-κB signaling downstream of STING pathway activation were both dominant-negative phenotypes. Consistent with this idea, we found that treatment with cycloheximide to allow for the degradation of a putative dominant-negative inhibitory factor enables both tumor intrinsic NF-κB signaling and IFN-β expression. Based on whole-genome sequencing and a genome-wide CRISPR screen, we have identified several individual candidate genes that, when knocked out, seem to augment both NF-κB signaling and IFN-β expression by tumor cells in response to STING pathway activation. Follow-up experiments with single cell clones will provide an authoritative answer to which candidate genes have the largest effect on IFN-β expression and what consequence this has for in vivo tumor growth.

References

1. Hanahan, D. & Weinberg, R. A. The hallmarks of cancer. *Cell* **100**, 57–70 (2000).
2. Fridman, W. H., Pagès, F., Sautès-Fridman, C. & Galon, J. The immune contexture in human tumours: impact on clinical outcome. *Nat. Rev. Cancer* **12**, 298–306 (2012).
3. Naito, Y. *et al.* CD8+ T cells infiltrated within cancer cell nests as a prognostic factor in human colorectal cancer. *Cancer Res.* **58**, 3491–3494 (1998).
4. Li, B. *et al.* Comprehensive analyses of tumor immunity: implications for cancer immunotherapy. *Genome Biol.* **17**, 174 (2016).
5. Galon, J. *et al.* Cancer classification using the Immunoscore: a worldwide task force. *J. Transl. Med.* **10**, 205 (2012).
6. Boon, T. & van der Bruggen, P. Human tumor antigens recognized by T lymphocytes. *J. Exp. Med.* **183**, 725–729 (1996).
7. Gubin, M. M. *et al.* Checkpoint blockade cancer immunotherapy targets tumour-specific mutant antigens. *Nature* **515**, 577–581 (2014).
8. Ohigashi, Y. *et al.* Clinical significance of programmed death-1 ligand-1 and programmed death-1 ligand-2 expression in human esophageal cancer. *Clin. Cancer Res. Off. J. Am. Assoc. Cancer Res.* **11**, 2947–2953 (2005).
9. Hino, R. *et al.* Tumor cell expression of programmed cell death-1 ligand 1 is a prognostic factor for malignant melanoma. *Cancer* **116**, 1757–1766 (2010).
10. Ribas, A. & Wolchok, J. D. Cancer immunotherapy using checkpoint blockade. *Science* **359**, 1350–1355 (2018).
11. Tumeh, P. C. *et al.* PD-1 blockade induces responses by inhibiting adaptive immune resistance. *Nature* **515**, 568–571 (2014).

12. Baumann, M. *et al.* Radiation oncology in the era of precision medicine. *Nat. Rev. Cancer* **16**, 234–249 (2016).

13. Ayers, M. *et al.* IFN-γ–related mRNA profile predicts clinical response to PD-1 blockade. *J. Clin. Invest.* **127**, 2930–2940 (2017).

14. Chen, D. S. & Mellman, I. Oncology meets immunology: the cancer-immunity cycle. *Immunity* **39**, 1–10 (2013).

15. Vogelstein, B., Lane, D. & Levine, A. J. Surfing the p53 network. *Nature* **408**, 307–310 (2000).

16. Petitjean, A. *et al.* Impact of mutant p53 functional properties on TP53 mutation patterns and tumor phenotype: lessons from recent developments in the IARC TP53 database. *Hum. Mutat.* **28**, 622–629 (2007).

17. Hafner, A., Bulyk, M. L., Jambhekar, A. & Lahav, G. The multiple mechanisms that regulate p53 activity and cell fate. *Nat. Rev. Mol. Cell Biol.* **20**, 199–210 (2019).

18. Schreiber, R. D., Old, L. J. & Smyth, M. J. Cancer immunoediting: integrating immunity's roles in cancer suppression and promotion. *Science* **331**, 1565–1570 (2011).

19. Shankaran, V. *et al.* IFNgamma and lymphocytes prevent primary tumour development and shape tumour immunogenicity. *Nature* **410**, 1107–1111 (2001).

20. Janeway, C. A. & Medzhitov, R. Innate immune recognition. *Annu. Rev. Immunol.* **20**, 197–216 (2002).

21. Brubaker, S. W., Bonham, K. S., Zanoni, I. & Kagan, J. C. Innate Immune Pattern Recognition: A Cell Biological Perspective. *Annu. Rev. Immunol.* **33**, 257–290 (2015).

22. Gallucci, S., Lolkema, M. & Matzinger, P. Natural adjuvants: endogenous activators of dendritic cells. *Nat. Med.* **5**, 1249–1255 (1999).

23. Matzinger, P. The danger model: a renewed sense of self. *Science* **296**, 301–305 (2002).
24. Tong, A.-J. *et al.* A Stringent Systems Approach Uncovers Gene-Specific Mechanisms Regulating Inflammation. *Cell* **165**, 165–179 (2016).
25. Stetson, D. B. & Medzhitov, R. Type I interferons in host defense. *Immunity* **25**, 373–381 (2006).
26. Tsou, C.-L. *et al.* Critical roles for CCR2 and MCP-3 in monocyte mobilization from bone marrow and recruitment to inflammatory sites. *J. Clin. Invest.* **117**, 902–909 (2007).
27. Ginhoux, F. & Jung, S. Monocytes and macrophages: developmental pathways and tissue homeostasis. *Nat. Rev. Immunol.* **14**, 392–404 (2014).
28. Roche, P. A. & Cresswell, P. Antigen Processing and Presentation Mechanisms in Myeloid Cells. *Microbiol. Spectr.* **4**, (2016).
29. Trombetta, E. S. & Mellman, I. Cell biology of antigen processing in vitro and in vivo. *Annu. Rev. Immunol.* **23**, 975–1028 (2005).
30. Ohl, L. *et al.* CCR7 Governs Skin Dendritic Cell Migration under Inflammatory and Steady-State Conditions. *Immunity* **21**, 279–288 (2004).
31. Reis e Sousa, C. Dendritic cells in a mature age. *Nat. Rev. Immunol.* **6**, 476–483 (2006).
32. Bousso, P. & Robey, E. Dynamics of CD8+ T cell priming by dendritic cells in intact lymph nodes. *Nat. Immunol.* **4**, 579–585 (2003).
33. Davis, M. M. & Bjorkman, P. J. T-cell antigen receptor genes and T-cell recognition. *Nature* **334**, 395–402 (1988).
34. Lieber, M. R. Site-specific recombination in the immune system. *FASEB J. Off. Publ. Fed. Am. Soc. Exp. Biol.* **5**, 2934–2944 (1991).

35. Arstila, T. P. *et al.* A direct estimate of the human alphabeta T cell receptor diversity. *Science* **286**, 958–961 (1999).

36. Casrouge, A. *et al.* Size estimate of the alpha beta TCR repertoire of naive mouse splenocytes. *J. Immunol. Baltim. Md 1950* **164**, 5782–5787 (2000).

37. Nemazee, D. Receptor editing in lymphocyte development and central tolerance. *Nat. Rev. Immunol.* **6**, 728–740 (2006).

38. Xing, Y. & Hogquist, K. A. T-cell tolerance: central and peripheral. *Cold Spring Harb. Perspect. Biol.* **4**, (2012).

39. Zhang, N. & Bevan, M. J. CD8(+) T cells: foot soldiers of the immune system. *Immunity* **35**, 161–168 (2011).

40. Voskoboinik, I., Smyth, M. J. & Trapani, J. A. Perforin-mediated target-cell death and immune homeostasis. *Nat. Rev. Immunol.* **6**, 940–952 (2006).

41. Rivoltini, L. *et al.* Human melanoma-reactive CD4+ and CD8+ CTL clones resist Fas ligand-induced apoptosis and use Fas/Fas ligand-independent mechanisms for tumor killing. *J. Immunol. Baltim. Md 1950* **161**, 1220–1230 (1998).

42. Martini, M. *et al.* IFN-gamma-mediated upmodulation of MHC class I expression activates tumor-specific immune response in a mouse model of prostate cancer. *Vaccine* **28**, 3548–3557 (2010).

43. Chawla-Sarkar, M. *et al.* Apoptosis and interferons: role of interferon-stimulated genes as mediators of apoptosis. *Apoptosis Int. J. Program. Cell Death* **8**, 237–249 (2003).

44. Wang, W. *et al.* CD8+ T cells regulate tumour ferroptosis during cancer immunotherapy. *Nature* **569**, 270–274 (2019).

45. Harlin, H. *et al.* Chemokine expression in melanoma metastases associated with CD8+ T-cell recruitment. *Cancer Res.* **69**, 3077–3085 (2009).

46. Spranger, S. *et al.* Up-regulation of PD-L1, IDO, and T(regs) in the melanoma tumor microenvironment is driven by CD8(+) T cells. *Sci. Transl. Med.* **5**, 200ra116 (2013).

47. Dong, H. *et al.* Tumor-associated B7-H1 promotes T-cell apoptosis: a potential mechanism of immune evasion. *Nat. Med.* **8**, 793–800 (2002).

48. Coulie, P. G., Van den Eynde, B. J., van der Bruggen, P. & Boon, T. Tumour antigens recognized by T lymphocytes: at the core of cancer immunotherapy. *Nat. Rev. Cancer* **14**, 135–146 (2014).

49. Aricò, E., Castiello, L., Capone, I., Gabriele, L. & Belardelli, F. Type I Interferons and Cancer: An Evolving Story Demanding Novel Clinical Applications. *Cancers* **11**, (2019).

50. Spaapen, R. M. *et al.* Therapeutic activity of high-dose intratumoral IFN-β requires direct effect on the tumor vasculature. *J. Immunol. Baltim. Md 1950* **193**, 4254–4260 (2014).

51. Indraccolo, S. Interferon-alpha as angiogenesis inhibitor: learning from tumor models. *Autoimmunity* **43**, 244–247 (2010).

52. Fuertes, M. B. *et al.* Host type I IFN signals are required for antitumor CD8+ T cell responses through CD8{alpha}+ dendritic cells. *J. Exp. Med.* **208**, 2005–2016 (2011).

53. Bachem, A. *et al.* Expression of XCR1 Characterizes the Batf3-Dependent Lineage of Dendritic Cells Capable of Antigen Cross-Presentation. *Front. Immunol.* **3**, (2012).

54. Broz, M. L. *et al.* Dissecting the tumor myeloid compartment reveals rare activating antigen-presenting cells critical for T cell immunity. *Cancer Cell* **26**, 638–652 (2014).

55. Roberts, E. W. *et al.* Critical Role for CD103(+)/CD141(+) Dendritic Cells Bearing CCR7 for Tumor Antigen Trafficking and Priming of T Cell Immunity in Melanoma. *Cancer Cell* **30**, 324–336 (2016).

56. Diamond, M. S. *et al.* Type I interferon is selectively required by dendritic cells for immune rejection of tumors. *J. Exp. Med.* **208**, 1989–2003 (2011).

57. Le Bon, A. *et al.* Direct stimulation of T cells by type I IFN enhances the CD8+ T cell response during cross-priming. *J. Immunol. Baltim. Md 1950* **176**, 4682–4689 (2006).

58. Hervas-Stubbs, S. *et al.* CD8 T cell priming in the presence of IFN-α renders CTLs with improved responsiveness to homeostatic cytokines and recall antigens: important traits for adoptive T cell therapy. *J. Immunol. Baltim. Md 1950* **189**, 3299–3310 (2012).

59. Newby, B. N. *et al.* Type 1 Interferons Potentiate Human CD8+ T-Cell Cytotoxicity Through a STAT4- and Granzyme B–Dependent Pathway. *Diabetes* **66**, 3061–3071 (2017).

60. Ourthiague, D. R. *et al.* Limited specificity of IRF3 and ISGF3 in the transcriptional innate-immune response to double-stranded RNA. *J. Leukoc. Biol.* **98**, 119–128 (2015).

61. Spranger, S., Dai, D., Horton, B. & Gajewski, T. F. Tumor-Residing Batf3 Dendritic Cells Are Required for Effector T Cell Trafficking and Adoptive T Cell Therapy. *Cancer Cell* **31**, 711-723.e4 (2017).

62. Spranger, S., Bao, R. & Gajewski, T. F. Melanoma-intrinsic β-catenin signalling prevents anti-tumour immunity. *Nature* (2015) doi:10.1038/nature14404.

63. Woo, S.-R. *et al.* STING-dependent cytosolic DNA sensing mediates innate immune recognition of immunogenic tumors. *Immunity* **41**, 830–842 (2014).

64. Ishikawa, H. & Barber, G. N. STING is an endoplasmic reticulum adaptor that facilitates innate immune signalling. *Nature* **455**, 674–678 (2008).

65. Sun, W. *et al.* ERIS, an endoplasmic reticulum IFN stimulator, activates innate immune signaling through dimerization. *Proc. Natl. Acad. Sci. U. S. A.* **106**, 8653–8658 (2009).

66. Jin, L. *et al.* MPYS, a novel membrane tetraspanner, is associated with major histocompatibility complex class II and mediates transduction of apoptotic signals. *Mol. Cell. Biol.* **28**, 5014–5026 (2008).

67. Sun, L., Wu, J., Du, F., Chen, X. & Chen, Z. J. Cyclic GMP-AMP Synthase Is a Cytosolic DNA Sensor That Activates the Type I Interferon Pathway. *Science* **339**, 786–791 (2013).

68. Burdette, D. L. *et al.* STING is a direct innate immune sensor of cyclic di-GMP. *Nature* **478**, 515–518 (2011).

69. Wu, J. *et al.* Cyclic GMP-AMP is an endogenous second messenger in innate immune signaling by cytosolic DNA. *Science* **339**, 826–830 (2013).

70. Ishikawa, H., Ma, Z. & Barber, G. N. STING regulates intracellular DNA-mediated, type I interferon-dependent innate immunity. *Nature* **461**, 788–792 (2009).

71. Luo, W.-W. *et al.* iRhom2 is essential for innate immunity to DNA viruses by mediating trafficking and stability of the adaptor STING. *Nat. Immunol.* **17**, 1057–1066 (2016).

72. Liu, S. *et al.* Phosphorylation of innate immune adaptor proteins MAVS, STING, and TRIF induces IRF3 activation. *Science* **347**, aaa2630 (2015).

73. Tanaka, Y. & Chen, Z. J. STING specifies IRF3 phosphorylation by TBK1 in the cytosolic DNA signaling pathway. *Sci. Signal.* **5**, ra20 (2012).

74. Abe, T. *et al.* STING recognition of cytoplasmic DNA instigates cellular defense. *Mol. Cell* **50**, 5–15 (2013).

75. Abe, T. & Barber, G. N. Cytosolic-DNA-mediated, STING-dependent proinflammatory gene induction necessitates canonical NF-κB activation through TBK1. *J. Virol.* **88**, 5328–5341 (2014).

76. Corrales, L. *et al.* Direct Activation of STING in the Tumor Microenvironment Leads to Potent and Systemic Tumor Regression and Immunity. *Cell Rep.* **11**, 1018–1030 (2015).

77. Borden, E. C. *et al.* Interferons at age 50: past, current and future impact on biomedicine. *Nat. Rev. Drug Discov.* **6**, 975–990 (2007).

78. van Pesch, V., Lanaya, H., Renauld, J.-C. & Michiels, T. Characterization of the Murine Alpha Interferon Gene Family. *J. Virol.* **78**, 8219–8228 (2004).

79. I, M., Je, D. & De, L. Differential viral induction of distinct interferon-alpha genes by positive feedback through interferon regulatory factor-7. *The EMBO journal* vol. 17 http://pubmed.ncbi.nlm.nih.gov/9822609/ (1998).

80. Sato, M. *et al.* Distinct and essential roles of transcription factors IRF-3 and IRF-7 in response to viruses for IFN-alpha/beta gene induction. *Immunity* **13**, 539–548 (2000).

81. Lee-Kirsch, M. A. The Type I Interferonopathies. *Annu. Rev. Med.* **68**, 297–315 (2017).

82. Ford, E. & Thanos, D. The transcriptional code of human IFN-β gene expression. *Biochim. Biophys. Acta BBA - Gene Regul. Mech.* **1799**, 328–336 (2010).

83. Thanos, D. & Maniatis, T. The high mobility group protein HMG I(Y) is required for NF-kappa B-dependent virus induction of the human IFN-beta gene. *Cell* **71**, 777–789 (1992).

84. Hiscott, J. *et al.* Triggering the interferon response: the role of IRF-3 transcription factor. *J. Interferon Cytokine Res. Off. J. Int. Soc. Interferon Cytokine Res.* **19**, 1–13 (1999).

85. Wathelet, M. G. *et al.* Virus infection induces the assembly of coordinately activated transcription factors on the IFN-beta enhancer in vivo. *Mol. Cell* **1**, 507–518 (1998).

86. Du, W. & Maniatis, T. An ATF/CREB binding site is required for virus induction of the human interferon beta gene [corrected]. *Proc. Natl. Acad. Sci. U. S. A.* **89**, 2150–2154 (1992).

87. Thanos, D. & Maniatis, T. Virus induction of human IFN beta gene expression requires the assembly of an enhanceosome. *Cell* **83**, 1091–1100 (1995).

88. Apostolou, E. & Thanos, D. Virus Infection Induces NF-kappaB-dependent interchromosomal associations mediating monoallelic IFN-beta gene expression. *Cell* **134**, 85–96 (2008).

89. Munshi, N. *et al.* Coordination of a Transcriptional Switch by HMGI(Y) Acetylation. *Science* **293**, 1133–1136 (2001).

90. Du, W. & Maniatis, T. The high mobility group protein HMG I(Y) can stimulate or inhibit DNA binding of distinct transcription factor ATF-2 isoforms. *Proc. Natl. Acad. Sci. U. S. A.* **91**, 11318–11322 (1994).

91. Reeves, R. & Beckerbauer, L. HMGI/Y proteins: flexible regulators of transcription and chromatin structure. *Biochim. Biophys. Acta* **1519**, 13–29 (2001).

92. Agalioti, T. *et al.* Ordered recruitment of chromatin modifying and general transcription factors to the IFN-beta promoter. *Cell* **103**, 667–678 (2000).

93. Agalioti, T., Chen, G. & Thanos, D. Deciphering the transcriptional histone acetylation code for a human gene. *Cell* **111**, 381–392 (2002).

94. Merika, M., Williams, A. J., Chen, G., Collins, T. & Thanos, D. Recruitment of CBP/p300 by the IFNβ Enhanceosome Is Required for Synergistic Activation of Transcription. *Mol. Cell* **1**, 277–287 (1998).

95. Kim, T. K., Kim, T. H. & Maniatis, T. Efficient recruitment of TFIIB and CBP-RNA polymerase II holoenzyme by an interferon-beta enhanceosome in vitro. *Proc. Natl. Acad. Sci. U. S. A.* **95**, 12191–12196 (1998).

96. Kim, J. L., Nikolov, D. B. & Burley, S. K. Co-crystal structure of TBP recognizing the minor groove of a TATA element. *Nature* **365**, 520–527 (1993).

97. Lomvardas, S. & Thanos, D. Nucleosome Sliding via TBP DNA Binding In Vivo. *Cell* **106**, 685–696 (2001).

98. Lomvardas, S. & Thanos, D. Modifying gene expression programs by altering core promoter chromatin architecture. *Cell* **110**, 261–271 (2002).

99. Diaz, M. O. *et al.* Homozygous deletion of the alpha- and beta 1-interferon genes in human leukemia and derived cell lines. *Proc. Natl. Acad. Sci. U. S. A.* **85**, 5259–5263 (1988).

100. Ye, Z. *et al.* Prevalent Homozygous Deletions of Type I Interferon and Defensin Genes in Human Cancers Associate with Immunotherapy Resistance. *Clin. Cancer Res. Off. J. Am. Assoc. Cancer Res.* **24**, 3299–3308 (2018).

101. Konno, H. *et al.* Suppression of STING signaling through epigenetic silencing and missense mutation impedes DNA damage mediated cytokine production. *Oncogene* **37**, 2037–2051 (2018).

102. Xia, T., Konno, H., Ahn, J. & Barber, G. N. Deregulation of STING Signaling in Colorectal Carcinoma Constrains DNA Damage Responses and Correlates With Tumorigenesis. *Cell Rep.* **14**, 282–297 (2016).

103. de Queiroz, N. M. G. P., Xia, T., Konno, H. & Barber, G. N. Ovarian Cancer Cells Commonly Exhibit Defective STING Signaling Which Affects Sensitivity to Viral Oncolysis. *Mol. Cancer Res. MCR* **17**, 974–986 (2019).

104. Vogel, C. & Marcotte, E. M. Insights into the regulation of protein abundance from proteomic and transcriptomic analyses. *Nat. Rev. Genet.* **13**, 227–232 (2012).

105. Huber, M. *et al.* Comparison of Proteomic and Genomic Analyses of the Human Breast Cancer Cell Line T47D and the Antiestrogen-resistant Derivative T47D-r. *Mol. Cell. Proteomics* **3**, 43–55 (2004).

106. Rueckert, C. *et al.* Cyclic dinucleotides modulate induced type I IFN responses in innate immune cells by degradation of STING. *FASEB J. Off. Publ. Fed. Am. Soc. Exp. Biol.* **31**, 3107–3115 (2017).

107. Gonugunta, V. K. *et al.* Trafficking-mediated STING degradation requires sorting to acidified endolysosomes and can be therapeutically targeted to enhance anti-tumor response. *Cell Rep.* **21**, 3234–3242 (2017).

108. Liang, Q. *et al.* Crosstalk between the cGAS DNA sensor and Beclin-1 autophagy protein shapes innate antimicrobial immune responses. *Cell Host Microbe* **15**, 228–238 (2014).

109. Zhong, B. *et al.* The ubiquitin ligase RNF5 regulates antiviral responses by mediating degradation of the adaptor protein MITA. *Immunity* **30**, 397–407 (2009).

110. Li, Q. *et al.* TRIM29 negatively controls antiviral immune response through targeting STING for degradation. *Cell Discov.* **4**, 1–13 (2018).

111. Wang, Y. *et al.* TRIM30α Is a Negative-Feedback Regulator of the Intracellular DNA and DNA Virus-Triggered Response by Targeting STING. *PLoS Pathog.* **11**, e1005012 (2015).

112. Stetson, D. B. & Medzhitov, R. Recognition of cytosolic DNA activates an IRF3-dependent innate immune response. *Immunity* **24**, 93–103 (2006).

113. Shi, Y. *et al.* Exosomal Interferon-Induced Transmembrane Protein 2 Transmitted to Dendritic Cells Inhibits Interferon Alpha Pathway Activation and Blocks Anti-Hepatitis B Virus Efficacy of Exogenous Interferon Alpha. *Hepatol. Baltim. Md* **69**, 2396–2413 (2019).

114. Hu, Y. *et al.* Multiple UBXN family members inhibit retrovirus and lentivirus production and canonical NFκB signaling by stabilizing IκBα. *PLOS Pathog.* **13**, e1006187 (2017).

115. Wang, P. *et al.* UBXN1 interferes with Rig-I-like receptor-mediated antiviral immune response by targeting MAVS. *Cell Rep.* **3**, 1057–1070 (2013).

116. Wang, Y.-B. *et al.* Ubiquitin-associated Domain-containing Ubiquitin Regulatory X (UBX) Protein UBXN1 Is a Negative Regulator of Nuclear Factor κB (NF-κB) Signaling. *J. Biol. Chem.* **290**, 10395–10405 (2015).

117. Panne, D. The enhanceosome. *Curr. Opin. Struct. Biol.* **18**, 236–242 (2008).

118. Ogawa, E., Mukai, K., Saito, K., Arai, H. & Taguchi, T. The binding of TBK1 to STING requires exocytic membrane traffic from the ER. *Biochem. Biophys. Res. Commun.* **503**, 138–145 (2018).

119. Dainichi, T., Matsumoto, R., Mostafa, A. & Kabashima, K. Immune Control by TRAF6-Mediated Pathways of Epithelial Cells in the EIME (Epithelial Immune Microenvironment). *Front. Immunol.* **10**, (2019).

120. Xia, Z.-P. *et al.* Direct activation of protein kinases by unanchored polyubiquitin chains. *Nature* **461**, 114–119 (2009).

121. Shi, M. *et al.* TRIM30α negatively regulates TLR-mediated NF-κB activation by targeting TAB2 and TAB3 for degradation. *Nat. Immunol.* **9**, 369–377 (2008).

122. Gunay-Aygun, M. *et al.* NBEAL2 is mutated in gray platelet syndrome and is required for biogenesis of platelet α-granules. *Nat. Genet.* **43**, 732–734 (2011).

123. Mayer, L. *et al.* Nbeal2 interacts with Dock7, Sec16a, and Vac14. *Blood* **131**, 1000–1011 (2018).

124. Aslan, J. E. & McCarty, O. J. T. Rho GTPases in platelet function. *J. Thromb. Haemost. JTH* **11**, 35–46 (2013).

125. Konno, H., Konno, K. & Barber, G. N. Cyclic dinucleotides trigger ULK1 (ATG1) phosphorylation of STING to prevent sustained innate immune signaling. *Cell* **155**, 688–698 (2013).

126. Senger, K. *et al.* Gene repression by coactivator repulsion. *Mol. Cell* **6**, 931–937 (2000).

127. Zawatzky, R., De Maeyer, E. & De Maeyer-Guignard, J. Identification of individual interferon-producing cells by in situ hybridization. *Proc. Natl. Acad. Sci. U. S. A.* **82**, 1136–1140 (1985).

128. Hu, J. *et al.* Chromosome-specific and noisy IFNB1 transcription in individual virus-infected human primary dendritic cells. *Nucleic Acids Res.* **35**, 5232–5241 (2007).

129. Hottiger, M. O., Felzien, L. K. & Nabel, G. J. Modulation of cytokine-induced HIV gene expression by competitive binding of transcription factors to the coactivator p300. *EMBO J.* **17**, 3124–3134 (1998).

130. Lipniacki, T., Paszek, P., Brasier, A. R., Luxon, B. A. & Kimmel, M. Stochastic regulation in early immune response. *Biophys. J.* **90**, 725–742 (2006).

131. Herrero, A. B., Rojas, E. A., Misiewicz-Krzeminska, I., Krzeminski, P. & Gutiérrez, N. C. Molecular Mechanisms of p53 Deregulation in Cancer: An Overview in Multiple Myeloma. *Int. J. Mol. Sci.* **17**, (2016).

132. Shen, Y. J. *et al.* Genome-derived cytosolic DNA mediates type I interferon-dependent rejection of B cell lymphoma cells. *Cell Rep.* **11**, 460–473 (2015).

133. Kitajima, S. *et al.* Suppression of STING Associated with LKB1 Loss in KRAS-Driven Lung Cancer. *Cancer Discov.* (2018) doi:10.1158/2159-8290.CD-18-0689.

134. Harding, S. M. *et al.* Mitotic progression following DNA damage enables pattern recognition within micronuclei. *Nature* **548**, 466–470 (2017).

135. Mackenzie, K. J. *et al.* cGAS surveillance of micronuclei links genome instability to innate immunity. *Nature* **548**, 461–465 (2017).

136. Barber, G. N. STING-dependent cytosolic DNA sensing pathways. *Trends Immunol.* **35**, 88–93 (2014).

137. Erdal, E., Haider, S., Rehwinkel, J., Harris, A. L. & McHugh, P. J. A prosurvival DNA damage-induced cytoplasmic interferon response is mediated by end resection factors and is limited by Trex1. *Genes Dev.* **31**, 353–369 (2017).

138. Vanpouille-Box, C. *et al.* DNA exonuclease Trex1 regulates radiotherapy-induced tumour immunogenicity. *Nat. Commun.* **8**, 15618 (2017).

139. Diamond, J. M. *et al.* Exosomes Shuttle TREX1-Sensitive IFN-Stimulatory dsDNA from Irradiated Cancer Cells to DCs. *Cancer Immunol. Res.* **6**, 910–920 (2018).

140. Ahn, J., Xia, T., Rabasa Capote, A., Betancourt, D. & Barber, G. N. Extrinsic Phagocyte-Dependent STING Signaling Dictates the Immunogenicity of Dying Cells. *Cancer Cell* **33**, 862-873.e5 (2018).

141. Gui, X. *et al.* Autophagy induction via STING trafficking is a primordial function of the cGAS pathway. *Nature* **567**, 262–266 (2019).

142. Anding, A. L. & Baehrecke, E. H. Autophagy in Cell Life and Cell Death. *Curr. Top. Dev. Biol.* **114**, 67–91 (2015).

143. Gulen, M. F. *et al.* Signalling strength determines proapoptotic functions of STING. *Nat. Commun.* **8**, 427 (2017).

144. Larkin, B. *et al.* Activation of STING in T cells induces type I IFN responses and cell death. *J. Immunol. Baltim. Md 1950* **199**, 397 (2017).

145. Wu, J. *et al.* STING-mediated disruption of calcium homeostasis chronically activates ER stress and primes T cell death. *J. Exp. Med.* **216**, 867–883 (2019).

146. Cerboni, S. *et al.* Intrinsic antiproliferative activity of the innate sensor STING in T lymphocytes. *J. Exp. Med.* **214**, 1769–1785 (2017).

147. Wang, H. *et al.* cGAS is essential for the antitumor effect of immune checkpoint blockade. *Proc. Natl. Acad. Sci.* **114**, 1637–1642 (2017).

148. Marcus, A. *et al.* Tumor-Derived cGAMP Triggers a STING-Mediated Interferon Response in Non-tumor Cells to Activate the NK Cell Response. *Immunity* **49**, 754-763.e4 (2018).

149. Ablasser, A. *et al.* Cell intrinsic immunity spreads to bystander cells via the intercellular transfer of cGAMP. *Nature* **503**, 530–534 (2013).

150. Gentili, M. *et al.* Transmission of innate immune signaling by packaging of cGAMP in viral particles. *Science* **349**, 1232–1236 (2015).

151. Berger, G. & Lawler, S. E. Novel non-nucleotidic STING agonists for cancer immunotherapy. *Future Med. Chem.* **10**, 2767–2769 (2018).

152. Banerjee, I. *et al.* Gasdermin D Restrains Type I Interferon Response to Cytosolic DNA by Disrupting Ionic Homeostasis. *Immunity* **49**, 413-426.e5 (2018).

153. Khiar, S. *et al.* Identification of a small molecule that primes the type I interferon response to cytosolic DNA. *Sci. Rep.* **7**, 2561 (2017).

154. Sharma, S. *et al.* Abstract 1932: discovery of ENPP1 inhibitors as agonists of STING pathway. *Cancer Res.* **78**, 1932 (2018).